ISSN 2071-3592

童綜合醫學雜誌

Tungs' Medical Journal

Volume 12 Number 1 June 2018

Editorial Office:

The Tungs' Medical Journal, Tungs' Taichung MetroHarbor Hospital.

No. 699, Sec. 8, Taiwan Blvd., Wuqi Dist., Taichung City 43503, Taiwan (R.O.C.)

E-Mail: Tungs_Journal@ms.sltung.com.tw

Tel.: 886-4-26581919 ext. 59045 Fax: 886-4-26582193

Printing Company:

Great C Printing Co.

Tel: 886-2-2302-3939 Fax: 886-2-2302-2036

Vol. 12 No. 1 January-June 2018

Tungs' Medical Journal

CONTENTS IN BRIEF

PATHOLOGY PAGE

IMAGE

Editorial

Immunotherapy in Prostate Cancer: Past, Current, and Future

Yen-Chuan Ou[1], and Hung-Lin Chen[2,*]

[1]Department of Urology, [2]Department of Medical Research, Tungs' Taichung MetroHarbor Hospital, Taichung, Taiwan

Received: May. 30, 2018; Accepted: May. 30, 2018

Abstract

Prostate cancer is one of the most prevalent cancers worldwide and is the fifth leading cause of deaths due to cancer in Taiwan. Reducing the morbidity and mortality of prostate cancer is a major concern for the Ministry of Health and Welfare of Taiwan. Immunotherapy has been the dominant field in oncology, particularly when checkpoint inhibitors become crucial factors in pharmaceutical industries. The progression of cancer immunotherapy has already achieved several milestones. However, exclusive characteristics of prostate cancer restrict the efficacy of immunotherapy. We reviewed recent clinical trials showing supporting and adverse outcomes of immunotherapy in metastatic castration-resistant prostate cancers, including cancer vaccines, checkpoint inhibitors, and adoptive T cells. To implement immunotherapy in prostate cancer, shaping an adequate microenvironment for the immune system is key. Although current outcomes of immunotherapy for prostate cancer have not been encouraging, these are expected in future.

Key words: Immunotherapy, Checkpoint inhibitor, CAR-T, Prostate cancer

Prostate cancer

The prevalence of prostate cancer is very high worldwide. In the United States, it is the most common cancer in men, with morbidity and mortality rates of 13% and 2.5%, respectively. Previous studies have shown that genetic background also has an important role in the mortality of prostate cancer. The death rate of prostate cancer is two times higher in African American men (4.2%) than in Asian and Pacific Islander men (2.1%).[1] The government of Taiwan has established a cancer registration database since 1989.[2] In the beginning, the database only included six cancer types, namely oral, colorectal, liver, lung, breast, and cervical cancers. Prostate cancer was omitted by the database until 2008. Since its enrollment in the cancer registration database, the number of patients with prostate cancer has been increasing every year. In 2013 and 2014, 4957 and 5160 patients, respectively, were diagnosed with prostate cancer,[2] with an increase of 149 cases and a growth rate of 3.01% (among the top five cancers). Thus far, prostate cancer has remained the fifth most common cancer in Taiwan,[2] with the major type being adenocarcinoma (approximately 97%). More than 35% of men aged 70–79 years (median age of patients diagnosed with prostate cancer, 73 years) are diagnosed with prostate cancer, with the disease being equally prevalent among the northern, middle, and southern parts of Taiwan.[2]

Patients with prostate cancer initially do not experience any clinical or life-threatening symptom, and the tumor growth is usually quite slow. Evidence has shown that, among men who died due to other causes, more than 33% aged between 70 and 79 years had prostate cancer. Therefore, death of most men due to prostate cancer was caused by reasons other than the cancer. However, one-third of prostate cancers are more aggressive and lead to death. A study has revealed that men frequently die due to prostate cancer at the age of 80 years in the United

*Correspondence to: Dr. Hung-Lin Chen, Department of Medical Research, Tungs' Taichung MetroHarbor Hospital, No. 699, Sec. 8, Taiwan Blvd., Wuqi Dist., Taichung City 43503, Taiwan, (R.O.C.)

States.[1] In Taiwan, the median age of men who died due to prostate cancer is 81 years. Research data has shown that 32.96% of prostate cancers are diagnosed at stage IV and more than 50% are diagnosed at late stages.[2] If prostate cancer is detected early, then death rates can be reduced. The common screening method for prostate cancer is the detection of prostate-specific antigen (PSA) in the peripheral blood, which was approved by the United States Food and Drug Administration (FDA) in 1994. For medical planning, approximately half (58.95%) of all patients with prostate cancer receive androgen deprivation (ADT) as the primary treatment. Secondary options are radiation (27.05%) and surgery (25.89%). Immunotherapy as the primary treatment for prostate cancer is performed in only 0.27% of cases.[2]

Immunotherapy in prostate cancer

Prostate cancer is a highly potential model for testing immunotherapy because of its multiple tumor-associated antigens, which are great targets for building up immune repertoires. Besides, prostate cancer does not progress as rapidly as other cancers, so that ample time is available for the immune system to develop antitumor responses. However, the microenvironment of prostate cancer is not immune-favorable. Evidence has shown that patients with prostate cancer have increasing numbers of regulatory T cells, which secrete transforming growth factor (TGF)-B, thereby causing immunosuppression. Moreover, prostate cancer reduced the human leukocyte antigen class I and increased the expression of Fas ligands. These characteristics lead to the suppression of antigen development and induce the apoptosis of immune cells.[1] In addition, the infiltration of T cells in the prostate is more difficult than that in other cancers. Although prostate cancer has several obstacles for boosting the immune response, recent progression of immunotherapy has shown several positive outcomes in prostate cancer.

Cancer vaccines

Sipuleucel-T (Provenge; Dendreon Corp) was the first prostate cancer vaccine approved by the FDA in 2010. It empowers the host to stimulate or recover the immune system for destroying prostate cancer tumor cells. The majority of patients who received sipuleucel-T carried asymptomatic or minimally symptomatic metastatic castration-resistant prostate cancer (mCRPC). For the production of sipuleucel-T vaccine, antigen-presenting cells are purified from patients' serum via leukapheresis and then cultured with PAP-GM-CSF medium. Prostatic acid phosphatase (PAP) is antigen-presented on the surface of prostate cancer. GM-CSF is the coactivator for the stimulation of antigen presentation in the immune system. After these stimulated antigen-presenting cells mature, they are replaced in the body and activate the T cells to recognize and kill prostate cancer cells presenting PAP on the surface.

A phase III clinical trial of sipuleucel-T enrolled 512 mCRPC patients. Two-thirds of all patients received sipuleucel-T and one-third received a placebo, and the outcomes revealed a prolonged overall survival (OS) of 25.8 vs. 21.7 months in patients receiving sipuleucel-T vs. placebo, respectively [hazard ratio (HR) = 0.77, p = 0.08]. However, the time to progression was not statistically different (3.7 vs. 3.6 months, respectively; HR = 0.95, p = 0.63).[3] Fever and flu-like symptoms were the major adverse events in patients receiving sipuleucel-T. Interestingly, sipuleucel-T seemed to improve the OS by mediating tumor growth and not by reducing PSA level and tumor size.

Immune checkpoint inhibitors

Immune checkpoint inhibitors have attracted much attention since recent clinical trials have demonstrated successful outcomes in multiple cancers. Because of increasingly improved OS and urgent demands of cancer patients, the FDA quickly approved these immunotherapy drugs for several cancer treatments, including non-small-cell lung cancer, melanoma, and bladder cancers. The mechanism of immune checkpoint inhibitors is to block the cell signals of immune checkpoint genes, leading to the inhibition of immunosuppression. These then expand particular T-cell clones that can recognize and kill cancer cells. Some researchers have shown that genomic biomarkers can be evaluated for the efficacy of immune checkpoint inhibitors.[4] For examples, cancers carrying higher neoantigens, increased expression of programmed death ligand-1 (PD-L1), and high levels of microsatellite instability have better responses to immune checkpoint inhibitors.

The first FDA-approved immune checkpoint inhibitor is an anti-CTLA-4 monoclonal antibody, ipilimumab. CLTA-4 is a cytotoxic T-lymphocyte-associated

protein 4, which functions as an "off" switch for T-cell proliferation. Ipilimumab inhibits the biological function of CLTA-4 to amplify T cells, which then attack cancer cells. Two clinical trials of anti-CLTA-4 antibodies for mCRPC treatment have shown improved progression-free survival (PFS), but improvement in OS was not so well noted.[5,6]

Another immune checkpoint inhibitor is an anti-PD-1 monoclonal antibody. Cancer cells escape from the immune system by expressing PD-L1, which binds to PD-1 on T cells, causing apoptosis of T cells. Anti-PD-1 monoclonal antibodies that block the interaction between PD-1 and PD-L1 lead to the proliferation of T-cell subgroups that distinguish cancer cells. Two small clinical trials of anti-PD-1 monoclonal antibodies for prostate cancer have been performed. One trial on nivolumab (Bristol-Myers Squibb, New York, NY, USA) showed no obvious responses in OS from 17 patients with mCRPC, although one patient reportedly had decreased PSA levels.[6] The other trial on pembrolizumab (Merck, Kenilworth, NJ, USA) enrolled 23 patients with mCRPC, among whom 13% had a partial response and 39% had a stable condition on cancer progression (KEYNOTE-028).[7] The limited responses to immune checkpoint inhibitors might be due to the low expression of PD-L1 in prostate cancer.[8]

The last potential immunotherapy drug is an indoleamine 2,3-dioxygenase 1 (IDO1) inhibitor. IDO1 is a rate-limiting enzyme in the kynurenine pathway, which converts the amino acid L-tryptophan (Trp) into L-kynurenine (Kyn) for amplifying regulatory T cells and halts the expansion of cytotoxic T cells. IDO1 is highly expressed in several cancers, including prostate cancer. Prostate cancer cells may survive from the immune system by expressing IDO1. A phase II clinical trial of an IDO inhibitor, indoximod, combined with sipuleucel-T in mCRPC began in 2012 and will end in 2018. Patients with mCRPC were provided with indoximod or placebo after receiving sipuleucel-T therapy. A total of 46 patients met inclusion criteria and were separated into two groups, one receiving indoximod (n = 22) and the other receiving placebo (n = 23). The current result has shown no significant difference in the adverse events, PSA progression, and immune responses. However, the median radiographic PFS was 10.3 months in the indoximod group and 4.1 months in the placebo group (p = 0.011), although OS remains under evaluation (NCT01560923).

Adoptive cell therapy

Adoptive cell therapy or chimeric antigen receptor T cells (CAR-T) was first applied for acute lymphoblastic leukemia and demonstrated astonishing results. CAR-T therapy requires the isolation of lymphocytes from patients' peripheral blood. These isolated lymphocytes are then transformed via gene editing to express transgenic antibodies for the recognition of cancer cells. After the expansion of CAR-T cells, patients receive CAR-T cells back for killing cancer cells.[9] Currently, a clinical trial of CAR-T that targets prostate-specific membrane antigen is ongoing. Although there is no conclusion yet, preliminary data have revealed no adverse events and the disease has remained stable for at least 6 months (NCT01140373).

Prospective

The best outcome of immunotherapy requires an immune-favorable microenvironment, including easy infiltration for T-cell migration, more neoantigens for T-cell-identifying cancer cells, and blocking immunosuppression signals for antitumor T-cell expansion.[10] Although prostate cancer has several neoantigens because of its high mutation burdens, the microenvironment is inadequate for the activation of the immune system. Creating a favorable microenvironment for the immune system provides an encouraging approach for immunotherapy in prostate cancer. Combining multiple therapies that simultaneously cause inflammation for T-cell infiltration and mitigate immunosuppression would be promising for the efficacy of immunotherapy in prostate cancer. Hormone therapy has been shown to increase PD-L1 levels and inflammation in prostate cancer. Radiotherapy has been proven to cause inflammation and enhance immune responses to cancer cells. Chemotherapy kills cancer cells and releases cancer antigens. These treatments boost immune responses in tumors and generate an optimal microenvironment for immunotherapy. Some combination strategies are under evaluation, such as enzalutamide (antiandrogens) with pembrolizumab (anti-PD-1 monoclonal antibody; NCT02861573) and Radium-223 (radiopharmaceutical) with atezolizumab (anti-PD-L1 antibody; NCT02814669). Although the outcomes of the mono immunotherapeutic agent in prostate cancer are not as good as expected, ongoing combination strategies

seem to move forward in the correct path. These studies will shed light on immunotherapy revolution in prostate cancer.

Reference

1. Bilusic M, Madan RA, and Gulley JL. Immunotherapy of prostate cancer: Facts and Hopes. Clin Cancer Res. 2017; 15; 23(22): 6764-6770
2. Cancer registry annual report 2015 Taiwan, Health Promotion Administration Ministry of Health and Welfare Taiwan, 2017
3. Kantoff PW, Higano CS, Shore ND, Berger ER, Small EJ, Penson DF, et al. Sipuleucel-T immunotherapy for castration-resistant prostate cancer. N Engl J Med 2010; 363: 411-22.
4. Spencer KR, Wang J, Silk AW, Ganesan S, Kaufman HL, Mehnert JM. Biomarkers for Immunotherapy: Current Developments and Challenges. Am Soc Clin Oncol Educ Book. 2016; 35: e493-503
5. Beer TM, Kwon ED, Drake CG, Fizazi K, Logothetis C, Gravis G, et al. Randomized, Double-Blind, Phase III Trial of Ipilimumab Versus Placebo in Asymptomatic or Minimally Symptomatic Patients With Metastatic Chemotherapy-Naive Castration-Resistant Prostate Cancer. J Clin Oncol 2017; 35: 40-7.
6. Kwon ED, Drake CG, Scher HI, Fizazi K, Bossi A, van den Eertwegh AJ, et al. Ipilimumab versus placebo after radiotherapy in patients with metastatic castration-resistant prostate cancer that had progressed after docetaxel chemotherapy (CA184-043): a multicentre, randomised, double-blind, phase 3 trial. Lancet Oncol 2014; 15: 700-12.
7. Topalian SL, Hodi FS, Brahmer JR, Gettinger SN, Smith DC, McDermott DF, et al. Safety, activity, and immune correlates of anti-PD-1 antibody in cancer. N Engl J Med 2012; 366: 2443-54.
8. Martin AM, Nirschl TR, Nirschl CJ, Francica BJ, Kochel CM, van Bokhoven A, et al. Paucity of PD-L1 expression in prostate cancer: innate and adaptive immune resistance. Prostate Cancer Prostatic Dis 2015; 18: 325-32
9. Hinrichs CS, Rosenberg SA. Exploiting the curative potential of adoptive T-cell therapy for cancer. Immunol Rev 2014; 257: 56-71.
10. Farkona S, Diamandis EP, Blasutig IM, Cancer immunotherapy: the beginning of the end of cancers? BMC Med 2016; 14: 73

免疫療法在攝護腺癌的進展：過去、現在、與未來

歐宴泉[1] 陳鴻霖[2,*]

梧棲童綜合醫療社團法人童綜合醫院 [1]泌尿科 [2]醫學研究部

受文日期：民國 107 年 05 月 30 日；接受刊載：民國 107 年 05 月 30 日

摘要

攝護腺癌是世界上普及率極高的癌症，也是台灣前十大癌症死因的第五名。如何降低攝護腺癌的發生率與死亡率是台灣衛生福利部的首要目標之一。免疫療法近期在癌症領域有許多傑出的臨床成效，促使免疫療法成為癌症治療領域中的焦點，尤其是免疫檢查點抑制劑已然是各大藥廠新藥發展的重要一環。但是因為攝護腺癌的先天特性讓免疫治療的療效並沒有達到預期的效果。本文中，我們回顧過往以及目前免疫療法在轉移性去勢抗性攝護腺癌的臨床試驗，包含攝護腺癌疫苗、免疫檢查點抑制劑與嵌合抗原受體 T 細胞療法。目前這些臨床試驗的結果正反兩面皆有，因此攝護腺癌是否適合免疫療法還在評估，尚未有確論。免疫療法若要在攝護腺癌有所突破，關鍵點在於改變攝護腺癌先天生理上的特性，塑造一個適合活化免疫系統的微型環境，改變微型環境需要組合式治療方案來達成。雖然現在單一免疫療法對於攝護腺癌的成效未振奮人心，但以組合式治療方案來改善適合免疫系統的微型環境，使得免疫療法在攝護腺癌治療上還有許多的未來發展性。

關鍵詞：攝護腺癌、免疫治療、癌症疫苗、免疫檢查點抑制劑、嵌合抗原受體 T 細胞

* 通訊作者：陳鴻霖博士 童綜合醫療社團法人童綜合醫院 43503 臺中市梧棲區臺灣大道八段 699 號

Tungs' Medical Journal 12 (2018) 6-19

Review Article

Non-alcoholic Fatty Liver Disease: A Review for the Pathogenic Mechanism and Management

Jui-Yao Lin[1], Kee-Ching Jeng[2], Pi-Deh Haung[3], Kuang-Ping Peng[1,*]

[1]Departments of Family medicine, [2]Medical Research, and [3]Gastroenterology, Tungs' Taichung MetroHarbor Hospital, Taichung, Taiwan

Received: Nov. 03, 2016; Accepted: Jul. 03, 2017

Abstract

Nonalcoholic fatty liver disease (NAFLD) is the most common chronic liver disease associated with metabolic syndrome worldwide. Patients with NAFLD are typically obese; however, nonobese individuals are also affected. NAFLD can vary from benign macrovesicular hepatic steatosis to more severe nonalcoholic steatohepatitis (NASH), hepatic fibrosis, liver cirrhosis, and hepatocellular carcinoma. Pathogenic mechanisms underlying NAFLD include multiple metabolic factors associated with obesity, insulin resistance, gut microbiota, ceramide, and genetics. Asymptomatic NAFLD can slowly progress to NASH and end-stage liver disease that requires liver transplantation. NAFLD/NASH are diagnosed based on abnormal liver chemistry, imaging studies, and liver biopsy. Fatty liver impairs regeneration and induces secondary replicative pathways, wherein proliferation of hepatic progenitor cells during chronic hepatocyte injury is followed by ductular reaction, leading to periportal fibrogenesis. Therefore, fibrosis score is a useful parameter for evaluating the severity of NASH. Current treatments of NAFLD/NASH include lifestyle modification for weight loss as well as treatment with vitamin E, thioglitazones, the antioxidant silymarin, farnesoid X receptor (FXR) agonists, and antifibrotic antibodies. Gut microbiota play an important role in NAFLD, illustrated by an increase in serum lipopolysaccharide (LPS) and liver Toll-like receptor 4 (TLR4) in animal models of NAFLD, and supplementation with probiotics reduces both indices and improve pathological lesions in these animal models. However, the therapeutic effect of these treatments in NAFLD/NASH await further studies.

Key words: Non-alcoholic fatty liver disease, Non-alcoholic steatohepatitis, Pathogenic mechanism, Treatments

Nonalcoholic fatty liver disease (NAFLD), the most common liver disease globally, is defined as the accumulation of excessive fat in the liver in the absence of excessive alcohol intake or other secondary causes. NAFLD represents a spectrum of hepatic disorders characterized by macrovesicular fatty liver, with histologic presentation ranging from steatosis and nonalcoholic steatohepatitis (NASH) to NAFLD-associated cirrhosis and hepatic cancer[1]. The risk of NAFLD to progress from fatty liver to liver disease with inflammation, fibrogenesis, and cell death renders NAFLD a medical challenge due to the lack of current established therapies. Clinical trials from the last decade did not yield a single intervention that has convincingly improved all important outcomes in all NAFLD patients. Therefore, it is imperative to elucidate the diagnosis, pathology, prevention, and new therapeutic approaches for NASH/NAFLD.

*Correspondence to: Dr. K.P. Peng, Department of Family Medicine, Tungs' Taichung MetroHarbor Hospital, No. 699, Sec. 8, Taiwan Blvd., Wuqi Dist., Taichung City 43503, Taiwan (R.O.C.)

Prevalence of NAFLD

NAFLD can range from asymptomatic nonalcoholic fatty liver (NAFL) to more severe NASH, hepatic fibrosis, liver cirrhosis, and hepatocellular carcinoma[1]. In the United States, the prevalence of NAFLD determined by ultrasonography is 19.0%, corresponding to 28.8 million adults (95% confidence interval [CI] 26.6–31.2)[2]. The global prevalence of NAFLD is 25.24% (95%CI 22.10–28.65), with

the highest prevalence in the Middle East (31.8%) and South America (30.5%) and the lowest in Africa (13.5%)[3].

In Japan, there is an estimated one million patients with NASH [4], whereas in Taiwan, the prevalence of NAFLD ranges from 11.4% to 41% and higher in population subgroups[5]. Although the disease remains largely asymptomatic, it can slowly progress to end-stage liver disease that might require liver transplantation eventually. In this review, the pathogenic mechanism underlying NAFLD/NASH will be discussed first.

Pathogenic mechanisms

Steatosis

The pathogenesis of NAFLD can be explained by the "multiple-hit" theory[6]. The first hit, which is the accumulation of triglycerides (i.e., lipid droplets) within the cytoplasm of hepatocytes (steatosis), is observed in more than 5% of the hepatocytes. This stage of benign hepatic steatosis, which can be attributed to insulin resistance, is reversible and self-limited; however, it renders the liver susceptible to necrosis and inflammatory changes. Liver accumulation of free cholesterol or ceramide is the second hit that leads to increased oxidative stress and subsequent endoplasmic reticulum (ER) stress. Although ER stress response maintains protein homeostasis, delayed or inadequate ER stress response might induce NASH with fat accumulation, insulin resistance, inflammation, apoptosis, and autophagy. Oxidative stress induces peroxidation of cardiolipin which originates from the inner mitochondrial membrane, leading to mitochondrial dysfunction and further generation of reactive oxygen species (ROS) as well as the formation of pro-inflammatory cytokines, apoptosis and gut-derived bacterial endotoxinemia[6,7].

Interference with triglyceride accumulation decreases hepatic steatosis in experimental animals[8]. Diacylglycerol acyl transferases (DGATs) catalyze the final incorporation of fatty acids into triglycerides, and DGAT2 antisense oligonucleotides can inhibit steatosis[8]. However, antisense oligonucleotides treatment also triggers more severe inflammation, oxidative stress, and fibrosis in the treated animals[9]. In contrast, overexpression of hepatic DGAT2 leads to hepatic steatosis in mice without liver injury or insulin resistance[10].

Gut microbiota

The frequency of small intestinal bacterial overgrowth and increased intestinal permeability, which are more frequently observed in patients with NASH and NAFLD than healthy controls[11,12], are potential sources of hepatotoxic oxidative injury. Among NAFLD patients, *Bacteroides* is increased twofold, whereas *Prevotella* is decreased in those with NASH. *Ruminococcus* was reported to be increased twofold in patients with stage 2 or greater fibrosis compared with those at a lower stage of NAFLD[13]. These bacteria generate ethanol and acetaldehyde, latter of which is easily absorbed into the portal blood stream and can initiate histological changes similar to those seen in NAFLD[14]. High concentrations of endogenous alcohol production were reported in humans[13] as well as in animals with intestinal blind-loops[15]. Particularly, patients with a high-carbohydrate diet or obese females with *Candida albicans* overgrowth were shown to have increased breath alcohol level[16,17].

Intestinal bacteria contribute to hepatic injury by releasing endotoxins as well. Rats injected with the endotoxin lipopolysaccharide (LPS) develop steatohepatitis, which can be improved by blocking cytokine response with anti-tumor necrosis factor (TNF-α) antibodies[18,19]. This finding is consistent with those in genetically obese mice with increased intestinal permeability and portal endotoxemia[20,21]. Patients with NAFLD also exhibit significant increases in markers of intestinal permeability and have a higher prevalence of small intestinal bacterial overgrowth[13]. Importantly, these changes correlate with the severity of hepatic steatosis.

Genes

Genetic factors are involved in the third hit of NAFLD pathogenesis. Palatine-like phospholipase 3 (*PNPLA3*), sorting and assembly machinery component 50 homolog (*SAMM50*), and parvin beta genes are important for hepatocyte regeneration[22-24]. Single nucleotide polymorphisms of these genes are associated with increased frequency, more severe histologic changes, and worsened progression of NAFLD. Variants in *PNPLA3* and pregnancy zone protein (*PZP*) genes are independent risk factors for NAFLD. Therefore, along with metabolic factors, genetics play an important role in the development of NAFLD[22-24].

Obesity and insulin resistance

The prevalence of NAFLD is higher in patients with obesity (90%) and type 2 diabetes mellitus (DM; 70%), which correlates with the increasing trend of obesity and metabolic syndrome in the modern world[25]. In Asia, the prevalence of NAFLD ranges from 15% and 30% in the general population and is over 50% in patients with type 2 DM and metabolic syndrome[25]. In the United States, the prevalence of NASH is about 3% but is predicted to be more than 25% in obese individuals[26].

Obesity may lead to insulin resistance and metabolic syndrome and thus is an important risk factor for NAFLD development (Table 1). Metabolic syndrome is defined as impaired glucose tolerance, hypertension, hypertriglyceridemia, low high-density lipoprotein level, and abdominal obesity. The clinical burden of NAFLD is not only confined to liver-related morbidity and mortality; NAFLD affects other organs and regulatory pathways as well[27]. NAFLD increases the risk of diseases related to metabolic syndrome such as type 2 DM, cardiovascular and cardiac diseases, and chronic kidney disease. Although the primary pathology of NAFLD pathology involves hepatic structure and function that causes morbidity and mortality from cirrhosis, liver failure, and hepatocellular carcinoma, majority of the deaths among patients with NAFLD are attributable to cardiovascular disease[27].

Insulin resistance may also be responsible for the development of NAFLD even in nonobese and lean individuals. Insulin resistance in the adipose tissue leads to continued lipolysis, increased plasma free fatty acid (FFA), and FFA influx into the hepatocytes[28]. Other potential risk factors for NAFLD are polycystic ovary syndrome, hypothyroidism, hypofunction of pituitary and sex glands, and sleep apnea [29].

Table 1. Etiology of non-alcoholic fatty liver disease (NAFLD)

Nutritional	**Drugs**
Obesity*	Glucocorticoids
Parenteral nutrition	Tamoxifen
Celiac disease	Amiodarone
Metabolic	Didanosine
Insulin resistance*	Zidovudine
Dyslipidemia*	**Others**
High ceramide production*	Inflammatory bowel disease
Fatty liver of pregnancy	Halogenated hydrocarbons
	Toxic mushrooms

*Most common causes of NAFLD. Adapted from refs [31,32]

Ceramides

According to the multiple-hit model, the pathological feature of the first hit hepatic steatosis includes increased lipolysis in peripheral adipose tissue, which leads to an increased influx of FFAs to the liver[30,31]. These FFAs are converted to various lipids, including triglycerides, diacylglycerol, and sphingolipids, or undergo oxidation in mitochondria, microsomes, or peroxisomes[32]. Ultimately, triglycerides are exported out of the liver as very low-density lipoproteins. However, in the presence of insulin resistance, the hepatic influx of FFAs exceeds the secretion of very low-density lipoproteins or fat oxidation, which ultimately results in increased hepatic levels of lipids including triglycerides and ceramides[32]. This excessive lipid deposition causes lipotoxicity and leads to cell dysfunction and cell death[33]. Hepatic concentrations of saturated fatty acids (i.e., palmitic acid) and mono-unsaturated fatty acids (i.e., oleic acid) were reported to be significantly increased in patients with NAFLD to contribute to the accumulation of ceramides [31,34,35]. Rats on high-saturated fat diet accumulated significant amounts of ceramides and sphingomyelin in the liver and hepatic nuclei[36]. Increased synthesis of ceramides in hepatic nuclei is associated with increased enzymes for ceramide metabolism including sphingomyolinase (SMase) and sphingomyelin synthase[37] (Fig. 1).

Ceramide regulates pro-inflammatory gene expression through the activation of nuclear transcription factor kappa-B (NF-κB) and promotes an inflammatory response [38]. Blocking *de novo* ceramide synthesis using myriocin can reduce macrovesicular lipid accumulation, hepatic triglyceride content, and the expression of suppressor of cytokine signaling 3, a cytokine-mediated gene that is also upregulated in NAFLD[39]. Conversely, ceramide generation in the liver may also be mediated by cytokines such as TNF-α and various associated death ligands (Table 2). Fas ligand (CD95L), a member of the TNF-α receptor family, is involved in caspase-mediated apoptosis and inflammatory pathways[40]. Importantly, there is a decrease in the expression of CD36, a fatty acid transport protein, and liver lipid content including total ceramide level, in *Fas* knockout mice fed on a

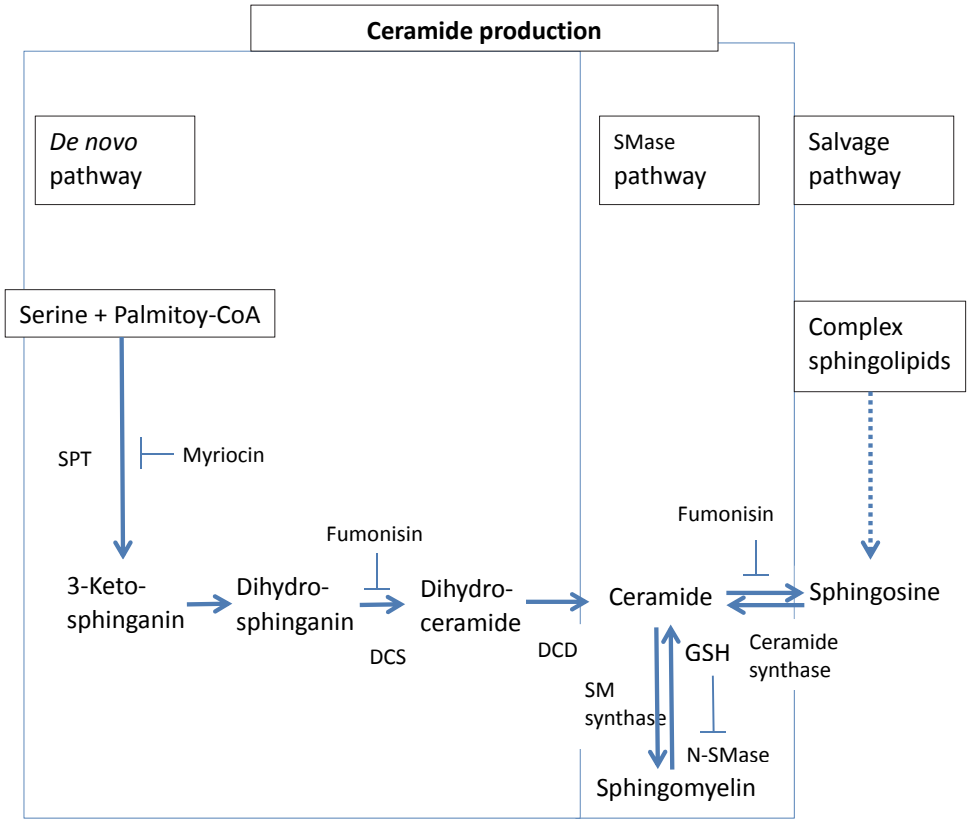

Fig. 1 Ceramide can synthesized by *de novo*, sphingomyelinase (SMase), or salvage pathways. Myriocin inhibits the serine palmitoyltransferase (SPT) enzyme that catalyzes the rate-limiting step in the *de novo* pathway. Fumanisin inhibits dihydroceramide synthase (DCS) and downregulates both the *de novo* and salvage pathways. The antioxidant glutathione (GSH) is known to inhibit dihydroceramide desaturase and neutral SMase (n-SMase) and to reduce ceramide production through the *de novo* and SMase pathways[32].

Table 2. Factors propmote ceramide production and its effects on the pathogenesis of steatosis and steatohepatitis

Effectors of ceramide production
Increased hepatic free fatty acid influx
Increased TNF-α
Decreased adiponectin
Increased IL-1
Production of ROS and oxidative stress
Physiological effects of ceramides
Increased cytokine expression
Insulin resistance
Mitochondrial dysfunction and decreased fat oxidation
Oxidative stress
Triggering of cellular apoptosis
Down-regulation of methionine adenosyltransferase (MAT) 1A expression and decrease in the redox ratio
Increased lipoprotein aggregation

Adapted from refs [32]

high-fat diet[41]. However, the role of ceramides in NASH/NAFLD awaits further investigation. Currently, whether hepatic steatosis in NASH/NAFLD is a direct result of ceramide accumulation in the liver or due to increased ceramide-mediated insulin resistance in adipose tissue that leads to increased plasma FFA and lipotoxicity remains unclear (Fig. 2).

Diagnosis

Most of the patients with NAFLD are asymptomatic and are often diagnosed based on abnormal liver function tests or abnormal imaging findings during evaluation for other reasons[42]. Patients with NASH have mild to moderate elevation (1.5 to 4 fold) of serum levels of alanine aminotransferase (ALT) and aspartate aminotransferase (AST), with greater elevation of ALT than AST (AST/ALT < 1)[43]. However, ALT and AST are not reliable markers of NASH because their levels can remain within normal limits in advanced NAFLD. A recent study showed that among 222 patients, 23% had normal ALT levels, and there

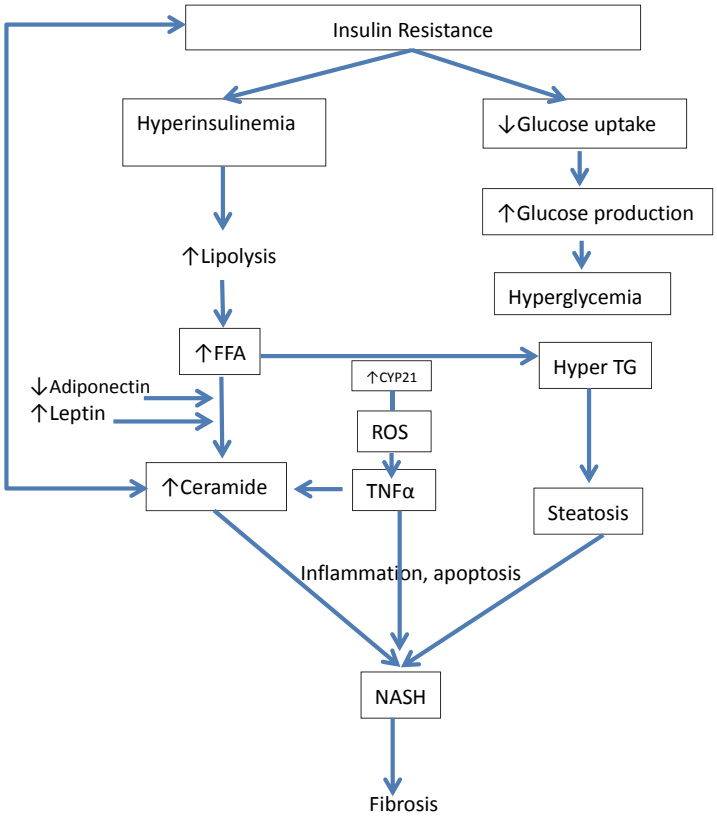

Fig. 2 Current concept of nonalcoholic fatty liver disease (NAFLD) pathogenesis. Obesity-induced insulin resistance initiates hyperinsulinemia and hyperglycemia. Increased free fatty acid (FFA) release due to the lipolysis of adipose tissue may accompany upregulation of pro-inflammatory cytokines, including tumor necrosis factor (TNF)-α and decreased adiponectin. These mediators converge in liver to facilitate ceramide production. Increased ceramide level further promotes hepatic insulin resistance and apoptosis through mitochondrial reactive oxygen species production. Decrease in adiponectin can impair ceramide clearance through conversion to sphingosine 1-phosphate, thus facilitating greater ceramide accumulation within the tissue. Increase in hepatic ceramide further contributes to the progression of steatosis to nonalcoholic steatohepatitis (NASH) and fibrosis[31,32].

was no difference in the rate of advanced fibrosis between those with normal and elevated ALT (26.8% vs. 18.1%, p = 0.19) [44]. Patients with other liver diseases such as viral hepatitis, hemochromatosis, and Wilson's disease have elevated AST and ALT; these diagnoses should be excluded from the differential diagnosis of NAFLD. A thorough history to identify potential causes such as significant alcohol use, starvation, medication use, and pregnancy-related hepatic steatosis is important. Tests for hepatitis A, B, and C virus infections are needed to distinguish those from NAFLD. Whereas polymerase chain reaction for circulating hepatitis C virus RNA is required to rule out hepatitis C [45], hemochromatosis and Wilson's disease are differentiated based on serum levels of ferritin, transferrin, and ceruloplasmin copper levels as well as a 24-hour urinary copper excretion test [46,47].

Transabdominal ultrasound, the most widely used modality for NAFLD detection because of its availability, low cost, and safety, cannot however differentiate NAFLD from simple steatosis, NASH, or hepatic fibrosis. Conversely, liver parenchyma may appear hypodense compared to spleen in a non-contrast computed tomography (CT) scan. Additionally, CT involves ionizing radiation and cannot differentiate different stages of NAFLD. Whereas transabdominal ultrasound is more sensitive than CT in detecting hepatic steatosis[23], magnetic resonance imaging (MRI) is more sensitive than CT for detection of hepatic steatosis based on the signal intensity that is distinct from that of the liver[23].

The gold standard for diagnosis of fatty liver disease is liver biopsy (Table 3). In addition, history is very important in distinguishing between alcoholic and nonalcoholic liver disease[3]. Fatty liver impairs

Table 3. Types of NAFLD by histology and outcome

Category	Histology	Outcome
Type 1	steatosis only	non-progressive
Type 2	steatosis plus lobular inflammation	benign course
Type 3	steatosis, lobular Inflammation and ballooning degeneration	NASH without fibrosis, may progress to cirrhosis
Type 4	steatosis, ballooning degeneration with Mallory bodies and/or fibrosis	NASH, may progress to cirrhosis

Adapted from refs [31]

regeneration and induces a secondary replicative pathway using bipotential, periportal, and hepatic progenitor cells. Hepatic progenitor cells proliferate during chronic hepatocyte injury, followed by ductular reaction, leading to periportal fibrogenesis. Ductular reaction worsens with increasing grade of NASH, portal inflammation, and extent of hepatocyte replicative arrest[48]. Therefore, fibrosis score is useful for evaluation of the severity NASH and is defined as follows: F0, no fibrosis; F1, portal fibrosis without septa; F2, few septa; F3, numerous septa without cirrhosis; and F4, cirrhosis.

Two noninvasive tests for fibrosis are serologic and radiologic tests. Serologic testing, albeit commercially available, cannot fully replace histologic analysis. Conversely, radiologic or ultrasonic measurement of elasticity can be used alone or in combination with serologic testing.

The NAFLD fibrosis score is used to assess the probability of fibrosis in patients with NAFLD. This scoring system consists of six variables: age, body mass index (BMI), blood glucose level, aminotransferase levels, platelet count, and albumin. Fibrosis score can separate NAFLD with and without advanced fibrosis and matches the stage of fibrosis. A high NAFLD fibrosis score cutoff (>0.676) was shown to be associated with advanced fibrosis (F3 to F4) in 82% of the patients with a sensitivity of 43% and specificity of 96%, whereas a low NAFLD fibrosis score cutoff value (<–1.455) had a negative predictive value of 88% with a sensitivity of 77% and a specificity of 71% [49].

Currently, four commercial serum marker systems are available: FibroTest/ FibroSure (Lab Corp), Hepascore (Quest Diagnostics), FibroSpect (Prometheus Corp), and the European Liver Fibrosis Study Group panel[50.33]. However, these tests are not currently available in Taiwan. AST/platelet ratio index can be calculated by routine laboratory tests. These blood tests are moderately useful for identifying clinically significant fibrosis or cirrhosis and can differentiate severe fibrosis (F2–F4) from low fibrosis (F0–F1)[50].

Magnetic resonance elastography (MRE) is performed with MRI[51] and involves placing a probe against the back of the patient. The probe emits low-frequency vibrations that pass through the liver and can be measured by the MRI spin echo sequence. Clinical utility of MRE has been confirmed by a meta-analysis of nine studies consisting of 232 patients with NAFLD that had fibrosis scores (F0/F1/F2/F3/F4) of 33.6%, 32.3%, 10.8%, 12.9%, and 10.4%, respectively. Mean area under the receiver operating characteristic curves (95%CIs) for MRE diagnosis of fibrosis stages F1, F2, F3, and F4 were 0.86 (0.82–0.90), 0.87 (0.82–0.93), 0.90 (0.84–0.94), and 0.91 (0.76–0.95), respectively[51].

Another modality for determination of liver fibrosis is acoustic radiation force impulse (ARFI) elastography developed by Siemens that integrates elastography and conventional B-mode ultrasonography[52]. Target liver area is examined by the image and shear wave speed (SWV, m/s) with the ARFI ultrasound probe which produces short pulses (262 ms at 2.67 MHz). However, ARFI elastography is only modestly accurate for determining fibrosis in NAFLD patients and therefore requires further histopathological assessment to assess the impact of hepatic inflammation and steatosis on SWV values as well as NAFLD fibrosis[53]. The utility of shear-wave elastography, which is currently available for measurement of liver stiffness at our institution, should be evaluated for the assessment of NAFLD fibrosis.

Fibroscan (Echosens, Paris, France) is another noninvasive ultrasound tool to determine liver stiffness[54] that explores a volume of liver parenchyma which can be approximated to a cylinder of 1 cm in diameter and 4 cm in length, 100 times greater than a given biopsy specimen; thus, this approach is a better representative of the entire hepatic parenchyma. Liver stiffness values (i.e., F0 4.4 to F4 36.2 kPa) were shown to be associated with increasing histological severity of hepatic fibrosis[54]. However, certain

conditions such as acute hepatitis, liver congestion, and cardiac failure can cause false high scores; therefore, patients with these conditions should not be evaluated with Fibroscan [55].

Management

Lifestyle modification

NAFLD is associated with obesity and metabolic syndrome; therefore, gradual weight loss is advocated as first-line intervention[3] (Table 4). Medical experts agree that dietary control and exercise are the preferred methods of weight loss[3].

A study reviewing the effect of exercise on 433 adult participants from eight studies[56] reported that the effect of exercise alone, aerobic or resistance-based, on fat mobilization was 30.2%, which could reach to 49.8% with diet and exercise. The study found that there was no difference between aerobic and resistance exercise intervention. Both exercise types reduced intrahepatic triglyceride levels in the absence of significant weight loss. An exercise program combined with dietary intervention should augment the reduction in intrahepatic triglyceride levels and improve glucose control and/or insulin sensitivity[56].

Another report[57] studied 100 obese patients with NASH aged between 35 and 50 years, with BMIs ranging from 30 to 35 kg/m^2. The results showed that moderate aerobic exercise and diet regimen reduced the levels of leptin, TNF-α, interleukin (IL)-6, IL-8, ALT, AST, total cholesterol, low-density lipoprotein, and triglycerides, homeostasis model assessment-insulin resistance index value, and BMI compared with the controls. Therefore, exercise-induced weight loss may modulate insulin resistance, levels of adiponectin, leptin, inflammatory cytokines, and markers of hepatic function in patients with NASH. Furthermore, loss of 7%–10% of body weight can reduce a significant amount of fat in liver and improve steatohepatitis.

Dietary control can achieve remarkable improvement of NASH[58]. A 46-year-old patient with a BMI of 40.7 kg/m^2 who was actively started on a low-calorie diet achieved a dramatic reduction in BMI to 28 kg/m^2 after four years. During the same period, his liver fibrosis as well as inflammation, steatosis, and ballooning degeneration improved, and his NAFLD activity score decreased from 4 to 0. Further evaluation revealed that the composition of fat deposits in

Table 4. Current treatments for NAFLD/NASH

Treatment strategy	Medication/intervention	Improvements
Lifestyle modification	Weight loss (7-10%)	ALT, histology
	Diet alone	ALT, histological markers
	Exercise alone	ALT, insulin, histological markers
	Diet and exercise	ALT, histological markers
	Bariatric surgery	Steatosis histology
Agents for metabolic syndrome		
PPARγ agonists	Thiazolidinediones	ALT, insulin, histology
Insulin sensitizing	Metformin	No additional benefits
GLP-1 R agonists	Incretin mimetics	Histology
Lipid-lowering	Statins	ALT, progression to NASH
Antioxidants	Vitamin (Vit) E	Histological markers in non-diabetic NASH
Anti-inflammatory	Pentoxifylline	ALT, histology
	n-3 PUFA	Steatosis
Probiotics	Lactobacillus	ALT, insulin resistance, anti-inflammatory markers
Hepatoprotective	Ursodeoxycholic acid	ALT, histology
	Sylimarin and Vit E	ALT, histology
Antifibrotic antibody	Simtuzumab	Histology

PPARγ: peroxisome proliferator-activated receptor gamma; GLP-1 R: glucagon-like peptide 1; PUFA: polyunsaturated fatty acids; ALT: alanine aminotransferase

liver tissue changed from macrovesicular to microvesicular droplets and eventually disappeared. Other than adiponectin, levels of all parameters including ALT, insulin resistance, ferritin, leptin, high-sensitivity C-reactive protein, and cytokeratin 18 were decreased with dietary restriction. However, no clear changes were observed in fibrosis markers[58].

Fish oil (n-3 polyunsaturated fatty acid, PUFA) is known to improve the lipid profile and reduce the levels of inflammatory markers[59]; however, more studies are necessary to elucidate its efficacy in metabolic syndrome. Although diet and exercise are superior to insulin sensitizers metformin and rosiglitazone in ALT normalization in NAFLD[60], maintaining body weight is challenging, and patients regain body weight that they had lost, which is associated with recurrence of NAFLD.

Pharmacotherapeutic strategies

Since NAFLD is associated with metabolic syndrome, management of obesity, DM, hypertension, and hyperlipidemia is important for the treatment of NAFLD. Pharmacotherapeutic strategies for NAFLD treatment target five areas: (1) primary metabolic targets; (2) oxidative stress and inflammation; (3) gut microbiota; (4) hepatoprotection; and (5) fibrosis[28, 31] (Table 4).

1. Agents targeting metabolic syndrome

Metformin, an insulin-sensitizing agent, is a first-line antidiabetic agent (1A level of evidence from the Centre for Evidence-Based Medicine [EBM]) that increases insulin sensitivity by upregulating AMP-activated protein kinase, which results in reduction of hepatic glucose production[61]. Currently metformin is not recommended specifically for NAFLD treatment.

Thioglitazones (pioglitazone [EBM level 1B] and rosiglitazone) are agonists of peroxisome proliferator-activated receptor gamma that controls transcription of insulin receptor genes involved in the transport, utilization, and production of glucose and lipids[62]. Thioglitazones redistribute fat from the liver and muscles to the adipose tissue through peroxisome proliferator-activated receptor gamma receptors and act as insulin sensitizers in NAFLD. Pioglitazone was shown to improve serum ALT level, steatosis, and steatohepatitis in nondiabetic patients with NASH but not the histological changes in the Placebo for the Treatment of Nondiabetic Patients with Nonalcoholic Steatohepatitis (PIVENS) trial [63]. However, clinicians should be cautious about the long-term safety and efficacy of thioglitazones, because they cause weight gain and increase the risk of congestive cardiac failure during NASH treatment[3].

L cells of the intestinal mucosa secrete glucagon-like peptide 1 (GLP-1), an incretin hormone secreted after nutrient ingestion[64]. GLP-1 increases insulin secretion by stimulating pancreatic β cells, decreases glucagon secretion, and delays gastric emptying. GLP-1 has a short half-life because of rapid degradation by dipeptidyl-peptidase IV (DPP-IV). In NAFLD patients, hepatic DPP-IV expression and serum DPP-IV activity are significantly higher and correlate with hepatic steatosis. Two GLP-1 receptor agonists, exenatide and liraglutide, are long-acting drugs due to their resistance to DPP-IV activity. Diabetic patients with NAFLD treated with exenatide or the DPP-IV inhibitor sitagliptin exhibited significant decreases in liver fat, transaminase levels, and hepatic steatosis[65,66]. However, further randomized controlled trials are needed to assess the utility and efficacy of incretin-based therapies for NAFLD.

Farnesoid X receptor agonist and others

Abnormal regulation of bile acid homeostasis has emerged as an important mechanism of liver injury. Bile acid homeostasis is critically regulated by farnesoid X receptor (FXR). FXR, which is known to exert tissue-specific effects by regulating bile acid synthesis and transport, also plays an important role in regulating lipid metabolism and suppressing NF-κB-induced inflammatory responses in the liver[67]. The molecular mechanism of FXR-mediated reduction of ceramide production might protect the liver from NAFLD and add a light to the prevention and treatment of NAFLD[68].

Lipid-lowering agents

Statins (EBM level 1B) are currently used as main-line therapies for hyperlipidemia[69]. NAFLD and hyperlipidemia frequently coexist as part of the metabolic syndrome. Statins may cause mild elevation of AST/ALT; however, they were also determined to be safe for patients with chronic liver diseases including NAFLD[69]. One randomized study[70] showed that the statin atorvastatin improved both biochemical and ultrasound evidence of NAFLD. However, there are

currently no randomized controlled studies evaluating the effect of statins on the histologic changes in NAFLD, and statins are not currently recommended for the specific treatment of NAFLD.

A low omega-3 (or n-3) and high omega-6 (n-6) PUFA consumption (EBM level 1B) may lead to an increase in the production of pro-inflammatory arachidonic acid derivatives (prostaglandins) and can impair hepatic lipid metabolism, predisposing to NAFLD[71]. Treatment with omega-3 fatty acids improves hepatic steatosis but not AST/ALT levels, and the optimal dose is currently not known, which requires further randomized controlled trials. At present, omega-3 fatty acid supplementation is not recommended for the treatment of NAFLD.

2. Antioxidants and anti-inflammatory agents

Oxidative stress leading to ER stress is considered as the main mechanism of progression of steatosis to steatohepatitis; thus, vitamin E has an important role as an antioxidant. In the PIVENS trial, the efficacy of vitamin E at 800 units per day was studied in patients with NASH[72]. Vitamin E (EBM level 1B) improves steatosis and steatohepatitis and decreases serum transaminases in nondiabetic patients but does not alleviate fibrosis histologically. Currently, vitamin E is recommended as a first-line drug in nondiabetic individuals with biopsy-proven NASH.

Anti-inflammatory agents

TNF-α activates ROS by lipid peroxidation and promotes necroinflammation, fibrogenesis, hepatic insulin resistance, and apoptosis[73]. Pentoxifylline, a xanthine derivative, can inhibit this inflammatory cytokine and is used in peripheral vascular disease for its ability to promote the relaxation of smooth muscle, flexibility of red blood cells, and deaggregation of platelets. Treatment with pentoxifylline at 400 mg for three times a day over a one-year period improved steatosis and lobular inflammation in a randomized placebo controlled trial without significant effect on ballooning degeneration[74]. Another study with a similar design[75] reported that while it did not improve metabolic outcomes, pentoxifylline reduced transaminase levels, hepatic steatosis, and ballooning degeneration. However, based on a recent review stating the positive effects of pentoxifylline, further studies are warranted to explore its potential therapeutic role in NAFLD.

3. Gut microbiota modifiers

Probiotics

Patients with NAFLD show not only liver pathology but also indications of intestinal permeability and small intestinal bacterial growth[8]. These changes correlated with the severity of hepatic steatosis. A recent animal study corroborated this claim and showed that serum LPS and liver toll-like receptor 4 (TLR4) levels were significantly increased during the progression of NAFLD with the decline of gut flora diversity and colonization resistance[76]. However, probiotic supplementation with live *Bifidobacterium infantis*, *Lactobacillus acidopilus*, and *Bacillus cereus* can improve gut microbiota structure and liver pathology. This effect is due to the reduction in the levels of serum LPS and liver TLR4[77] and may explain the successful outcomes of a small randomized study where supplementation with a tablet containing 500 million *Lactobacillus bulgaricus* and *Streptococcus thermophilus* was reported to improve liver AST levels in patients with NAFLD[78]. Therefore, probiotics may provide a new approach to prevent and treat NAFLD.

4. Hepatoprotective agents

Ursodeoxycholic acid extracted from the bile of certain bears is used as a folk medicine. This compound is also a naturally occurring secondary bile acid in humans that is produced by intestinal bacteria as a metabolic byproduct. Ursodeoxycholic acid has cytoprotective lipid-modifying properties and can reduce serum ALT levels in patients with NAFLD; however, a long-term study failed to show its ability to improve any of the liver histologic findings[79-81]. Therefore, ursodexycholic acid is not considered as a treatment option for NAFLD.

Silymarin is derived from the milk thistle plant (*Silybum marianum*) and has been used for centuries as a natural remedy for diseases of the liver and biliary tract. Silymarin is a potent and selective FXR agonist and maintains a higher plasma high-density lipoprotein cholesterol (HDL-C) and a lower LDL-C level, with no effects on body weight, food intake, or liver transaminase levels in animals[82]. A clinical trial showed that silymarin plus vitamin E, together with a hypocaloric diet, ameliorated hepatic function and the noninvasive NAFLD index[83]. Therefore, silymarin can be used as an alternative therapeutic agent if other drugs fail or as a complementary treatment

associated with other therapeutic regimens.

Orlistat is a reversible enteric and pancreatic lipase inhibitor that promotes fat malabsorption and decreases FFA influx into the liver, leading to weight loss and improved insulin sensitivity. In a randomized trial[84], orlistat was shown to reduce serum ALT and AST levels and hepatic steatosis. Another study demonstrated that treatment with orlistat could significantly reduce weight for more than 9% and improve serum transaminase levels and liver histology regardless of the dose[85]. Orlistat is currently approved for weight loss in obese patients but not recommended solely for the treatment of NAFLD.

5. Antifibrotic antibody

Hepatic fibrosis leads to liver cirrhosis at the advanced stage. Lysyl oxidase-like molecule 2 (LOXL2) can crosslink type 1 collagen and promote fibrosis[86]. Serum LOXL2 level also correlates with the stage of hepatic fibrosis[87]. Therefore, simtuzumab, a humanized antifibrotic monoclonal antibody (IgG4) against LOXL2, may stop the fibrotic process. In a small study[88], patients with liver disease of diverse etiology tolerated simtuzumab treatment well. In multicenter clinical trials, simtuzumab exerted dose-dependent antifibrotic effects and lowered portal pressure in patients with compensated cirrhosis due to NASH. This treatment is effective in patients with advanced hepatic fibrosis but not cirrhosis secondary to NASH[89].

Conclusion

NAFLD is often incidentally detected by abnormal liver function tests. Management of the disease relies on good preventive measures, a better understanding of the underlying mechanisms of the disease, reliable noninvasive diagnostic tests, and effective therapies. Lifestyle modification to achieve targeted weight loss, vitamin E, pioglitazone, FXR agonists, and antifibrotics may be helpful in nondiabetic NASH patients. In addition, a supplementation with probiotics may be included for treatment (Table 4), as they reduces serum LPS and liver TLR-4 levels and improve the pathological changes in animal models of NAFLD. Although metabolic syndrome is important in NAFLD, its heterogenetic pathogenic mechanisms should be emphasized. Therefore, treatment strategies should be individualized further.

References

1. Chalasani N, Younossi Z, Lavine JE, et al. The diagnosis and management of non-alcoholic fatty liver disease: practice Guideline by the American Association for the Study of Liver Diseases, American College of Gastroenterology, and the American Gastroenterological Association. Hepatol 2012; 55: 2005-23.
2. Lazo M, Hernaez R, Eberhardt MS, et al. Prevalence of non-alcoholic fatty liver disease in the United States: the Third National Health and Nutrition Examination Survey, 1988-1994. Am J Epidemiol 2013; 178: 38-45.
3. Younossi ZM, Koenig AB, Abdelatif D, Fazel Y, Henry L, Wymer M. Global epidemiology of nonalcoholic fatty liver disease- Meta-analytic assessment of prevalence, incidence, and outcomes. Hepatol 2016; 64: 73-84.
4. The Japanese Society of Gastroenterology, in: Evidence-based Clinical Practice Guideline for Nonalcoholic Fatty liver Diseases/Nonalcoholic Steatohepatitis 2014, Nankodo Co., Ltd., Tokyo, 2014.
5. Hsu CS, Kao JH. Non-alcoholic fatty liver disease: An emerging liver disease in Taiwan. J Formosan Med Asso 2012; 111: 527-35.
6. Takaki A, Kawai D, Yamamoto K. Molecular mechanisms and new treatment strategies for non-alcoholic steatohepatitis (NASH). Int J Mol Sci 2014; 15: 7352-79.
7. Bozaykut P, Sahin A, Karademir B, Ozer NK. Endoplasmic reticulum stress related molecular mechanisms in nonalcoholic steatohepatitis. Mech Ageing Dev 2016; 157: 17-29.
8. Choi CS, Savage DB, Kulkarni A, et al. Suppression of diacylglycerol acyltransferase-2 (DGAT2), but not DGAT1, with antisense oligonucleotides reverses diet-induced hepatic steatosis and insulin resistance. J Biol Chem 282, 22678-88.
9. Yamaguchi K, Yang L, McCall S, et al. Inhibiting triglyceride synthesis improves hepatic steatosis but exacerbates liver damage and fibrosis in obese mice with nonalcoholic steatohepatitis. Hepatol 2007; 45: 1366-74.
10. Monetti M, Levin MC, Watt MJ, et al. Dissociation of hepatic steatosis and insulin resistance in mice overexpressing DGAT in the liver. Cell Metab 2007; 6: 69-78.
11. Miele L, Valenza V, La Torre G, et al. Increased intestinal permeability and tight junction alterations in nonalcoholic fatty liver disease. Hepatol 2009; 49: 1877-87.
12. Boursier J, Mueller O, Barret M, et al. The severity of nonalcoholic fatty liver disease is associated with gut dysbiosis and shift in the metabolic function of the gut microbiota. Hepatol 2016; 63: 764-75.
13. Cope K, Risby T, Diehl AM. Increased gastrointestinal ethanol production in obese mice: implications for fatty liver disease pathogenesis. Gastroenterol 2000; 119: 1340-7.
14. Mezey E, Imbembo AL, Potter JJ, et al. Endogenous ethanol production and hepatic disease following jejunoileal bypass for morbid obesity. Am J Clin Nutr 1975; 28: 1277-83.
15. Baraona E, Julkunen R, Tannenbaum L, Lieber CS. Role of intestinal bacterial overgrowth in ethanol production and metabolism in rats. Gastroenterol 1986; 90: 103-10.
16. Kaji H, Asanuma Y, Yahara O, et al. Intragastrointestinal alcohol fermentation syndrome: report of two cases and review of the literature. J Forensic Sci Soc 1984; 24: 461-71.

17. Nair S, Cope K, Risby TH, Diehl AM. Obesity and female gender increase breath ethanol concentration: potential implications for the pathogenesis of nonalcoholic steatohepatitis. Am J Gastroenterol 2001; 96: 1200-4.
18. Pappo I, Bercovier H, Berry E, et al: Antitumor necrosis factor antibodies reduce hepatic steatosis during total parenteral nutrition and bowel rest in the rat. JPEN J Parenter Enteral Nutr 1995; 19: 80-2.
19. Kirsch R, Clarkson V, Verdonk RC, et al. Rodent nutritional model of steatohepatitis: effects of endotoxin (lipopolysaccharide) and tumor necrosis factor alpha deficiency. J Gastroenterol Hepatol 2006; 21: 174-82.
20. Brun P, Castagliuolo I, Di Leo V, et al. Increased intestinal permeability in obese mice: new evidence in the pathogenesis of nonalcoholic steatohepatitis. Am J Physiol Gastrointest Liver Physiol 2007; 292: G518.
21. Jin X, Yu CH, Lv GC, Li YM. Increased intestinal permeability in pathogenesis and progress of nonalcoholic steatohepatitis in rats. World J Gastroenterol 2007; 13: 1732-6.
22. Chalasani N, Guo X, Loomba R, et al. Genome-wide association study identifies variants associated with histologic features of nonalcoholic Fatty liver disease. Gastroenterology 2010; 139: 1567-76.
23. Kitamoto T, Kitamoto A, Yoneda M, et al. Genome-wide scan revealed that polymorphisms in the PNPLA3, SAMM50, and PARVB genes are associated with development and progression of nonalcoholic fatty liver disease in Japan. Hum Genet 2013; 132: 783-92.
24. Bhatt SP, Nigam P, Misra A, Guleria R, Pandey RM, Pasha MA. Genetic variation in the patatin-like phospholipase domain-containing protein-3 (PNPLA-3) gene in Asian Indians with nonalcoholic fatty liver disease. Metab Syndr Relat Disord 2013; 11: 329-35.
25. Wong VW. Nonalcoholic fatty liver disease in Asia: a story of growth. J Gastroenterol Hepatol 2013;28:18-23.
26. Vernon G, Baranova A, Younossi ZM. Systematic review: the epidemiology and natural history of non-alcoholic fatty liver disease and non-alcoholic steatohepatitis in adults. Aliment Pharmacol Ther 2011; 34: 274-85.
27. Byrne CD, Targher G. NAFLD: a multisystem disease. J Hepatol 2015; 62(1 Suppl): S47-64.
28. Ahmed M. Non-alcoholic fatty liver disease in 2015. World J Hepatol 2015; 18; 7: 1450-9.
29. Loria P, Carulli L, Bertolotti M, Lonardo A. Endocrine and liver interaction: the role of endocrine pathways in NASH. Nature Rev Gastroenterol Hepatol 2009; 6: 236-47 .
30. Gentile CL, Pagliassotti MJ. The role of fatty acids in the development and progression of nonalcoholic fatty liver disease. J Nutr Biochem 2008; 19: 567-76.
31. Tolman KG, Dalpiaz AS. Treatment of no-alcoholic fatty liver disease. Therapeutics and Clinical Risk Management 2007; 3: 1153-63.
32. Pagadala M, Kasumov T, McCullough AJ, Zein NN, Kirwan J. Role of ceramides in nonalcoholic fatty liver disease. Trends Endocrinol Metab 2012; 23: 365-71.
33. Trauner M, Arrese M, Wagner M. Fatty liver and lipotoxicity. Biochim Biophys Acta 2010; 1801: 299-310.
34. Puri P, Baillie RA, Wiest MM, et al. A lipidomic analysis of nonalcoholic fatty liver disease. Hepatology. 2007; 46: 1081-90.
35. Wei Y, Wang D, Topczewski F, Pagliassotti MJ. Saturated fatty acids induce endoplasmic reticulum stress and apoptosis independently of ceramide in liver cells. Am J Physiol Endocrinol Metab 2006; 291: E275-81.
36. Chocian G, Chabowski A, Zendzian-Piotrowska M, Harasim E, Łukaszuk B, Górski J. High fat diet induces ceramide and sphingomyelin formation in rat›s liver nuclei. Mol Cell Biochem 2010; 340: 125-31.
37. Albi E, Lazzarini R, Viola Magni M. Phosphatidylcholine/sphingomyelin metabolism crosstalk inside the nucleus. Biochem J 2008; 410: 381-9.
38. Summers SA. Ceramides in insulin resistance and lipotoxicity. Prog Lipid Res 2006; 45: 42-72.
39. Yang G, Badeanlou L, Bielawski J, Roberts AJ, Hannun YA, Samad F. Central role of ceramide biosynthesis in body weight regulation, energy metabolism,and the metabolic syndrome. Am J Physiol Endocrinol Metab 2009; 297: E211-24.
40. Comi C. Fas-mediated T-cell apoptosis in chronic inflammatory demyelinating polyneuropathy. J Peripher Nerv Syst 2011; 16(Suppl 1): 45-7.
41. Wueest S, Rapold RA, Schumann DM, et al. Deletion of Fas in adipocytes relieves adipose tissue inflammation and hepatic manifestations of obesity in mice. J Clin Invest 2010; 120: 191-202.
42. Choudhury J, Sanyal AJ. Clinical aspects of fatty liver disease. Semin Liver Dis 2004; 24: 349-62.
43. Armstrong MJ, Houlihan DD, Bentham L, et al. Presence and severity of non-alcoholic fatty liver disease in a large prospective primary care cohort. J Hepatol 2012; 56: 234-40.
44. Verma S, Jensen D, Hart J, Mohanty SR. Predictive value of ALT levels for non-alcoholic steatohepatitis (NASH) and advanced fibrosis in non-alcoholic fatty liver disease (NAFLD). Liver Int 2013; 33: 1398-405.
45. Recommendations for Testing, Managing, and Treating Hepatitis C. Joint panel from the American Association of the Study of Liver Diseases and the Infectious Diseases Society of America. http://www.hcvguidelines.org/ Accessed on August 01, 2016.
46. Brewer GJ, Yuzbasiyan-Gurkan V.Wilson disease. Medicine 1992; 71: 139-64.
47. Chalasani N, Younossi Z, Lavine JE, et al. The diagnosis and management of non-alcoholic fatty liver disease: practice guideline by the American Gastroenterological Association, American Association for the Study of Liver Diseases, and American College of Gastroenterology. Gastroenterol 2012; 142: 1592-609.
48. Richardson MM, Jonsson JR, Powell EE, et al. Progressive fibrosis in nonalcoholic steatohepatitis: association with altered regeneration and a ductular reaction. Gastroenterol 2007; 133: 80-90.
49. Angulo P, Hui JM, Marchesini G, et al. The NAFLD fibrosis score: a noninvasive system that identifies liver fibrosis in patients with NAFLD. Hepatol 2007; 45: 846-54.
50. Chou R, Wasson N. Blood tests to diagnose fibrosis or cirrhosis in patients with chronic hepatitis C virus infection: a systematic review. Ann Intern Med 2013; 158: 807-20.
51. Singh S, Venkatesh SK, Loomba R, et al. Magnetic resonance elastography for staging liver fibrosis in non-alcoholic fatty liver disease: a diagnostic accuracy systematic review and individual participant data pooled analysis. Eur Radiol 2016; 26: 1431-40.
52. De Robertis R, D'Onofrio M, Demozzi E, Crosara S, Canestrini S, Mucelli RP. Noninvasive diagnosis of cirrhosis: A review of different imaging modalities. World J Gastroenterol 2014; 20: 7231.
53. Liu H, Fu J, Hong R, Liu L, Li F. Acoustic radiation force

impulse elastography for the non-invasive evaluation of hepatic fibrosis in non-alcoholic fatty liver disease patients: a systematic review & meta-analysis. PLoS One 2015; 10: e0127782.
54. Yoneda M, Fujita K, Inamori M, Nakajima A, Yoneda M, Tamano M, Hiraishi H. Transient elastography in patients with non-alcoholic fatty liver disease (NAFLD). Gut 2007; 56: 1330-1.
55. Al-Ghamdi AS. Fibroscan®: A noninvasive test of liver fibrosis assessment. Saudi J Gastroenterol 2007; 13: 147-9.
56. Golabi P, Locklear CT, Austin P, Afdhal S, Byrns M, Gerber L, Younossi ZM.Effectiveness of exercise in hepatic fat mobilization in non-alcoholic fatty liver disease: Systematic review. World J Gastroenterol 2016; 22: 6318-27.
57. Abd El-Kader SM, Al-Shreef FM, Al-Jiffri OH. Biochemical parameters response to weight loss in patients with non-alcoholic steatohepatitis. Afr Health Sci 2016; 16: 242-9.
58. Kawanaka M, Nouso K, Yano S, Nakamura J, Nishino K, Suehiro M, Kawamoto H. Casereport of diet-related improvements of non-alcoholic steatohepatitis evaluated by four consecutive liver biopsies. Hepatol Res 2016 Jun 29. Doi:10.1111/hepr.12768.
59. Al-Gayyar MM, Shams ME, Barakat EA. Fish oil improves lipid metabolism and ameliorates inflammation in patients with metabolic syndrome: impact of nonalcoholic fatty liver disease. Pharm Biol 2012; 50: 297-303.
60. Akyüz F, Demir K, Ozdil S, et al. The effects of rosiglitazone, metformin, and diet with exercise in nonalcoholic fatty liver disease. Dig Dis Sci 2007; 52: 2359-67.
61. Ismail-Beigi F. Clinical practice. Glycemic management of type 2 diabetes mellitus. N Engl J Med 2012; 366: 1319-27.
62. Mehta SR. Advances in the treatment of nonalcoholic fatty liver disease. Ther Adv Endocrinol Metab 2010; 1: 101-15.
63. Chalasani NP, Sanyal AJ, Kowdley KV, et al. Pioglitazone versus vitamin E versus placebo for the treatment of non-diabetic patients with non-alcoholic steatohepatitis: PIVENS trial design. Contemp Clin Trials 2009; 30: 88-96.
64. Tushuizen ME, Bunck MC, Pouwels PJ, van Waesberghe JH, Diamant M, Heine RJ. Incretin mimetics as a novel therapeutic option for hepatic steatosis. Liver Int 2006; 26: 1015-7.
65. Iwasaki T, Yoneda M, Inamori M, et al. Sitagliptin as a novel treatment agent for non-alcoholic Fatty liver disease patients with type 2 diabetes mellitus. Hepatogastroenteral 2011; 58: 2103-5.
66. Itou M, Kawaguchi T, Taniguchi E, Oriishi T, Sata M. Dipeptidyl peptidase IV inhibitor improves insulin resistance and steatosis in a refractory nonalcoholic fatty liver disease patient: A case report. Case Rep Gastroenterol 2012; 6: 538-44.
67. Wang YD, Chen WD, Wang MH, Yu D, Forman BM, Huang WD. Farnesoid X receptor antagonizes nuclear factor κB in hepatic inflammatory response. Hepatol 2008; 48: 1632-43.
68. Jiang CT, Xie C, Li F, Zhang LM, Nichols RG, Krausz KW. Intestinal farnesoid X receptor signaling promotes nonalcoholic fatty liver disease. J Clin Invest 2015; 125: 386-402.
69. Nseir W, Mahamid M. Statins in nonalcoholic fatty liver disease and steatohepatitis: updated review. Curr Atheroscler Rep 2013; 15: 305.
70. Athyros VG, Mikhailidis DP, Didangelos TP, et al. Effect of multifactorial treatment on non-alcoholic fatty liver disease in metabolic syndrome: a randomised study. Curr Med Res Opin 2006; 22: 873-83.
71. Di Minno MN, Russolillo A, Lupoli R, Ambrosino P, Di Minno A, Tarantino G. Omega-3 fatty acids for the treatment of non-alcoholic fatty liver disease. World J Gastroenterol 2012; 18: 5839-47.
72. Sanyal AJ, Chalasani N, Kowdley KV, et al. Pioglitazone, vitamin E, or placebo for nonalcoholic steatohepatitis. N Engl J Med 2010; 362: 1675-85.
73. Pessayre D, B. Fromenty B, Mansouri A. Mitochondrial injury in steatohepatitis. Eur J Gastroenterol Hepatol 2004; 16: 1095-105.
74. Zein CO, Yerian LM, Gogate P, et al. Pentoxifylline improves nonalcoholic steatohepatitis: a randomized placebo-controlled trial. Hepatol 2011; 54: 1610-9.
75. Van Wagner LB, Koppe SW, Brunt EM, et al. Pentoxifylline for the treatment of non-alcoholic steatohepatitis: a randomized controlled trial. Ann Hepatol 2013; 10: 277-86.
76. Xue L, He J, Gao N, et al. Probiotics may delay the progression of nonalcoholic fatty liver disease by restoring the gut microbiota structure and improving intestinal endotoxemia. Sci Rep 2017; 7: 45176.
77. Aller RD, De Luis DA, Izaola O, et al. The effect of a probiotic on liver aminotranspherases in nonalcoholic fatty liver disease patients: a double blind randomized clinical-trial. Eur Rev Med Pharmacol Sci 2011; 15: 1090-5.
78. Dufour JF, Oneta CM, Gonvers JJ, et al: Randomized placebo-controlled trial of ursodeoxycholic acid with vitamin e in nonalcoholic steatohepatitis. Clin Gastroenterol Hepatol 2006; 4: 1537-43.
79. Leuschner UF, Lindenthal B, Herrmann G, et al. High-dose ursodeoxycholic acid therapy for nonalcoholic steatohepatitis: a double-blind, randomized, placebo-controlled trial. Hepatol 2010; 52: 472-9.
80. Lindor KD, Kowdley KV, Heathcote EJ, et al. Ursodeoxycholic acid for treatment of nonalcoholic steatohepatitis: results of a randomized trial. Hepatol 2004; 39: 770-8.
81. Gu M, Zhao P, Huang J, et al. Silymarin ameliorates metabolic dysfunction associated with diet-induced obesity via activation of Farnesyl X receptor. Front Pharmacol 2016; 7: 345.
82. Aller R, Izaola O, Gómez S, et al. Effect of silymarin plus vitamin E in patients with non-alcoholic fatty liver disease. A randomized clinical pilot study. Eur Rev Med Pharmacol Sci 2015; 19: 3118-24.
83. Ismail-Beigi F. Clinical practice. Glycemic management of type 2 diabetes mellitus. N Engl J Med 2012; 366: 1319-27.
84. Shields WW, Thompson KE, Grice GA, Harrison SA, Coyle WJ. The effect of metformin and standard therapy versus standard therapy alone in nondiabetic patients with insulin resistance and nonalcoholic steatohepatitis (NASH): a pilot trial. Therap Adv Gastroenterol 2009; 2: 157-63.
85. Mehal WZ, Iredale J, Friedman SL. Scraping fibrosis: expressway to the core of fibrosis. Nat Med 2011; 17: 552-3.
86. Murawaki Y, Kusakabe Y, Hirayama C. Serum lysyl oxidase activity in chronic liver disease in comparison with serum levels of prolyl hydroxylase and laminin. Hepatol 1991; 14: 1167-73.
87. Talal AH, Feron-Rigodon M, Madere J, Subramanian GM, Bornstein JD. 1319 Simutuzumab, an antifibrotic monoclonal antibody against Lysyl Oxidase-Like 2(LOXL2)

enzyme, appears safe and well tolerated in patients with liver disease of diverse etiology (Abstract) J Hepatol 2013; 58 Suppl 1: S532.
88. Gilead Sciences. In: Data supporting the development of three investigational agents for the treatment of nonalcoholic steatohepatitis (NASH) and primary sclerosing cholangitis (PSC). The International Liver Congress 2016 in Barcelona, Spain.
89. Hossain N, Pushpjeet Kanwar P, and Smruti R. Mohanty SR. A comprehensive updated review of pharmaceutical and nonpharmaceutical treatment for NAFLD. Gastroenterol Res Pract 2016; 2016: 7109270.

非酒精性脂肪肝病：致病機轉及治療回顧

林瑞瑤[1] 鄭啟清[2] 黃彼得[3] 彭洸萍[1,*]

童綜合醫療社團法人童綜合醫院 [1]家醫部 [2]醫研部 [3]胃腸肝膽科

受文日期：民國 105 年 11 月 03 日；接受刊載：民國 106 年 07 月 03 日

摘要

非酒精性脂肪肝病 (NAFLD) 是與代謝癥候症相關的最常見慢性肝病，普遍見於全世界。雖然脂肪肝病人中，普遍是屬過度肥胖，但亦有非肥胖者。NAFLD 依照其嚴重程度可分為脂肪肝、脂肪性肝炎 (non-alcoholic steatohepatitis，NASH)、肝纖維化、肝硬化、肝癌。其致病機轉包括代謝相關的體重過重、糖尿病、神經醯胺 (ceramide) 過度產生、腸道細菌及基因等。無症狀的脂肪肝會慢慢形成脂肪肝炎，導致肝病末期，需要移植肝臟的治療。診斷脂肪肝病需做肝功能生化檢查、影像檢查及取肝生檢體切片。由於脂肪肝阻擾再生功能，引發肝前驅細胞增生反應，也導致門脈纖維化的反應，因此肝切片纖維化指數，可以評估脂肪性肝炎 NASH 的嚴重度。目前治療 NAFLD/NASH 方法，包括調整生活習慣、控制體重、補充維生素 E、降血脂藥、降血糖藥、降膽汁藥、抗纖維抗體等。由於腸道細菌是致病的關鍵原因之一以及動物研究證實 NAFLD 嚴重度與血液中的內毒素及肝臟鐸類受體 TLR-4 的表現增高有關，補充益生菌不但可降低這兩項指標，還能改善脂肪肝的病變。然而還需繼續深入研究，這些新的方法是否能真正有效的改善脂肪肝病變。

關鍵詞：非酒精性脂肪肝病、脂肪性肝炎、病因、治療

* 通訊作者：彭洸萍醫師 童綜合醫療社團法人童綜合醫院 家醫部 43503 臺中市梧棲區臺灣大道八段 699 號

Tungs' Medical Journal 12 (2018) 20-29

Original Article

The Impact of Brain Magnetic Resonance Image Analysis via Independent Component Analysis in Conjunction with Skull Stripping

San-Kan Lee[1,2,3], Shih-Wei Wang[4], Yung-Chieh Chang[3,4], Jyh-Wen Chai[3,5], Clayton Chi-Chang Chen[3], Yi-Ying Wu[3], Chu-Jing Sung[6], Wen-Hsien Chen[3], Hung-Chieh Chen[3], Ching-Wen Yang[7], Hsian-Min Chen[6,8,*], Yen-Chieh Ouyang[4], Chein-I Chang[9]

[1]President Office, Tungs' Taichung MetroHarbor Hospital, Taichung, Taiwan
[2]Medical Consultant, [3]Department of Radiology, [6]Center for QUantitative Imaging in Medicine (CQUIM), Department of Medical Research, [7]Computer Center, Taichung Veterans General Hospital, Taichung, Taiwan
[4]Department of Electrical Engineering, National Chung Hsing University, Taichung, Taiwan
[5]Section of Radiology, College of Medicine, China Medical University, Taichung, Taiwan
[8]Department of Biomedical Engineering, Hungkuang University, Taichung, Taiwan
[9]Remote Sensing Signal and Image Processing Laboratory, Department of Computer Science and Electrical Engineering, University of Maryland, Baltimore County, Baltimore, MD 21250, USA

Received: Jan. 05, 2017; Accepted: May. 26, 2017

Abstract

Background and purpose: Lately, independent component analysis (ICA) has garnered considerable attention in magnetic resonance imaging (MRI) because of its ability to offer valuable clinical information in medical diagnosis. However, the source separation ability of ICA-based approaches is substantially limited by the two major issues, the lack of adequate image sequences used to acquire MR images to implement the ICA and brain skull interference that can markedly impede the MR image analysis. By developing two approaches to address and resolve these issues, this study aims to investigate whether pre-processing or post-processing, which separates the skull and non-brain intracranial tissue from MR images (skull stripping [SS]), improves the performance of the ICA in conjunction with support vector machine (SVM).

Methods: We introduced two processes, SS and SVM, in conjunction with the ICA (ICA+SVM). While SS removed the skull interference, SVM resolved the dilemma caused by inadequate independent components. Besides, we evaluated the sensitivity, specificity, accuracy, and Tanimoto index (TI) to statistically assess the results of the cerebrospinal fluid (CSF), gray matter (GM), and white matter (WM) with the ground truth data of the synthetic brain images.

Results: The average sensitivity, specificity, accuracy, and TI of the CSF, GM, and WM classification of synthetic data were 0.90, 0.98, 0.97, and 0.80, respectively, using the ICA conjunction with the SVM method, followed by SS, which was higher than that in other experiments.

Conclusion: This study suggests that that SS after ICA+SVM could remove the non-brain tissue to offer excellent results.

Keywords: Independent component analysis (ICA), Magnetic resonance (MR) analysis, Skull stripping, Support vector machine (SVM)

*Correspondence to: Hsian-Min Chen, Center for QUantitative Imaging in Medicine (CQUIM), Department of Medical Research, Taichung Veterans General Hospital, No. 1650 Taiwan Boulevard Sec. 4, Taichung, 40705, Taiwan (R.O.C.)

Introduction

In recent years, independent component analysis (ICA) has witnessed widespread utility in functional

magnetic resonance imaging (fMRI)[1-4]. However, its applications to MRI did not gain similar momentum as fMRI until recently when Nakai et al. applied the ICA for contrast enhancement of the gray matter (GM) and white matter (WM) in MR image analysis[5]. The primary reason for this differential utility of the ICA between fMRI and MRI is that these two ICA applications differ entirely because of the use of the mixing matrix by the ICA for signal source separation and one cannot be directly applied to the other. As samples for fMRI are collected along a temporal sequence with the number of samples, denoted by *L*, typically higher than the number of signal sources to be separated, denoted by *p*, the ICA implemented in fMRI is, in fact, undercomplete (UC) as ICA underrepresents a mixed model (UC-ICA). Thus, the ICA aims to resolve an overdetermined system with *L* equations (specified by the number of samples) and *p* unknowns (represented by signal sources to be separated). Regrettably, Nakai et al. overlooked this issue by assuming that the number of sensors (*L*) is more than or equal to the number of sources (*p*) where the number of sensors corresponds to the combinations of acquisition parameters echo time (TE) and repetition time (TR), and a signal source is signified by a tissue cluster characterized by a unique combination of T1 and T2 relaxation times.

The use of random initial projection vectors by the ICA to produce independent components (ICs) is another crucial issue not addressed by Nakai et al. The issue with this random approach is that the final sets of projection vectors produced by two distinct random initial projection vectors are typically different. Thus, such serious inconsistency undermines the repeatability of the ICA, thereby making it unstable.

Of the two issues mentioned, an inadequate number of MR images and inconsistency in ICA results, the former triggers the latter. Precisely, if there were more signal sources than MR images, at least, two or more signal sources will be forced to be blended into one single IC. Thus, this paper develops two approaches to address and resolve these issues.

The first approach comprises a process of skull stripping (SS) in combination with the ICA to remove the skull and background noise before the MR image analysis. Apparently, the removal of the skull and background noise offers two benefits as follows: (a) no ICs are required to accommodate these signal sources, thereby reducing the number of ICs required for the MR image analysis; (b) reducing the misinterpretation caused by these signal sources to augment the MR image analysis.

The second approach comprises the inclusion of the support vector machine (SVM) classifier as a follow-up process of the ICA to mitigate inconsistent results of the ICA. As the GM, WM, and cerebrospinal fluid (CSF) are of substantial interest in the MR image analysis, three ICs are adequate for their classification. Although these three MR substances could be randomly classified by only three ICs resulting from the use of random initial conditions, their classification results are consistent because when a specific MR substance is classified, all other signal sources are annihilated and so is its inconsistency. Notably, the proposed approaches illustrated with experiments using synthetic images are available on the website (www.bic.mni.mcgill.ca/brainweb/).

Hence, by developing two approaches to address and resolve these issues, this study aims to investigate whether pre-processing or post-processing, which separates the skull and non-brain intracranial tissue from MR images (SS), improves the performance of the ICA in conjunction with SVM.

Materials and Methods

Synthetic Brain MRI Data

For experiments in this study, we used the axial T1-weighted, T2-weighted, and proton density MR brain images (with 5-mm section thickness, 0% noise, and 0% intensity non-uniformity) simulated by the MRI simulator of McGill University (Montreal, Canada; www.bic.mni.mcgill.ca/brainweb/)[6].

ICA

The ICA is based on the assumption that data are linearly mixed by a set of separate statistically independent unknown signal sources by which these signal sources could be used to unmix MR images consistent with the criterion of mutual information. Precisely, let $\mathbf{x}$ be a linearly mixed signal source vector expressed by

$$\mathbf{x} = \mathbf{A}\mathbf{s} \tag{1}$$

where $\mathbf{A}$ is an unknown $L \times p$ mixing matrix and $\mathbf{s} = (s_1, s_2, \ldots, s_p)^T$ is also an unknown p-dimensional signal source vector that needs to be separated. The

ICA aims to process the observed mixed signal source $\mathbf{x}$ in Eq. (1) and determine an unmixing matrix $\mathbf{W}$ so that the *p* unknown signal sources in the signal source vector $\mathbf{s}$ could be separated by an unmixing equation [1,7,8] given by the following:

$$\mathbf{s} = \mathbf{W}\mathbf{x} \tag{2}$$

Despite establishing its practicality in several applications, the ICA cannot be blindly applied without extra care. In particular, MRI is known to overlook several critical issues, one of which is the mixing matrix $\mathbf{A}$ used in the fMRI and MRI analyses. When applying the ICA to fMRI, the signal sources are one-dimensional (1D), and the used ICA is typically UC where the number of observations (*L*) of the mixing matrix $\mathbf{A}$ in Eq. (1) is always higher than the number of signal sources (*p*) to be unmixed, i.e., $L > p$. In this case, no solutions exist for Eq. (1). Thus, a general approach to mitigate this dilemma is to use the dimensionality reduction, such as the principal component analysis, as a pre-processing step to reduce *L* to *p* to create the mixing matrix $\mathbf{A}$ as a square matrix. Conversely, if the ICA is applied as multispectral images to MR images, the signal sources to be unmixed are 2D rather than 1D signals considered in fMRI. Thus, the resulting ICA is, indeed, overcomplete (OC) as the number of multispectral MR images (*L*) used in the mixing matrix $\mathbf{A}$ is smaller than the number of signal signals (*p*), i.e., $L < p$, wherein one single IC must be used to incorporate multiple signal sources because of the lack of data dimensionality. Hence, various problems that are never encountered in the UC-ICA, such as the ICA used in fMRI, become chief issues in the OC-ICA. For instance, in MRI, the data dimensionality of *L* used in the mixing matrix $\mathbf{A}$ signifies the number of multispectral MR band images that are ascertained by pulse sequences used for the MRI acquisition such as T1, PD, T2, and the number of signal sources (*p*) used in the $\mathbf{A}$ suggests the number of brain tissue substances of interest such as the GM, WM, and CSF.

SS

Our extensive experiments demonstrated that the brain skull is a significant signal source that appears in approximately every single IC generated by the ICA with variable levels of energy strength. Thus, if the brain skull could efficiently be segmented from MR images before the ICA implementation, its interfering effect on ICs could be either minimized or eliminated to augment the ability of the ICA unmixing. Recently developed watershed-based algorithms for SS [9-11] could be used to attain our objective in this study.

Figure 1 illustrates how SS using a watershed-based algorithm [9-11] is used to process a brain image. First, construct a 3D image intensity histogram, as shown in Fig. 1(b), of an original gray level image shown in Fig. 1(a) where the altitude of a pixel represents its gray level value. Then, implement a watershed-based algorithm [9-11] that classifies image pixels into basins where the regions circumscribed by red curves (Fig. 1(c)) are basins segmented by the watershed-based processing. Figure 1(d) presents the result after the merging process. After that, the basin located at the center is selected (Fig. 1(d)) because the brain tissue is located at the center of a brain MR image. Finally, the image (Fig. 1(d)) is used for SS, and the resulting skull-stripped brain image is further smoothed by morphological processing (Fig. 1(e)).

SVM

The SVM finds a broad application in pattern classification and analysis[12] and is primarily developed as a binary classifier that determines an optimal hyperplane, which separates two classes of training samples (support vectors) as farther as possible by maximizing the margin of separation between classes away from the hyperplane. Unlike most classifiers, the SVM uses and includes only a few so-called "confusing data" samples, referred to as slack variables in its optimization problems, to maximize the margin of separation among these samples. Furthermore, it uses a nonlinear kernel to map the original data space into a higher dimensional space to resolve the linear inseparability issue.

Based on the statistical learning theory, Vapnik was the first to envision the SVM[13]. Consider a two-category classification problem with a given set of training data $\{(\mathbf{r}_i, d_i)\}_{i=1}^n$ where $\{\mathbf{r}_i\}_{i=1}^n$ are *n* samples with their related binary decisions $\{d_i\}_{i=1}^n$ specified by either +1 or –1. Let us assume that the SVM is specified by a linear discriminate function $g(\mathbf{r}) = \mathbf{w}^T\mathbf{r} + b$ where $\mathbf{w}$ is a weight vector and *b* is a bias. Precisely, given a set of training data, $\{(\mathbf{r}_i, d_i)\}_{i=1}^n$, the SVM finds a weight vector $\mathbf{w}$ and bias *b* that satisfy

$$d_i = \begin{cases} +1; \text{ if } \mathbf{w}^T\mathbf{r}_i + b \geq 0 \\ -1; \text{ if } \mathbf{w}^T\mathbf{r}_i + b < 0 \end{cases} \tag{3}$$

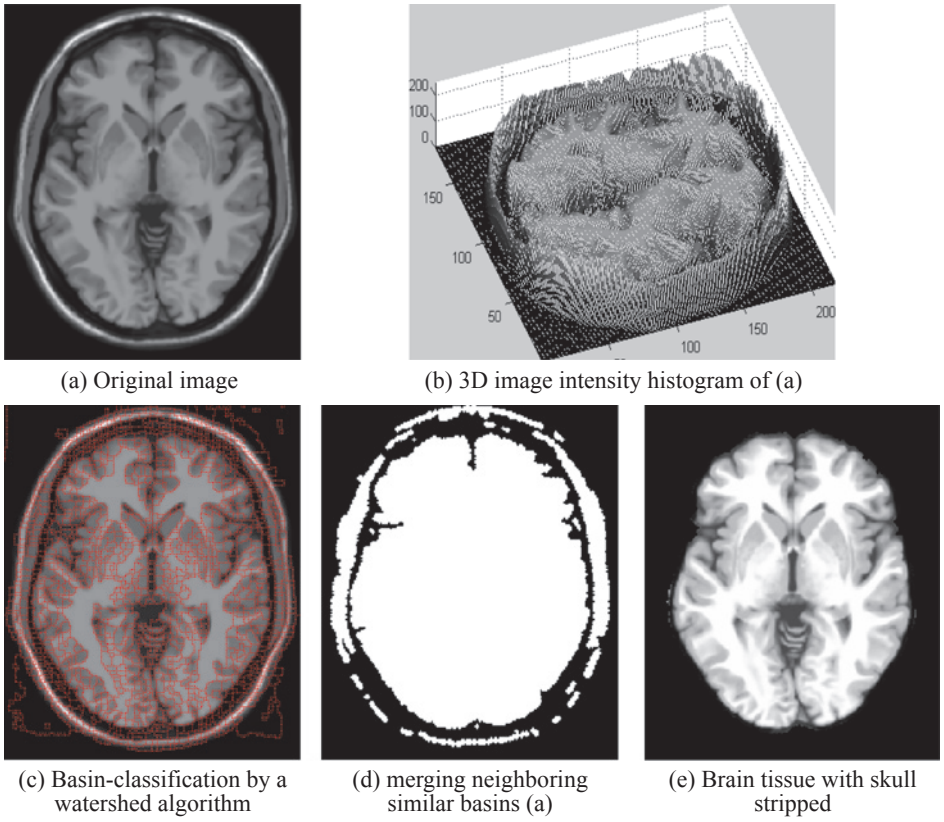

(a) Original image (b) 3D image intensity histogram of (a)

(c) Basin-classification by a watershed algorithm (d) merging neighboring similar basins (a) (e) Brain tissue with skull stripped

Fig. 1 An illustration of SS processing of a brain image using a watershed-based algorithm.

and maximize the margin of separation defined by the distance between a hyperplane and closest data samples. Specifically, Eq. (3) could be re-derived by incorporating its binary decision into the discriminant function as follows:

$$d_i(\mathbf{w}^T\mathbf{r}_i + b) \geq 1 \text{ for } 1 \leq i \leq n \quad (4)$$

For a linearly separable problem, the SVM attempts to position a class boundary so that the margin from the nearest example is maximized. Based on Eq. (4) the distance ρ between a sample vector $\mathbf{r}$ and its projected vector on the hyperplane $g(\mathbf{r}) = \mathbf{w}^T\mathbf{r} + b = 0$ is specified by $\rho = g(\mathbf{r}) / \| \mathbf{w} \|$ with $\mathbf{w}$ the normal vector of the hyperplane. Since $g(\mathbf{r})$ takes only +1 or –1, the distance ρ is then defined by

$$\rho = \begin{cases} 1/\| \mathbf{w} \| \text{ if } d_i = +1 \\ -1/\| \mathbf{w} \| \text{ if } d_i = -1 \end{cases} \quad (5)$$

Using Eq. (5), we defined the margin of separation between two classes, signified by ρ as $\rho = 2 / \| \mathbf{w} \|$. By Eqs. (3)–(5), the SVM defined an optimal weight vector $\mathbf{w}$ minimizing

$$\Phi(\mathbf{w}) = (1/2)\mathbf{w}^T\mathbf{w} = (1/2) \| \mathbf{w} \|^2 \quad (6)$$

subject to constraints specified in Eq. (4).

In addition, an optimal solution to the above optimization problem is provided by

$$\mathbf{w}^{\text{SVM}} = \sum_{i=1}^{n} \alpha_i^{\text{SVM}} d_i \mathbf{r}_i \quad (7)$$

$$1 = d_s = (\mathbf{w}^{\text{SVM}})^T \mathbf{r} \ + b \Rightarrow b = 1 - (\mathbf{w}^{\text{SVM}})^T \mathbf{r}^s \quad (8)$$

where $\mathbf{r}^s$ is the support vector on the hyperplane with its decision $d_s = +1$.

Further details about the SVM are available elsewhere[13].

Evaluation methods

Apparently, the sensitivity, specificity, and accuracy are three commonly used criteria for the medical diagnosis[14]. The formulas are defined by Eqs. (9)-(11).

$$\textbf{Sensitivity} = \frac{\textbf{TP}}{\textbf{TP} + \textbf{TN}} \quad (9)$$

$$\textbf{Specificity} = \frac{\textbf{TN}}{\textbf{TN} + \textbf{FP}} \quad (10)$$

$$\mathbf{Accuracy} = \frac{\mathbf{TP} + \mathbf{TN}}{\mathbf{TP} + \mathbf{FP} + \mathbf{TN} + \mathbf{FN}} \tag{11}$$

where **TP**, **TN**, **FN**, and **FP** are true positives, true negatives, false negatives, and false positives, respectively.

Besides, another useful measure for quantitative study and analysis is the Tanimoto index (TI), which was developed by Tanimoto[14] and used for multispectral MR images, defined as:

$$\mathrm{TI} = \frac{|A \cap B|}{|A \cup B|} \tag{12}$$

where A and B are two datasets and $|X|$ is the size of a set X. Based Eq. (12), $\mathrm{TI} = 0$ implies that both datasets A and B are entirely different and $\mathrm{TI} = 1$ suggests that both datasets, A and B are the same set.

Results

Synthetic Brain Image Experiments

We used synthetic images, described in the data section, for experiments to objectively assess the ability and limitations of the ICA regarding the quantitative and qualitative analysis. In this study, we designed the experiments in two parts as follows: (a) brain MR images with the skull and background (BKG), including SVM and ICA+SVM; and (b) brain MR images without BKG, including SS+ICA+SVM and ICA+SVM+SS. As the SVM is a supervised classifier, we assumed four classes of significant interest, BKG, CSF, GM, and WM. Thus, for each of these four classes, we selected nine training samples, marked by bright points in the BKG image and dark points in the CSF, GM, and WM images (Fig. 2). Of note, the selection of these samples was performed by radiologists in the Taichung Veterans General Hospital, Taichung, Taiwan.

Example 1: SVM with BKG

Example 1 included the brain skull in MR images for consideration but used a classifier, SVM, rather than the ICA to perform the signal separation. Fig. 3 illustrates the impact of the BKG on the SVM performance when the BKG is considered as an additional signal class. In this case, three MR images and four signal classes, GM, WM, CSF, and BKG, are present.

Example 2: ICA+SVM with BKG

In example 2, the BKG is deterministic, considered

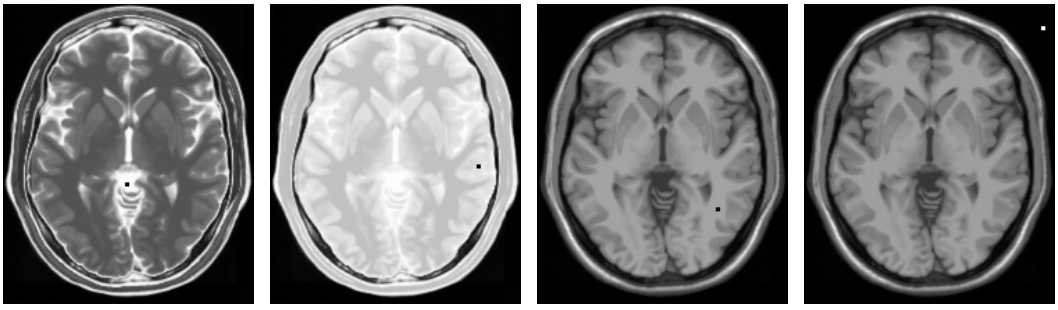

CSF GM WM BKG

Fig. 2 Training samples for each of the four classes, CSF, GM, WM, and BKG.

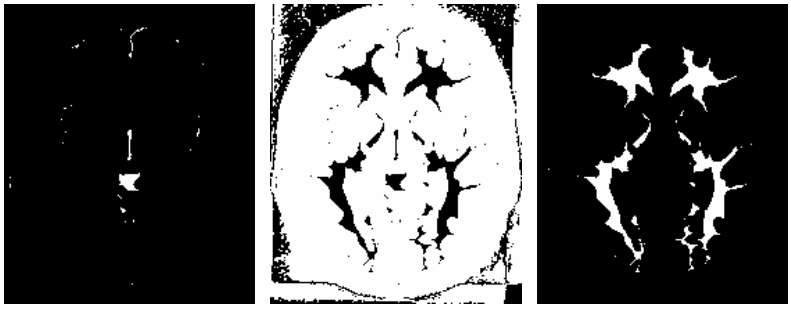

CSF GM WM

Fig. 3 SVM classification results with BKG.

part of the sample mean, and removed by sphering before the ICA, followed by the SVM. Notably, to the results of our experiments are strikingly close and similar irrespective of the constant value set for the gray level values of the BKG (such as 128, 255, or any gray level value). Fig. 4 shows the ICA results by using brain images with setting for the zero gray level values of the BKG, and the SVM classification results by using ICs images.

In examples 1 and 2, we conducted experiments to assess the impact of the BKG on classification. In the following examples, however, we assessed an additional impact of brain SS on the classification.

Example 3: SS +ICA+SVM

Example 3 combined both ICA and SVM by first pre-processing SS to remove the brain skull and, then, using the ICA to separate signal sources in three ICs, which were further categorized by the SVM. As expected, the results were better than those in Examples 1 and 2 (Fig. 5).

Example 4: ICA+SVM+SS

Example 4 is in contrast to Example 3 where the SS process was conducted after ICA+SVM as post-processing. Fig. 6 shows that post-processing the ICA+SVM results by SS were considerably different from those obtained in pre-processing (Fig. 5).

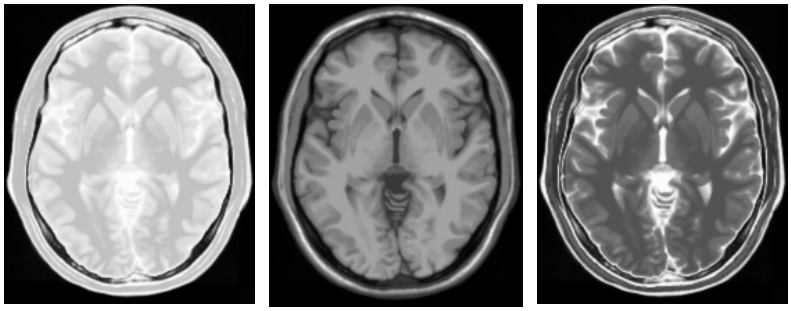

PDWI T1WI T2WI

(a) Brain MR images with BKG=0

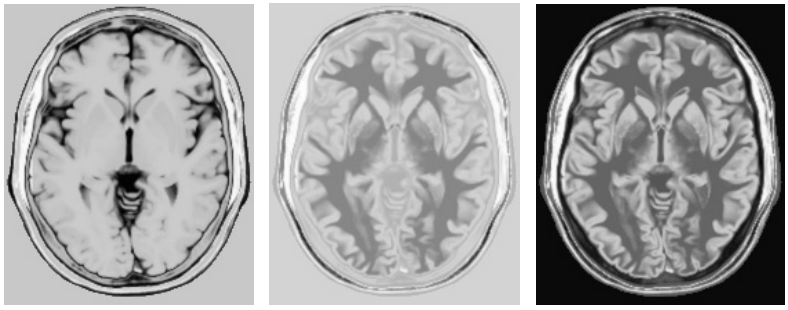

IC1 IC2 IC3

(b) Three FastICA-generated ICs by using Brain MR Images with BKG=0

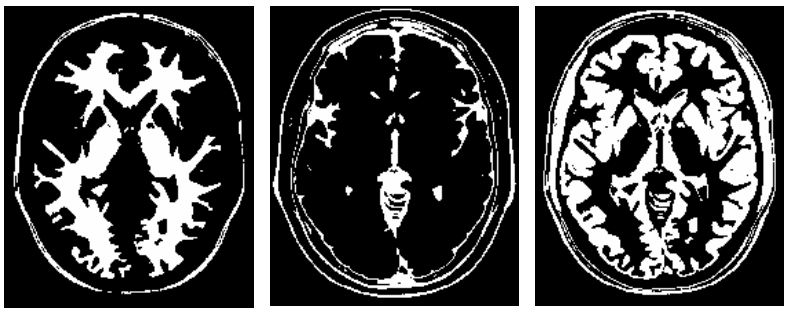

(c) SVM classification

Fig. 4 (a) Brain MR images with BKG = 0. (b) Fast ICA-generated ICs by using MR images with BKG = 0. (c) SVM classification results from (b).

Tables 1–4 present the sensitivity, specificity, accuracy, and TI of the results from experiments conducted in examples 1–4, respectively.

Our experiments revealed that the skull and background noise of MR brain images are significant signal sources exhibited in ICs that exert tremendous

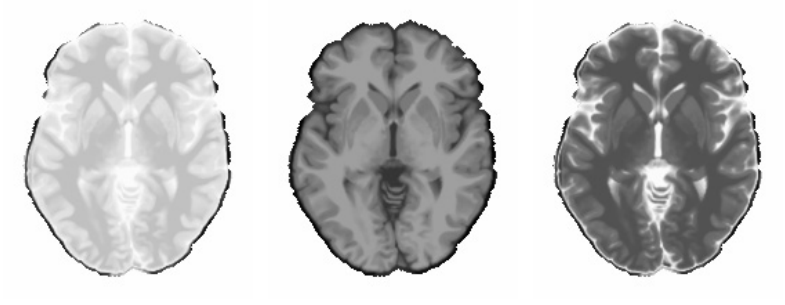

PD T1 T2

(a) Brain MR images without BKG and skull by SS

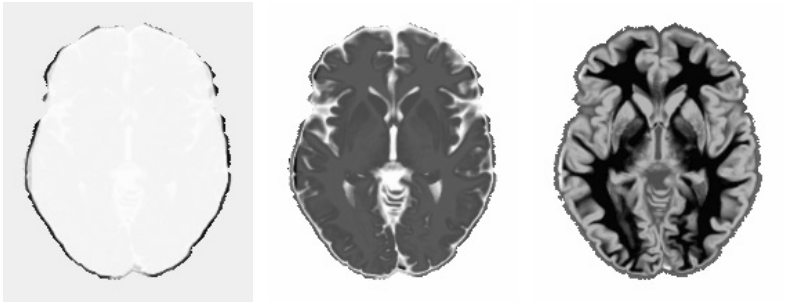

IC1 IC2 IC3

(b) Three FastICA-generated ICs without BKG and skull by SS

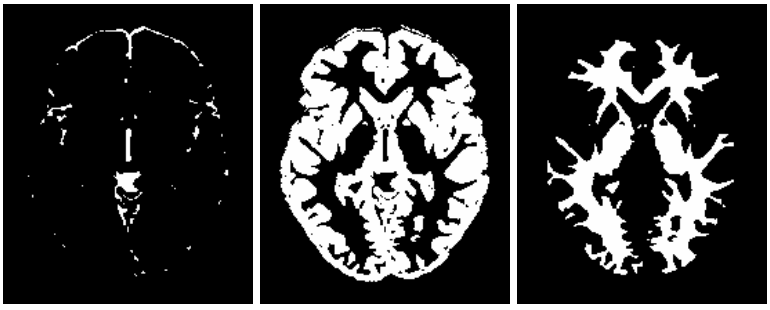

CSF GM WM

(c) SVM classification

Fig. 5 The results are SVM classifier in conjunction with the ICA as a follow-up process.

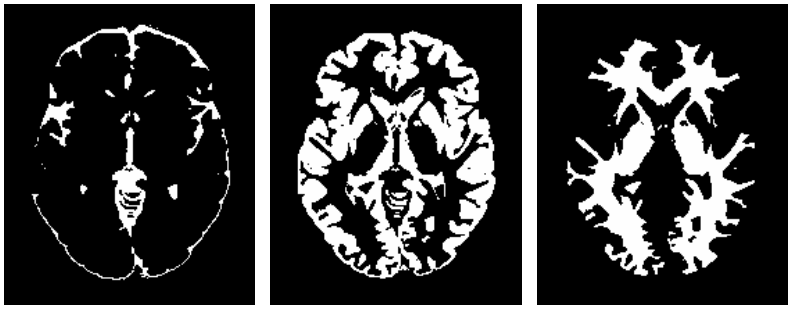

CSF GM WM

Fig. 6 The results are using ICA+SVM algorithms and SS as post-processing.

Table 1. Sensitivity results of examples 1–4 for the synthetic data (from the 11th to the 28th slice)

Approaches	CSF	GM	WM	GM+WM	Overall average
SVM	0.6565	0.3338	0.4941	0.4140	0.4948
ICA + SVM	0.8059	0.9728	0.9218	0.9473	0.9002
SS + ICA + SVM	0.5367	0.9873	0.8421	0.9147	0.7887
ICA + SVM + SS	0.7914	0.9728	0.9218	0.9473	0.8953

Table 2. Specificity results of examples 1–4 for the synthetic data (from the 11th to the 28th slice)

Approaches	CSF	GM	WM	GM+WM	Overall average
SVM	0.6018	0.8530	0.9109	0.8820	0.7886
ICA + SVM	0.9299	0.8742	0.9540	0.9141	0.9194
SS + ICA + SVM	0.9945	0.8906	0.9988	0.9447	0.9613
ICA + SVM + SS	0.9844	0.9633	0.9957	0.9795	0.9811

Table 3. Accuracy results of examples 1–4 for the synthetic data (from the 11th to the 28th slice)

Approaches	CSF	GM	WM	GM+WM	Overall average
SVM	0.6001	0.7472	0.8276	0.7874	0.7250
ICA + SVM	0.9212	0.8955	0.9500	0.9228	0.9222
SS + ICA + SVM	0.9637	0.9111	0.9758	0.9435	0.9502
ICA + SVM + SS	0.9712	0.9659	0.9846	0.9753	0.9739

Table 4. Tanimoto index of examples 1–4 for the synthetic data (from the 11th to the 28th slice)

Approaches	CSF	GM	WM	GM+WM	Overall average
SVM	0.1009	0.1668	0.3929	0.2799	0.2202
ICA + SVM	0.4081	0.6429	0.7391	0.6910	0.5967
SS + ICA + SVM	0.4924	0.6788	0.8376	0.7582	0.6696
ICA + SVM + SS	0.6551	0.8501	0.9033	0.8767	0.8028

interfering effects on the MR image analysis. The preliminary results in Tables 1-4 illustrated that the ICA+SVM+SS could efficiently enhance the impact of the skull and background noise on MR brain images.

Discussions

The proposed ICA+SVM+SS method in this study offers several advantages in the classification of normal GM and WM brain tissues, especially the CSF volume, the efficient quantification of which has been termed challenging in previous studies. First, the method reduces the computational cost of data processing because it only requires one set of training samples to process the entire multi-slice images. Besides, the same saving is applicable in minimizing the operator's burden. Second, and more importantly, it avoids potential operator interferences from multiple selections of training samples and markedly enhances the reproducibility of the supervised classifier. Of note, this method facilitates the clinical applicability of 3D MRI data analysis, which offers a higher number of image slices with a high-spatial resolution. In this study, the latter typically hindered the effective image analysis because of the enormous computational burden. In addition, the proposed method could proficiently classify 3D MRI data by using small sets of training data, without operation and computational complexity.

This study addresses several major concerns arising from applications of the ICA in the MR image analysis and introduces techniques to resolve these issues. Of note, the most significant and paramount issue is the occurrence of BKG effects on MR images. Thus, the pre-processing technique comprises brain SS before ICA, which does not necessitate the ICA to

produce an individual IC to separate the brain skull. In this study, we used the SVM as a post-processing method to classify the ICA-generated ICs and mitigate the effect of the BKG on the data analysis. Finally, we assessed whether pre-processing or post-processing, which separates the skull and non-brain intracranial tissue from MR images (i.e., SS), improves the performance in ICA-SVM. The results revealed that by implementing the extraction-based classification technique, SVM, in conjunction with the ICA as post OC-ICA processing method to categorize substances of interest, the pre-processing technique comprising SS could eliminate the known unwanted substances to reduce the false-positive rate, which performs significantly better in terms of the classification of three primary brain tissue substances.

Conclusions

In conclusion, this study establishes the importance of performing SS, which is significantly better regarding the classification of three primary brain tissue substances. Thus, SS implemented before ICA-SVM could decrease the number of *p* in OC-ICA situation to enhance the performance in ICA conjunction with SVM, and implementing SS after ICA-SVM could remove the non-brain tissue to perform better.

Acknowledgements

We thank the support from Ministry of Science and Technology(MOST 104-2221-E-075A-00, NSC 102-2221-E-075A-001-MY3; and Taichung Veterans General Hospital grants (TCVGH-1025506C; TCVGH-1047315C; TCVGH-1045502C).

References

1. Hyvarinen A, Karhunen J, Oja E. Independent Component Analysis, John Wiley & Sons, 2001; 391-414.
2. Burgess GC, Kandala S, Nolan D, Laumann TO, Power JD, Adeyemo B, et al. Evaluation of Denoising Strategies to Address Motion-Correlated Artifacts in Resting-State Functional Magnetic Resonance Imaging Data from the Human Connectome Project. Brain Connect. 2016; 6(9): 669-680.
3. Cochereau J, Deverdun J, Herbet G, Charroud C, Boyer A, Moritz-Gasser S, et al. Comparison between resting state fMRI networks and responsive cortical stimulations in glioma patients. Hum Brain Mapp. 2016; 37(11): 3721-3732.
4. Du Y, Pearlson GD, Liu J, Sui J, Yu Q, He H, et al. A group ICA based framework for evaluating resting fMRI markers when disease categories are unclear: application to schizophrenia, bipolar, and schizoaffective disorders. Neuroimage. 2015; 122: 272-80.
5. Nakai T, Muraki S, Bagarinao E, Miki Y, Takehara Y, Matsuo K, et al. Application of independent component analysis to magnetic resonance imaging for enhancing the contrast of gray and white matter. NeuroImage. 2004; 21: 251-260.
6. http://www.bic.mni.mcgill.ca/brainweb/
7. Bell AJ, Sejnowski TJ. An information-maximization approach to blind separation and blind deconvolution. Neural Computation. 1995; 7: 1129-1159.
8. Hyvarinen A, Oja E. A fast fixed-point for independent component analysis. Neural Computation. 1997; 9: 1483-1492.
9. Hahn HK, Peitgen H. The Skull Stripping Problem in MRI Solved by a Single 3D Watershed Transform. Proc. MICCAI, LNCS 1935: 134-143, Springer, Berlin, 2000.
10. Gonzalez RC, Woods RE. Digital Image Processing. 3rd ed., Pearson, 2007; 617-624.
11. Vincent L, Soille P. Watersheds in Digital Spaces: An Efficient Algorithm Based on Immersion Simulations. IEEE Trans on Pattern Analysis and Machine Intelligence. 1991; 13: 583-598.
12. Theodoridis S, Koutroumbas K. Pattern Recognition, 2nd, Academic Press, 2003; 77-85.
13. Vapnik VN. Statistical Learning Theory, John Wiley & Sons, 1998; 493-521.
14. Tofts P. Quantitative MRI of the Brain: Measuring Changes Caused by Disease, John Wiley & Sons Ltd, 2003; 17-54.

獨立成份分析結合去腦殼方法於腦部磁振造影影像研究之影響

李三剛[1,2,3] 王士偉[4] 張詠傑[3,4] 蔡志文[3,5] 陳啟昌[3] 吳奕螢[3] 宋秋瑾[6]
陳文賢[3] 陳虹潔[3] 楊晴雯[7] 陳享民[6,8,*] 歐陽彥杰[4] 張建禕[9]

童綜合醫療社團法人童綜合醫院 [1]院長
臺中榮民總醫院 [2]顧問 [3]放射線部 [6]醫學研究部醫學影像量化研究中心 [7]資訊室
[4]中興大學 電機工程學系
[5]中國醫藥大學 醫學院放射科
[8]弘光科技大學 生物醫學工程系
[9]美國馬里蘭大學巴爾地摩校區 資訊科學及電機工程學系

受文日期：民國 106 年 01 月 05 日；接受刊載：民國 106 年 05 月 26 日

摘要

背景和目的：近來，獨立成分分析法於磁振造影影像研究中扮演很重要的角色，它可以在醫學診斷中提供有價值的臨床訊息。然而，在使用獨立成分分析方法時會產生兩個主要問題，限制其訊號分離的能力。主要是由於缺乏足夠的造影波序以得到磁振影像張數，及腦殼等非腦組織對獨立成份分析時的干擾。
方法：為了解決上述兩個問題，本文介紹了去腦殼和支持向量器兩種處理過程來解決獨立成分分析法使用時之問題。去腦殼主要是消除腦殼等非腦組織對獨立成分分析分離主要三種組織之干擾，而支援向量器是用於補救由不足獨立成分所造成的困境。
結果：本論文利用靈敏度，特異性，準確性和 Tanimoto 指數，來評估合成腦部磁造影影像之腦脊髓液，灰白質分類的結果。其中利用獨立成份分析結合支援向量器後再去腦殼的平均數據分別為 0.90、0.98、0.97 和 0.80，此實驗結果皆高於其他實驗的方法。
結論：本論文利用去腦殼方法對腦部磁振造影影像進行非腦組織與腦組織的分離預處理及後處理，的確可提高獨立成分分析結合支援向量器的性能。由實驗結果可證明，獨立成分分析結合支援向量器分析後，再進行去腦殼處理，除了可以去除非腦組織外，也可以達到腦部主要組織分類的最佳效果。

關鍵詞：獨立成份分析、磁振造影影像分析、去腦殼、支援向量器

* 通訊作者：陳享民博士 臺中榮民總醫院 醫學研究部醫學影像量化研究中心 台中市西屯區 (407) 台灣大道 4 段 1650 號

Tungs' Medical Journal 12 (2018) 30-37

Original Article

Design of the Visual Behavior Questionnaire for Taiwanese Children Aged 5-12 Years (VBQ-T30) and its Preliminary Report

Han Chin Kuo*

Department of Ophthalmology, Tungs' Taichung MetroHarbor Hospital

Received: Mar. 08, 2017; Accepted: Apr. 10, 2017

Abstract

Myopia is a global issue. In addition to being a refractive-error problem, high myopia may lead to significant degeneration of the eyes and diseases such as retinopathy or maculopathy. This problem is more serious in East Asian countries, where the "myopia epidemic" has not been successful controlled. A systematic approach targeting multiple aspects across various priority levels is needed to decrease the incidence and prevalence of myopia. Therefore, we designed a myopia questionnaire (VBQ-T30) that probes daily visual behaviors of individual children along with family and school factors that affect these behaviors. The pre-test and pre-test survey of the VBQ-T30 questionnaire indicate that it is a reliable and valid tool. Data from the responses to VBQ-T30 questions provides researchers with information concerning the behaviors of young children at home and in school that generate risk and protective factors associated with the development of myopia. This information should help in the development of systematic policies for myopia prevention.

Keywords: Myopia, Myopia control, Visual behaviors, Systematic approach

Background

Myopia has become a worldwide public health problem as its incidence and prevalence have risen among new generations [1–5]. This "myopia epidemic" is more serious in East Asian countries like Taiwan, Singapore, Japan, Korea, and China[3–5]. The prevalence of myopia increased from 36.7% in 1983 to 61% in 2000 among children aged 12 years in Taiwan[4]. Furthermore, a similarly high rate exists among the 12-year-old children in Hong Kong, 64% in 1991 and 61% in 2012[5]. Although efforts have been made to prevent myopia onset and progression among children in these countries, the high prevalence has not decreased, and this will lead to a large number of adults suffering from high myopia in the future. Early-onset myopia, which occurs at a younger age (e.g., in elementary school children) may progress to high myopia, owing to the continuous increase in myopia diopter until 18 years of age. High myopia is frequently associated with complications, such as vitreous opacity, maculopathy, retinal breakage, and even retinal detachment, due to significant eyeball deformity (axial elongation).

Most myopia cases are acquired, and the "Near-Work" theory has been established to explain the cause of acquired myopia[6]. This theory suggests that long periods of near-work like reading, writing, or use of electronic devices during childhood/teenager stages is the main cause of myopia onset and progression. Children and teenagers' lengthy near-work could be associated with individual, school, family, cultural, and other factors.

Research and current preventive strategies have focused mainly on individual-level factors such as the use of pharmaceutical regimens (use of cycloplegic eye drops) and personal guidelines about proper visual behaviors. For instance, studies have

*Correspondence to: Han Chin Kuo, Department of Ophthalmology, Tungs' Taichung MetroHarbor Hospital, No. 699, Sec. 8, Taiwan Blvd., Wuqi Dist., Taichung City 43503, Taiwan (R.O.C.)

demonstrated that the use of atropine may be effective in myopia control[8–10]. MIT (Myopia Investigation Study in Taipei), a population-based study supported by the Taipei city government, suggested that children should have adequate outdoor activities and limited near-work activities [11–12]. Genetic and optometric factors like wearing Ortho-K or contact lenses have also been evaluated in some studies[6–7,13–16].

However, studies with an emphasis on children's proper visual behaviors (more outdoor activities and less near-work), and use of cycloplegics (tropicamide/atropine) may not be enough. This is because the children's daily visual burden is largely influenced by school and familiar factors, and many school policies and parental attitudes/practices are often inconsistent with the behavior guidelines for myopia prevention in Taiwan. For instance, the academic burden may be too heavy with too much homework and too many exams and too stressful because of the comparison/ranking in the Taiwanese education system or there may be high parental expectations pertaining to academic performance. We therefore propose to develop a systematic strategy to control the "myopia epidemic," an expansion of our surveys to such environments is warranted to identify the highest influencing factors.

Purpose

A common flaw in some myopia studies is the lack of stratification among different "near tasks" like reading, writing, painting, or instrument-learning, which vary in the visual burden they impose on an individual. The size of visual objectives is often neglected, too. For instance, the "use of cellphones, computers, or tablets" was analyzed as a single variable in the MIT survey, disregarding the various screen sizes among these electronic devices[11–12]. We designed a 30-question Visual Behavior Questionnaire (VBQ-T30) for Taiwanese children aged 5–12 years that was aimed at obtaining data for studies addressing the above problems. The questionnaire covered numerous details about the children's daily visual behaviors and the family/school factors that determine these behaviors. We hope that the VBQ-T30 will be used to identify specific environmental factors for myopia in a comprehensive manner.

Methods

Design of the questionnaire

We first constructed a conceptual framework to include known causes of myopia based on literature review and our own clinical experiences. We categorized environmental factors according to their proximity to the event of myopia into proximal, intermediate, or distal causes. The risk/protective factors based on the visual distance (near-work theory) were divided into three categories: "near works"(≤ 50 cm), "intermediate-distance" (>50 cm to ≤3 m) and "Far-distance" (>3 m). The genetic factors and "therapy" factors, although relatively irrelevant to visual behaviors, were also included in this framework. The important factors to be controlled or measured were selected using this framework, and 30 questions probing these factors were constructed, thus creating the questionnaire (VBQ-T30). The VBQ-T30 questionnaire includes one part for parents and another part for children, and it can be completed in 30 minutes.

Pre-test of the VBQ-T30

We recruited 18 parents and their children for a preliminary VBQ-T30 test. After completing the VBQ-T30, the participants answered another survey that inquired about their opinion of the questionnaire to assess the soundness of the VBQ-T30.

Assessment of reliability

In question 4 of VBQ-T30, the parents recorded the length of time spent by their children doing homework. In question 25, the children assessed their homework burden. The consistency of the two questions was compared to assess the reliability of the VBQ-T30.

Assessment of validity

We used question 13 of the VBQ-T30 to test the assumption that parents working in the ophthalmologic department of hospitals or eye clinics have professional knowledge about myopia control in children. We compared the knowledge scores between the parents working in the ophthalmologic department and those not working in such departments.

Results

The conceptual framework

We identified 13 environmental factors (X1–X13) that could lead to development of myopia based on literature review and our clinical experience (Fig 1). In addition to genetic factors (X14), these 13 environmental factors were divided into three types of causative factors (distal, intermediate, and proximal) according to their proximity to the myopia event. [6–37]

The questionnaire

The purpose of our survey was to gather information about the children's daily visual behaviors and the direct factors influencing these behaviors in familiar and school environments. Therefore, genetic factors (X14), all distal causative factors (X1–X4), along with geographic, economic, governmental, and cultural factors, were controlled in this survey. Health-care factors (intermediate cause) and "treatment" factors (proximal cause) were controlled for the same reason[8–10,14–17].

We constructed a total of 30 questions (Q1–Q30) that were included in the VBQ-T30 (Attachment 1). In addition to questions 1 and 2 (family and parental data) and question 11 (the use of cycloplegic eye drops), 27 questions were related to X5 personal factors, X6 family factors, X7 school factors, and X8 community factors of intermediate causality, as well as X10 near-work factors, X11 intermediate-distance factors, and X12 far-distance factors of proximal causality. Table 1 represents the details of these factors and related questions. We designed the VBQ-T30 for children aged 5–12 and their parents. However, we found differences in children's daily visual behaviors and their parents' raising practices that depended on school stages [kindergarten, low (grade 1–2), middle (grade 3–4), and high (grade 5–6)] of elementary school. Thus, we re-designed our questionnaire using "K," "L," "M," and "H" in front of every question to denote the suitability of each question for kindergarten, low-grade, middle-grade, and high-grade stages of elementary school, respectively.

The pre-test and survey

A total of 18 children and their parents were enrolled into the VBQ-T30 pre-test with an 8-question survey (Attachment 2) following completion of the VBQ-T30 to assess the soundness of the questionnaire. The tables below represent the results of the

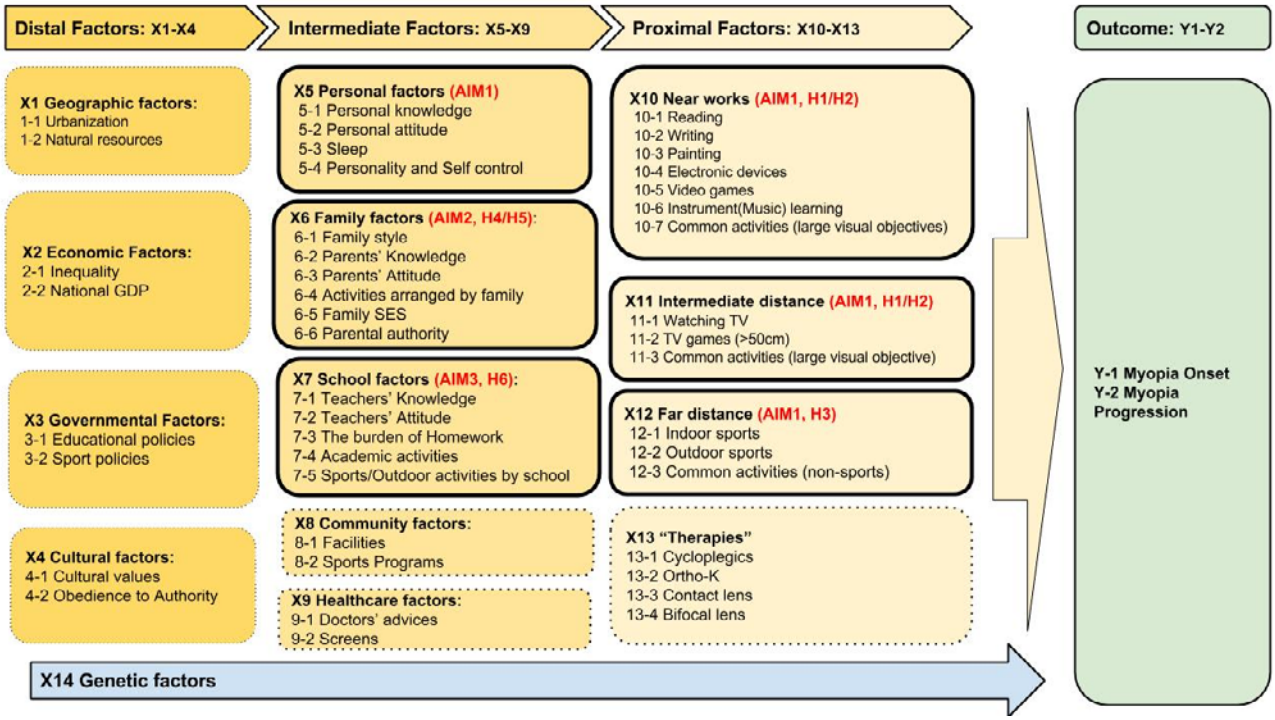

Fig. 1 The environmental factors about myopia.

Table 1. Factors X5-X12 with related questions (Mark *: question in the children part of questionnaire)

Factors	Related Question #
X5-1 Child's knowledge about myopia	Q30/Children's knowledge about myopia control*
X5-2 Child's attitude toward myopia	Q4/Daily routine, Q23/Electronic devices*, Q28/Outdoor activity*, Q27/Outdoor activity*
X5-3 Sleep	Q4/Daily routine
X5-4 Personality and Self-control	Q20/Academic activities*, Q17/Personality, Q22/Sports*, Q28/Reading*, Q24/ Electronic devices*, Q21/After-school activities
X6-1 Family style	Q1/Family member, Q2/Parental data, Q3/Family authority
X6-2 Parents' knowledge about myopia	Q13/Parents' knowledge about myopia, Q19/Parents practice of myopia control
X6-3 Parents' attitude related to myopia	Q12, Q14, Q15/Parents' attitude, Q19/Parent's practice of myopia control
X6-4 Sports/Outdoor activities offered by family:	Q9-3/Sports, Q22/Sports*, Q27/Outdoor activities*
X6-5 Family SES	Q2/Parental data
X6-6 Parental authority	Q3/Parental authority, Q14-2/Parents' authority on academic performance
X7-1 Teachers' knowledge	Q25/Homework*, Q26/Teacher's practice*
X7-2 Teachers' attitude	Q25/Homework*, Q26/Teacher's practice*
X7-3 Burden of homework	Q4/Daily routine, Q25/Homework*, Q26/Teacher's practice
X7-4 Academic activities	Q25/Academic activities
X7-5 Sports/outdoor activities by school	Q4/Daily routine, Q27/Sports*
X10-1 Reading	Q5/Reading, Q23/Reading*
X10-2 Writing:	Q4/Daily routine, Q25/Homework*
X10-3 Painting	Q9-2/Non-instrument static talent learning
X10-4 Cell phone/Tablet/Computer	Q8/Electronic devices, Q24/Electronic devices*
X10-5 Video games	Q8/Electronic devices, Q24/Electronic devices*
X10-6 Instrument learning	Q9-1/Instrument learning
X10-7 Common activities	Q18/Home job
X11-1 Watching TV	Q7/Watching TV
X11-2 TV Games (>50cm)	Q7-4/Watching TV
X11-3 Common activities	Q24/Home job
X12-1 Indoor sports	Q9-3/Sports, Q11/Physical skill, Q22/Sports*
X12-2 Outdoor sports	Q9-3/Sports, Q11/Physical skill, Q22/Sports*
X12-3 Common activities	Q27/Outdoor activities*, Q28/Breaks at school*

survey for the VBQ-T30 pre-test.

The results Table 2 reflect the soundness of the VBQ-T30 in seven out of eight items. However, 6 of 18 parents (33%) responded that the children's daily activities had changed over the past year, and there were difficulties answering some questions due to these changes in habitual activities.

Reliability and validity

Our results Table 3, 4 suggested that the reliability and validity of the VBQ-T30 were good.

Discussion

Our questionnaire has several remarkable features. The VBQ-T30 covers a lot of details about children's daily visual behaviors at the individual level, which include behaviors recognized by parents like watching TV and using electronic devices, and more private activities like academic burdens (reading, doing homework, after-school tutoring, and instrument-learning). In addition, we included protective factors like outdoor and sporting activities in our questionnaire.

Table 2. Soundness of VBQ-T30

Items	Poor/Negative response	Good/Positive response	% of good response
Time-spending	>30 minutes: 2	≤30 minutes: 16	88%
Length of VBQ-T	2	16	88%
Recall difficulty (Too long for a year)	0	18	100%
Recording difficulty (Too long for a year)	6	12	66%
Clarity of questions	0	18	100%
Sensitivity	0	18	100%
Loss of points	0	18	100%
Repeated points	0	18	100%

Table 3. Assessment of the reliability (Question 4 and Question 25)

Number of children reported 7 hours per week in homework by parents (Q4)	Number of children responding "heavy" or "very heavy" in homework by themselves(Q25)	Consistency rate
9 out of 14	10 out of 14	71%

Table 4. Assessment of the validity

	Parents with ophthalmological/optometric background (n=7)	Parents without ophthalmological/optometric background (n=11)
Mean knowledge score	Average:2.00 (min:1, max:3)	Average: 1.36 (min:1, max:2)

Calculation of knowledge score: 1 point by mentioning common idea like "electronic devices" or "gesture of reading/writing. Another point was added by mentioning other knowledge like "book reading" or "outdoor activities".

The VBQ-T30 probes into family and school factors that influence children's visual behaviors directly. We focused particularly on family factors because the parents were directly involved in answering the survey. In contrast, school factors were covered less, because the children's schoolteachers were not contacted directly in our survey.

Four different versions of the VBQ-T30 were applied to four different age groups of children (5–6 years, kindergarten; grade 1-2; grade 3-4; and grade 5-6). Therefore, the results allow for the detection of specific problems in each age group.

The survey taken after our preliminary test validated the soundness of the VBQ-T30. However, 6 out of 18 parents (33%) responded that changing behaviors over the course of a year made it difficult to estimate customary daily behaviors of their children. This is a dilemma for myopia surveys, as it would be hard to detect any myopia progression inside a shorter period. One solution to this problem could be to request that parents and their children take the VBQ-T30 test every 6 months during a year. However, this would likely increase the budget for the survey substantially.

None of the parents in the pre-test survey raised any sensitivity issues or expressed memory difficulties regarding their children's visual behavior over the past year. Therefore, we do not anticipate any significant response and recall bias for the VBQ-T30 test. Several questions had to be answered twice in this test, once by parents, and a second time by children. For instance, parents recorded the number of hours spent per week doing homework by their children in question 4, and their children graded the degree of homework burden in question 25. The consistency of response in these two questions helped indicate the reliability of the VBQ-T30 test. Moreover, parents working in the ophthalmologic department of hospitals or eye clinics showed a higher level of knowledge about myopia control compared with those without (2.00 vs. 1.36, $p < 0.05$, Table 4). This suggests that VBQ-T30 is a valid tool for preliminary assessment of factors involved in development of myopia in children. However, due to the small sample size, further assessments on both reliability and validity are warranted.

Conclusion

The VBQ-T30 test is a thorough survey about children's daily visual behaviors, and the underlying

factors affecting these behaviors, such as familial and school factors. The questionnaire helps in extracting overall data for prevention of myopia and progression control among Taiwanese children aged between 5–12 years. Identification of these factors is important to design interventions for control of myopia with a systematic approach in Taiwan. The preliminary test and its pre-test survey suggest the VBQ-T30 is reliable and provides valid information once completed. A further assessment with a larger sample size is warranted.

References

1. Matamoros E, Weber M, Korobelnik J, Leveziel N. Prevalence of myopia in France. Medicine 2015; 94: e1976.
2. Vistale S, Sperduto R, Ferris III F. Increased prevalence of myopia in the United States between 1971-1972 and 1999-2004. Arch Ophthalmol 2009; 127: 1632-9.
3. Jung SK, Lee JH, Kakizaki H, Lee D. Prevalence of myopia and its association with body stature and educational level in 19-year-old male conscripts in Seoul, South Korea. Invest Ophthalmol Vis Sci 2012; 53: 5579-83.
4. Lin LLK, Shih YF, Hsiao CK, Chen CJ, Lee LA, Hung PT. Epidemiologic study of the prevalence and severity of myopia among schoolchildren in Taiwan in 2000. J Formos Med Assoc 2001; 100: 684-91.
5. Lam CSY, Lam CH, Cheng SCK, Chan LYL. Prevalence of myopia among Hong Kong Chinese schoolchildren: Changes over two decades. Ophthalmic Physiol Opt 2012;32:17-24.
6. Morgan I, Rose K. How genetic is school myopia? Prog Retin Eye Res 2005; 24: 1-38.
7. Ho DW, Yap MK, Ng PW, Fung WY, Yip SP. Association of high myopia with crystallin beta A4 (CRYBA4) gene polymorphisms in the linkage-identified MYP6 locus. PLoS ONE 2012; 7: e40238.
8. Shih YF, Chen CH, Chou AC, Ho TC, Lin LLK, Hung PT. Effect of different concentrations of atropine on controlling myopia in myopic children. J Ocul Pharmacol Ther 1999; 15: 85-90.
9. Shih KC, Chan TCY, Ng ALN, Lai JSM, Li WWT, Cheng ACK, et al. Use of Atropine for prevention of childhood myopia progression in clinical practice. Eye Contact Lens 2016; 42: 16-23.
10. Clark T, Clark R. Atropine 0.01% eyedrops significantly reduce the progression of childhood myopia. J Ocul Pharmacol Ther 2015; 31: 541-5.
11. Tsai DC, Lin LJ, Huang N, Hsu CC, Chen SS, Chiu AW, et al. Study design, rationale and methods for a population-based study of myopia in schoolchildren: the Myopia Investigation study in Taipei. Clin Exp Ophthalmol 2015; 43: 612-620.
12. Hsu CC, Huang N, Lin PY, Tsai DC, Tsai CY, Woung LC, Liu CJ, et al. Prevalence and risk factors for myopia in second-grade primary school children in Taipei: A population-based study. J Chin Med Assoc 2016; 79: 625-632.
13. Chen X, Sankaridurg P, Donovan L, Lin Z, Li L, Martinez A, et al. Characteristic of peripheral refractive errors of myopic and non-myopic Chinese eyes. Vision Res 2010;50:31-5.
14. Charm J, Cho P. High myopia-partial reduction ortho-K: A 2-year randomized study. Optom Vis Sci 2013; 90: 530-9.
15. Cho P, Cheung S. Retardation of myopia in Orthokeratology (ROMIO) study: A 2-year randomized clinical trial. Invest Ophthalmol Vis Sci 2012; 53: 7077-85.
16. Aller TA, Wildsoet C. Bifocal soft contact lenses as a possible myopia control treatment: a case report involving identical twins. Clin Exp Optom 2008; 91: 394-9
17. Gwiazda J. Treatment options for myopia. Optom Vis Sci 2009; 86: 624-8.
18. Saw SM, Nieto FJ, Katz J, Schein OD, Levy B, Chew SJ. Factors related to the progression of Myopia in Singaporean children. Optom Vis Sci 2000; 77: 549-54.
19. Sherwin JC, Reacher MH, Keogh RH, Khawaja AP, Mackey DA, Foster PJ. The association between time spent outdoors and myopia in children and adolescents: A systematic review and meta-analysis. Ophthalmology 2012; 119: 2141-51
20. Jones-Jordan LA, Sinnott LT, Cotter SA, Kleinstein RN, Manny RE, Mutti DO, et al. Time outdoors, visual activity, and myopia progression in juvenile-onset myopes. Invest Ophthalmol Vis Sci 2012; 53: 7169-75.
21. Jones LA, Sinnott LT, Mutti DO, Mitchell GL, Moeschberger ML, Zadnik K. Parental history of myopia, sports and outdoor activities, and future myopia. Invest Ophthalmol Vis Sci 2007; 48: 3524-32.
22. Guggenheim JA, Northstone K, McMahon G, Ness AR, Deere K, Mattocks C, et al. Time outdoors and physical activity as predictors of incident myopia in childhood: A prospective cohort study. Invest Ophthalmol Vis Sci 2012; 53: 2856-65.
23. Rose KA, Morgan IG, Ip J, Kifley A, Huynh S, Smith W, Mitchell P. Outdoor activity reduces the prevalence of myopia in children. Ophthalmology 2008; 115: 1279-85.
24. Lu B, Congdon N, Liu X, Choi K, Lam DSC, Zhang M, et al. Associations between near work, outdoor activity, and myopia among adolescent students in rural China. Arch Ophthalmology 2009; 127: 769-75.
25. Dirani M, Tong L, Gazzard G, Zhang X, Chia A, Young TL, Rose KA, Mitchell P, Saw SM. Outdoor activity and myopia in Singapore teenage children. Br J Ophthalmol 2009; 93: 997-1000.
26. Saxena R, Vashist P, Tandon R, Pandey RM, Bhardawaj A, Menon V, et al. Prevalence of myopia and its risk factors in urban school children in Delhi: The North India Myopia study (NIM study). PLoS ONE 2015; 10: e0117349.
27. Donald O, Mutti G, Lynn M, Melvin L. Moeschberger, Jones LA, et al. Parental myopia, near work, school achievement, and children's refractive error. Invest Ophthal and Vis Sci 2002; 43: 3633-40.
28. Saw SM, Wu HM, Seet B, Wong TY, Yap E, Chia KS, et al. Academic achievement, close up work parameters, and myopia in Singapore military conscripts. Br J Ophthalmol 2001; 85: 855-60.
29. Jones-Jordan LA, Mitchell GL, Cotter SA, et al. Visual activity before and after the onset of Juvenile myopia. Invest Ophthalmol Vis Sci 2011; 52: 1841-50.
30. Peckham CS, Gardiner PA, Goldstein H. Acquired myopia in 11-year-old children. Br Med J 1977: 1: 542-5.
31. Mutti, Donald; Zadnik, Karla. Has near work's star fallen? Optom Vis Sci 2009; 86: 76-8.
32. Konstantopoulos A, Yadegarfar G, Elgohary M. Near work, education, family history, and myopia in Greek conscripts. Eye 2008; 22: 542-6.

33. Cordain L, Eaton SB, Brand Miller J, Lindeberg S, Jensen C. An evolutionary analysis of the etiology and pathogenesis of juvenile-onset myopia. Acta Ophthalmol Scand 2002; 80: 125-35.
34. Parssinen O, Lyyra A. Myopia and Myopia Progression Among Schoolchildren: A three-year follow-up study. Invest Ophthalmol Vis Sci 1993; 34: 2794-802.
35. Wu P, Tsai C, Hu C, Yang Y. Effects of outdoor activities on myopia among rural school children in Taiwan. Ophthalmic Epidemiol 2010; 17: 338-42.
36. Deng L, Gwiazda J, Thorn F. Children's refractions and visual activities in the school year and summer. Optom Vision Sci 2010; 87: 406-13.
37. Zhan MZ, Saw SM, Hong RZ, Fu ZF, Yang H, Shui YB, Yap MK, Chew SJ. Refractive errors in Singapore and Xiamen, China--a comparative study in school children aged 6 to 7 years. Optom Vis Sci 2000; 77: 302-8.

Attachments:

1. VBQ-T30, Visual Behavior Questionnaire for Taiwanese Children Aged 5-12
2. Survey of the VBQ-T30 pre-test

台灣 5-12 歲學童視覺行為問卷調查（VBQ-T30）之設計與初報

郭翰欽*

童綜合醫療社團法人童綜合醫院　眼科

受文日期：民國 106 年 03 月 08 日；接受刊載：民國 106 年 04 月 10 日

摘要

近視已經是一個全球的問題。高度近視不只是一個屈光問題，它更會造成眼球的退化與病變，例如視網膜病變或黃斑部病變。近視問題在許多東亞國家尤其嚴重，但是多年來近視控制在這些國家並沒有成功。為了有效控制近視的發生率與盛行率，系統性（多層次 / 多面向、並分別優先順序）的介入是需要的。因此我們設計了這份問卷（VBQ-T30），它不只調查個人層次的視覺行為，還包括直接影響學童視覺行為的家庭與學校因素。VBQ-T30 經過了初步試填與評估，顯示了 VBQ-T30 在基本上是一個可信賴與有效的工具。它的運用可以提供近視研究者，有關兒童近視的危險與保護因子、橫跨個人家庭與學校的多面向資料。這些資料對於將來擬定系統性的近視預防政策將有所助益。

關鍵詞：近視、近視控制、視覺行為、系統性介入

* 通訊作者：郭翰欽醫師　童綜合醫療社團法人童綜合醫院　眼科　43503 臺中市梧棲區臺灣大道八段 699 號

Tungs' Medical Journal 12 (2018) 38-42

Case Report

A Case of: Uncommon Cause of Left Flank Pain

Ho-Hsiang Chen[1], Chien-Jung Chang[2], Suan-Hung Yu[3,*]

[1]RN, Emergency Medicine NP, Department of Nursing, [2]Division of Cardiology, Department of Medicine, [3]M.D., Department of Emergency Medicine, Tungs' Taichung Metro Harbor Hospital

Received: Jun. 24, 2016; Accepted: Aug. 02, 2016

Abstract

Nutcracker syndrome (NS) is a vascular compression disorder in which the left renal vein becomes entrapped between the superior mesenteric artery and the aorta, which can result in flank pain and/or hematuria. Imaging studies, such as color Doppler ultrasonography and computed tomography, are frequently used to diagnose NS. Endovascular stenting has recently become the mainstream treatment for NS. However, NS remains underdiagnosed. NS should be considered as a differential diagnosis if patients present with symptoms of left flank pain, hematuria, proteinuria, and chronic fatigue syndrome.

Key words: Nutcracker syndrome, Flank pain, Hematuria, Endovascular stent

Introduction

Nutcracker syndrome (NS) refers to compression of the left renal vein between the superior mesenteric artery and the aorta.[1,2] It can cause hypertension and/or hematuria due to rupture of the thin-walled septum separating the veins from the collecting system. NS presents with variable symptoms, such as abdominal or flank pain, with or without microscopic hematuria, pelvic congestion, varicoceles in males, proteinuria, and chronic fatigue syndrome.[3] NS is not typically diagnosed in the emergency room because color Doppler ultrasonography (US), computed tomography (CT), and magnetic resonance imaging (MRI) are not routinely performed in emergency settings.[4] Therefore, a detailed medical history, physical examination, basic laboratory tests, and clinic imaging are used to exclude other causes of hematuria.[5]

*Correspondence to: Suan-Hung Yu, MD., Department of Emergency Medicine, Tungs' Taichung Metro Harbor Hospital, No. 699, Sec. 8, Taiwan Blvd., Wuqi Dist., Taichung City 43503, Taiwan (R.O.C.)

Case Report

A 51-year-old female presented with a 1-month history of intermittent left flank pain. She had visited a urologist as an outpatient and was diagnosed with ureteral stones. Due to worsening symptoms and a mild fever for 2 days, she visited our emergency department. Her past history included neurotic depression, hypertension, and urolithiasis. She underwent lithotripsy of the right ureter 1 year before presentation at a urology outpatient department. Physical examination showed no costovertebral angle tenderness or palpable abdominal tenderness. Urine analysis was negative for hematuria, pyuria, and proteinuria. Non-color sonography detected stones in the bilateral kidneys but no hydronephrosis. Due to the absence of hematuria and hydronephrosis, ureteral stone as the cause of left flank pain was ruled out. Abdominal CT was performed to investigate the presence of left renal infarction or acute pyelonephritis found the compression of the left renal vein between the abdominal aorta and superior mesentery artery (Fig. 1), suggestive of NS. A cardiologist was consulted for further investigation. Left renal phlebography showed engorgement of the distal left renal vein, left lumbar veins, and gonadal vein (Fig.

2), whereas manometry showed that the pressure gradient from the distal left renal vein to the inferior vena cava was 4 mmHg, which confirmed a diagnosis of NS. Her symptoms had improved by placement of an endovascular stent (16 × 2 mm; Boston Scientific, Marlborough, MA, USA) within the stenotic site of the left renal vein via the right femoral vein (Fig. 3). Her total hospital stay for endovascular stenting was 2 days. Anticoagulation therapy with orfarin at 5 mg/day was administered for 9 months and then stopped due to the development of diffuse ecchymosis. Ten months later, repeated abdominal CT, which was performed due to the development of low back pain, revealed patency of the stent and expansion of the left renal vein caused by the stent (Fig. 4). No other disposition or stent-related thrombosis was detected.

Discussion

NS is characterized by impaired blood outflow that is often accompanied by distention of the distal portion of the vein, which results in a variation of symptoms among individuals. The diagnosis of NS is often difficult and commonly delayed. Diagnostic and treatment criteria are not well established, and the natural history of NS is not well understood. Therefore, this disease is underestimated according to clinical statistics.[6]

For a precise diagnosis of NS, a detailed history, physical examination, and appropriate clinical imaging by Doppler US, CT, or MRI are required. Contrast-enhanced CT is the easiest and fastest method to diagnose NS. CT can detect engorgement of the

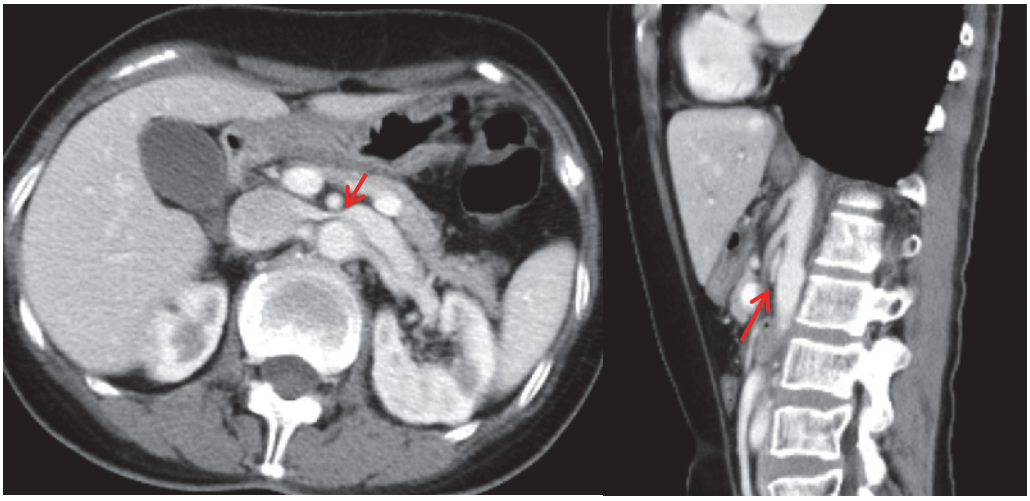

Fig. 1 CT showed compression of left renal vein by superior mesenteric artery and abdominal aorta.

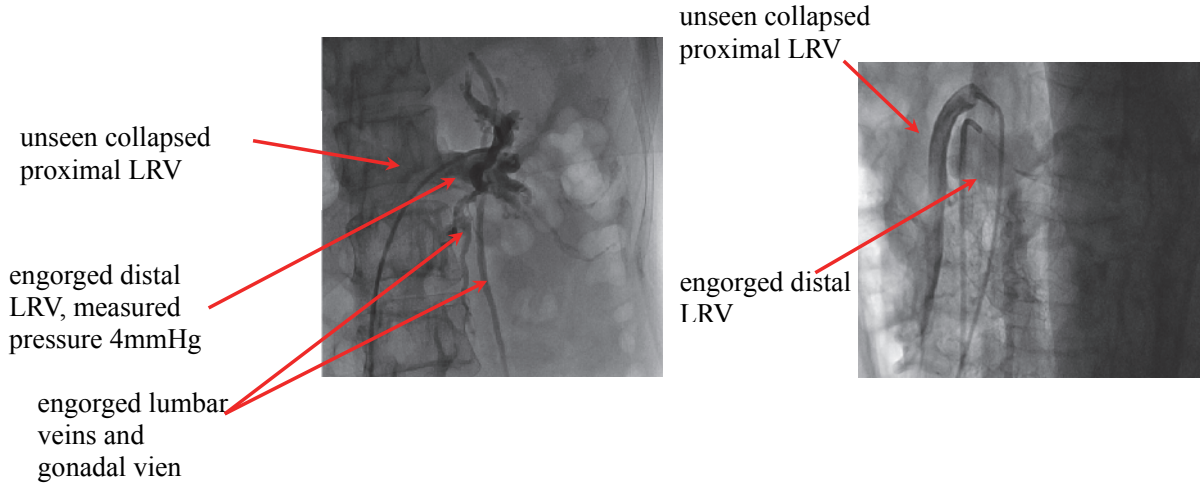

Fig. 2 Angiogram found distal left renal vein, left lumbar veins and gonadal vein engorgement.

distal left renal vein and compression of the proximal left renal vein. A pressure gradient of >3 mmHg in the left renal vein calculated by phlebography and manometry is used to confirm the diagnosis of NS.[4]

NS is rarely considered as a diagnosis for patients complaining of left flank pain. Hematuria is the most common symptom of NS. The presence of flank pain and hematuria often leads to a diagnosis of urolithiasis, particularly when the patient has a history of urolithiasis. Hematuria in NS is caused by an increase in venous pressure with vessel wall rupture into the collecting system.[1,7] Chronic fatigue syndrome is also a common symptom of NS. Our patient had major depression that overwhelmed the symptom of fatigue, which is thought to be associated with lumbar venous congestion with backache, particularly during exercise. Although proteinuria is a common symptom of NS,[8] it was probably intermittent in the present case.

Recently, articles have proposed different treatments for NS. Current treatments include stenting of the left renal vein and surgical transposition of the vessels. In a retrospective 6-month follow-up study of 61 patients with NS who underwent endovascular stenting, gross hematuria and pain had improved with a success rate of 96.7% (59 patients). However, in less than 24 months, three patients developed serious side effects, which included stent migration into the right atrium, the hilum of the left renal vein, and the inferior vena cava.[9] Stenting of the left renal vein is a relatively safe and efficient technique to provide long-term patency of the left renal vein.[5,10,11] Although the efficacy of this technique continues to improve, it is important to consider the risks of stent disposition and thrombosis.[9] Transposition of the left renal vein is also an effective treatment strategy, but the anatomy of the patient must be carefully evaluated to decide how to transpose the superior mesenteric

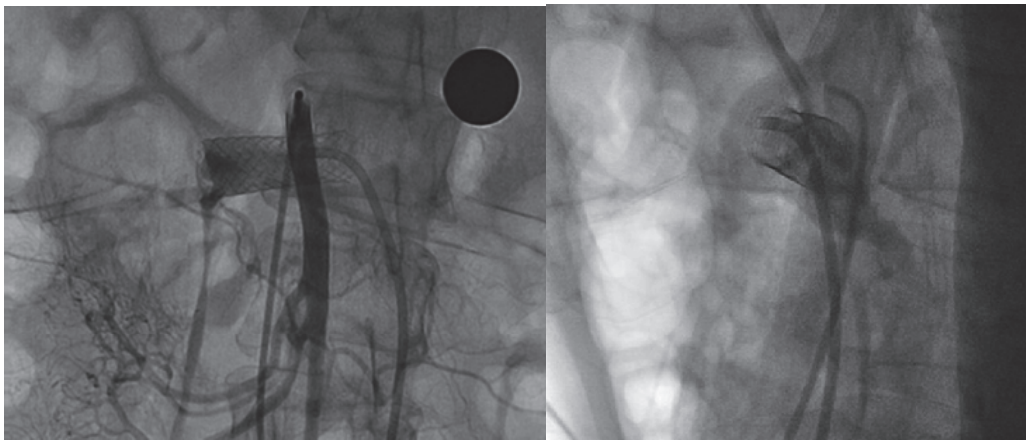

Fig. 3 Angiography after endovascular stenting.

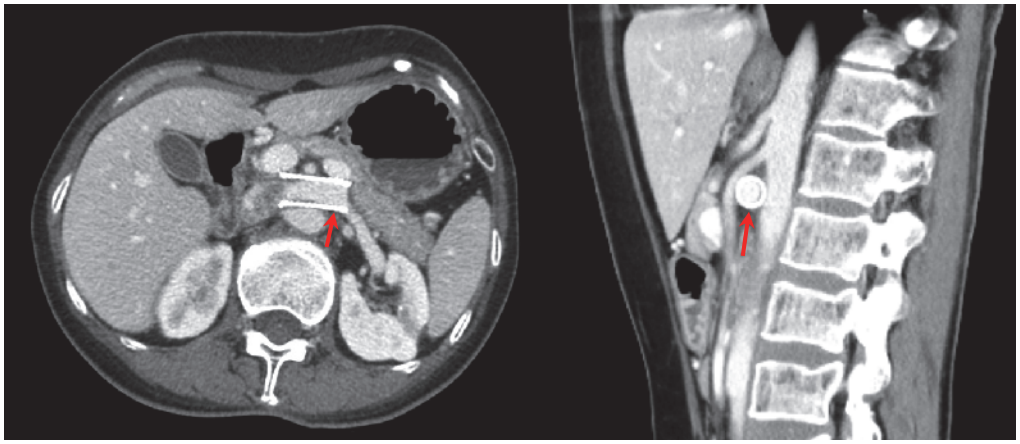

Fig. 4 CT showed the stent in the left renal vein.

artery to a lower position away from the left renal vein.[12] Our patient was followed-up as an outpatient for 10 months. During this time, there was no complication of thrombosis, stent displacement, or other abnormalities. Endovascular stenting is becoming the mainstream treatment for NS due to the increasing number of studies reporting good long-term outcomes.[9]

To date, there are insufficient reported cases of NS for a qualitative systematic review or meta-analysis to determine whether it is necessary to screen all suspected cases of NS for recurrent hematuria, left flank pain, and urolithiasis. In conclusion, for patients who present with these symptoms, NS should be considered as a differential diagnosis using color Doppler US, CT, or MRI.

Conflicts of interest

All authors have no conflicts of interest to declare.

References

1. Chen Y-M, Wang I-K, Ng K-K, Huang C-C. Nutcracker syndrome: an overlooked cause of hematuria. Chang Gung medical journal 2002; 25: 700-5.
2. Erben Y, Gloviczki P, Kalra M, et al. Treatment of nutcracker syndrome with open and endovascular interventions. Journal of Vascular Surgery: Venous and Lymphatic Disorders 2015; 3: 389-96.
3. He Y, Wu Z, Chen S, et al. Nutcracker syndrome—how well do we know it? Urology 2014; 83: 12-7.
4. Ahmed K, Sampath R, Khan M. Current trends in the diagnosis and management of renal nutcracker syndrome: a review. European Journal of Vascular and Endovascular Surgery 2006; 31: 410-6.
5. Policha A, Lamparello P, Sadek M, Berland T, Maldonado T. Endovascular Treatment of Nutcracker Syndrome. Annals of Vascular Surgery 2016.
6. Poyraz AK, Firdolas F, Onur MR, Kocakoc E. Evaluation of left renal vein entrapment using multidetector computed tomography. Acta Radiologica 2013; 54: 144-8.
7. Kurklinsky AK, Rooke TW. Nutcracker phenomenon and nutcracker syndrome. Mayo Clinic Proceedings; 2010: Elsevier. p. 552-9.
8. Mazzoni MB, Kottanatu L, Simonetti GD, et al. Renal vein obstruction and orthostatic proteinuria: a review. Nephrology Dialysis Transplantation 2011; 26: 562-5.
9. Chen S, Zhang H, Shi H, Tian L, Jin W, Li M. Endovascular stenting for treatment of Nutcracker syndrome: report of 61 cases with long-term followup. The Journal of urology 2011; 186: 570-5.
10. Wang X, Zhang Y, Li C, Zhang H. Results of endovascular treatment for patients with nutcracker syndrome. Journal of vascular surgery 2012; 56: 142-8.
11. Wu Z, Zheng X, He Y, et al. Stent migration after endovascular stenting in patients with nutcracker syndrome. Journal of Vascular Surgery: Venous and Lymphatic Disorders 2016; 4: 193-9.
12. Said SM, Gloviczki P, Kalra M, et al. Renal nutcracker syndrome: surgical options. Seminars in vascular surgery; 2013: Elsevier. p. 35-42.

左腰痛之罕見個案：胡桃鉗症候群

陳和庠[1] 張建榮[2] 余宣宏[3,*]

童綜合醫療社團法人童綜合醫院 [1]護理部急診專科護理師 [2]心臟科主治醫師 [3]急診部主治醫師

受文日期：民國 105 年 06 月 24 日；接受刊載：民國 105 年 08 月 02 日

摘要

胡桃鉗症候群是指左腎靜脈經過上腸系膜動脈和主動脈之間時遭受壓迫而引起腰部疼痛或血尿。常用的的影像學包括彩色都卜勒超音波，電腦斷層掃描作為診斷胡桃夾症候群。近期文獻顯示血管內支架對於胡桃鉗症候群有顯著的治療成效。但由於因影像學並非常規檢查，因此如果病人有左腰痛，血尿，蛋白尿和慢性疲勞症狀的症狀，我們必須留意胡桃鉗症候群，以鑑別造成血尿的其他原因。

關鍵詞：胡桃鉗症候群、腰痛、血尿、血管內支架

* 通訊作者：余宣宏醫師 童綜合醫療社團法人童綜合醫院急診部主治醫師 43503 臺中市梧棲區臺灣大道八段 699 號

Case Report

Cardiac Tamponade Caused by Primary Synovial Sarcoma of the Pericardium: A Case Report

Chung-Pei Chang[1], Ya-Ling Yang[2], Maw-Sheng Sun[1,*]

[1]Departments of Anesthesiology and [2]Cardiology, Show Chwan Memorial Hospital

Received: Jul. 22, 2016; Accepted: Sep. 16, 2016

Abstract

A primary synovial sarcoma of the pericardium is extremely rare. Here, we report a case of a 47-year-old man who was admitted with sudden onset of chest pain and shortness of breath. Computed tomography and epicardial echocardiography showed a large pericardial mass located predominantly at the rostral portion of the left atrium. He was considered to have cardiac tamponade caused by the pericardial tumor, and he was urgently treated with surgical excision under careful general anesthesia. A subsequent histological analysis confirmed the diagnosis of a primary pericardial synovial sarcoma. In conclusion, we presented an extremely rare case of a primary pericardial synovial sarcoma.

Key words: Primary pericardial synovial sarcoma, Cardiac tamponade, General anesthesia

Case report

A 47-year-old man with no history of disease presented to the emergency department with severe chest pain and shortness of breath. Physical examination revealed a fixed raised jugular venous pulse and very quiet heart sounds. Chest radiography demonstrated a grossly enlarged cardiothoracic ratio and left pleural effusion. Subsequent epicardial echocardiography revealed a large mass in the pericardial space, which was predominantly over the left atrium and lateral wall of the left ventricle, as well as large pericardial effusion impairing the movements of both ventricles. Computed tomography of the thorax demonstrated a large, heterogeneous soft-tissue-density lesion in the pericardium at the rostral portion of the left atrium. The lesion extended to the right superior mediastinum between the superior vena cava and ascending aorta. The lesion also encased the pulmonary artery (Fig. 1). The patient was considered to have cardiac tamponade associated with the tumor. To relieve his symptoms and prevent fatal complications, tumor resection was planned. An intraoperative transesophageal echocardiogram confirmed the presence of a large mass in the pericardial space over the left side, which compressed both ventricles of the heart (Fig. 2).

Following median sternotomy, a reddish, friable, necrotic tumor weighing about 578 g was removed. Histological analysis of the mass revealed epithelial and spindle cells with abundant mitotic activity, indicating a cellular tumor (Fig. 3).

On immunohistochemical analysis, the tumor was positive for cytokeratin, vimentin, mic-2, and bcl-2. Additionally, there was focal immunoreactivity for CD34, calretinin, and smooth muscle antigen, confirming a diagnosis of biphasic synovial sarcoma. At subsequent follow-up three months later, he was referred for adjuvant radiotherapy and chemotherapy.

Discussion

Primary tumors of the heart are uncommon, with an incidence of 0.0017% to 0.003%[1-3]. They

*Correspondence to: Maw-Sheng Sun, MD., Department of Anesthesiology, Show Chwan Memorial Hospital, No. 542, Sec. 1, Chung-Shan Rd., Changhua, 500, Taiwan (R.O.C.)

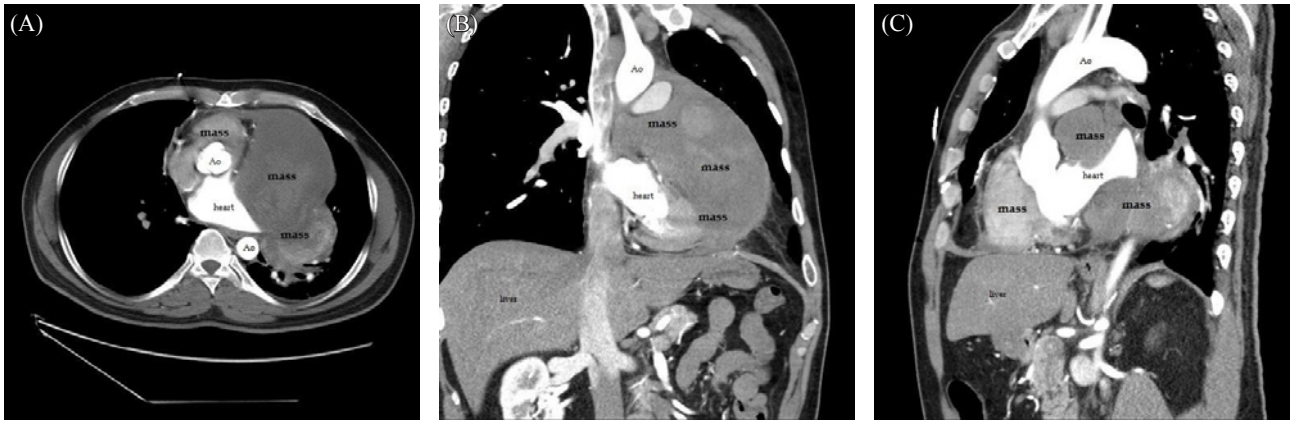

Fig. 1 The post-contrast CT (A, B, C) revealed a huge heterogeneous mass with hematoma formation; the ventricles were compressed by tumor. Ao: aorta

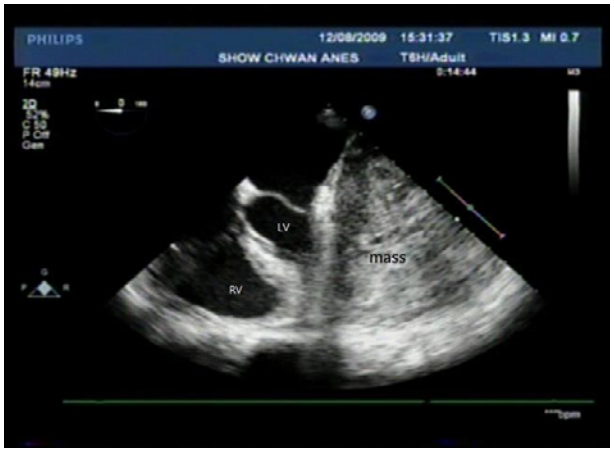

Fig. 2 A huge mass within the pericardial space over the left side compressed both ventricles of the heart.
LV: left ventricle, RV: right ventricle

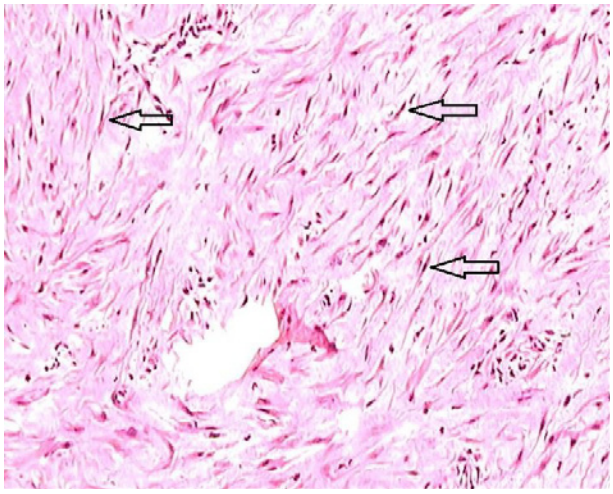

Fig. 3 The specimen showed high cellular spindle tumor cells (arrows), hypocellular fibrotic tissue and blood clot.

mainly comprise benign atrial myxomas, and the majority of malignant tumors are sarcomas. Histologically, angiosarcoma is the most common malignant tumor of the heart, followed by undifferentiated sarcoma, osteosarcoma, leiomyosarcoma, myxosarcoma, synovial sarcoma, and neurofibrosarcoma. A primary pericardial synovial sarcoma is an extremely rare tumor, and only few cases have been reported in the literature[4]. Although these tumors are initially asymptomatic during their early development, they present with local invasion causing arrhythmias and tamponade; blood flow obstruction causing dyspnea, chest pain, or heart failure; or embolic episodes at the cerebral coronary and retinal vascular beds. The awkward tumor site and clinical features associated with an advanced tumor at presentation make it challenging to obtain adequate biopsy material and reach a diagnosis[5-7].

On identification, the standard treatment of a primary pericardial synovial sarcoma is surgical excision, followed by adjuvant chemoradiotherapy. Surgical intervention is performed to not only alleviate symptoms but also avoid potential complications[8,9]. The tumor can be approached by a median sternotomy or left or right thoracotomy, depending on its location in the heart. Surgical treatment strategies include simple excision, as in our patient, excision with pericardial patch reconstruction, autotransplantation after tumor excision, and orthotopic cardiac transplantation, and the most appropriate approach is selected according to the extent and location of the tumor. Heart–lung transplantation has been reported

as an option in patients with primary cardiac synovial sarcomas with no evidence of metastatic spread[10]. In our patient, this approach was not an option because of metastatic involvement of the superior mediastinum.

A pericardial synovial sarcoma, like any other cardiac sarcoma, has a poor prognosis. The most common causes of death are local recurrence, even after complete macroscopic resection, and metastasis[11]. Adjuvant radiation therapy for a synovial sarcoma is known to help reduce the local recurrence rate in cases with or without positive margins and to prolong survival. However, cardiac radiation can lead to long-term cardiac damage. On comparing different regimens of chemotherapy, ifosfamide and doxorubicin combination therapy appears to be the most successful. However, the overall survival advantage associated with chemotherapy remains to be established in larger randomized multicenter trials[8,11].

In the present case, the anesthetic technique should be tailored to the presence of cardiac tamponade. The principal hemodynamic feature of cardiac tamponade is a decrease in cardiac output from a reduced stroke volume with an increase in central venous pressure.

As stoke volume remains relatively fixed, cardiac output becomes primarily dependent on the heart rate[12]. Induction of general anesthesia in a patient with a pericardial tumor is extremely dangerous and may cause cardiac arrest. In such patients, large-bore intravenous access is mandatory. Additionally, monitoring of the intra-arterial and central venous pressures is desirable. The anesthetic technique should maintain a high sympathetic tone until the tamponade is relieved[13]. Cardiac depression, vasodilation, and slowing of the heart rate should be avoided. Awake intubation with maintenance of spontaneous ventilation is theoretically desirable; however, coughing, straining, hypoxemia, and respiratory acidosis are detrimental and should be avoided. Ketamine is the anesthetic of choice for induction and maintenance of anesthesia until tumor removal. Epinephrine at a low dose (10 μg) may be useful as a temporary inotrope and chronotrope. Generous intravenous fluid administration is useful to maintain venous return[14].

In conclusion, we presented an extremely rare case of a primary pericardial synovial sarcoma. Surgical excision is the standard treatment for cardiac tamponade caused by tumor compression. Before surgery, the correct anesthesia protocol, including adequate monitors, large-bore intravenous access, ketamine induction, and possible awake intubation, should be selected to ensure successful surgery in patients with a pericardial synovial sarcoma.

References

1. Vander Salm TJ. Unusual primary tumors of the heart. Semin Thorac Cardiovasc Surg 2000; 12: 89-100. [PMID: 10807431 DOI: 10.1053/ct.2000.5080]
2. Khan H, Chaubey S, Edlin J, Wendler O. Primary cardiac synovial sarcoma. A rare tumor with poor prognosis. Asian Cardiovasc Thorac Ann 2014; 22: 835-838. [PMID: 24887816 DOI: 10.1177/0218492313483584]
3. Schaffer LR, Caltharp SA, Milla SS, Kogon BF, Cundiff CA, Dalal A, Quigley PC, Shehata BM. Rare presentation of four primary pediatric cardiac tumors. Cardiovasc Pathol 2016; 25: 72-77. [PMID: 26419627 DOI: 10.1016/j.carpath.2015.08.011]
4. Hudzik B, Miszalski-Jamka K, Glowacki J, Lekston A, Gierlotka M, Zembala M, Polonski L, Gasior M. Malignant tumors of the heart. Cancer Epidemiol 2015; 39: 665-672. [PMID: 26239627 DOI: 10.1016/j.canep.2015.07.007]
5. Akerström F, Santos B, Alguacil AM, Orradre JL, Lima P, Zapardiel S. Pericardial synovial sarcoma. Thorac Cardiovasc Surg 2011; 59: 175-177. [PMID: 21480141 DOI: 10.1055/s-0030-1250336]
6. Suster S, Moran CA. Primary synovial sarcomas of the mediastinum: a clinicopathologic, immunohistochemical, and ultrastructural study of 15 cases. Am J Surg Pathol 2005; 29: 569-578. [PMID: 15832079]
7. Phatak P, Khanagavi J, Aronow WS, Puri S, Yusuf Y, Puccio C. Pericardial synovial sarcoma: challenges in diagnosis and management [version 2; referees: 2 approved, 1 approved with reservations]. F1000Res 2014; 3: 15. [PMID: 24715974 DOI: 10.12688/f1000research.3-15.v2]
8. Myers P, Konstantinidis S, Karatzas N, Milas F, Panos A. Pericardial synovial sarcoma of the heart; is it always worth operating? J Cardiovasc Surg (Torino) 2011; 52: 749-751. [PMID: 21894142]
9. Saraiva J, Antunes PE, Carvalho L, Antunes MJ. Primary Malignant Cardiac Tumors: Surgical results. Rev Port Cardiol 2016; 35: 199-204. [PMID: 26992743 DOI: 10.1016/j.repce.2016.03.003]
10. Perek B, Tomaszewska I, Stefaniak S, Bartczak A, Jemielity M. Early and long-term outcomes of pericardiotomy in the treatment of primary cardiac tamponade. Kardiochir Torakochirurgia Pol 2015; 12: 191-194. [PMID: 26702272 DOI: 10.5114/kitp.2015.54451]
11. White RW, Rushbrook J, Sivananthan MU, McGoldrick JP. Primary cardiac synovial sarcoma with imminent tricuspid valve obstruction. Ann Thorac Surg 2009; 87: 322. [PMID: 19101330 DOI: 10.1016/j.athoracsur.2008.03.067]
12. Sánchez-Enrique C, Nuñez-Gil IJ, Viana-Tejedor A, De Agustín A, Vivas D, Palacios-Rubio J, Vilchez JP, Cecconi A, Macaya C, Fernández-Ortiz A. Cause and Long-Term Outcome of Cardiac Tamponade. Am J Cardiol 2016; 117: 664-669. [PMID: 26718232 DOI: 10.1016/j.amjcard.2015.11.023]

13. Maxwell BG, Harrington KB, Kelly NE. Anesthetic management for reentry sternotomy in a patient with a full stomach and pericardial tamponade from left ventricular rupture. Ann Card Anaesth 2013; 16: 51-53.
[PMID: 23287087 DOI: 10.4103/0971-9784.105371]

14. Grocott HP, Gulati H, Srinathan S, Mackensen GB. Anesthesia and the patient with pericardial disease. Can J Anaesth 2011; 58: 952-966.
[PMID: 21789738 DOI: 10.1007/s12630-011-9557-8]

原發性心包膜滑膜肉瘤所造成的心包填塞：病例報告

張中沛[1] 楊雅玲[2] 孫懋昇[1,*]

秀傳紀念醫院 麻醉科[1] 心臟內科[2]

受文日期：民國 105 年 07 月 22 日；接受刊載：民國 105 年 09 月 16 日

摘要

心包膜的原發性滑膜肉瘤是極其罕見的。我們報告了一位 47 歲男性因為突發性胸痛和呼吸急促而急診入院的病例。經由電腦斷層掃描和胸前心臟超音波檢查，我們在左心房二尖瓣的位置發現了一個明顯的巨大心包膜腫瘤。該病患因此被診斷為心包膜腫瘤所造成的心包填塞，並且立即在全身麻醉之下進行手術切除治療。隨後的組織學分析證實為原發性心包膜滑膜肉瘤。

關鍵詞：原發性心包膜滑膜肉瘤、心包填塞、全身麻醉

* 通訊作者：孫懋昇醫師 秀傳紀念醫院麻醉科主任 500 彰化縣彰化市中山路一段 542 號

Tungs' Medical Journal 12 (2018) 48-54

Case Report

Esophageal Gastrointestinal Stromal Tumor: One Case Report and Review of Literatures

Cheng-Yu Hsu[1], Chung-Cheng Liu[1,*], Lien-Fu Lin[1], Jong-Shiaw Jin[2], Chia-Herng Yue[3]

[1]Department of Gastroenterology, [2]Pathology, [3]General Surgery, Tungs' Taichung Metroharbor Hospital, Taichung, Taiwan

Received: Nov. 03, 2016; Accepted: Dec. 23, 2016

Abstract

Esophageal gastrointestinal stromal tumors (GIST) are rare, and complete surgical resection is the standard treatment. Because of their rarity, the natural clinical course, management, and prognosis of esophageal GISTs remain unclear. In particular, small (<2 cm) esophageal GISTs and microGISTs (<1 cm) pose management challenges. We report the case of a 55-year-old female. Her esophageal microGIST, located in the upper third of the esophagus, maintained a stable size of 0.8 cm for 5 years. The pathological risk assessment for this lesion was "very low risk of malignancy." We present the case of this patient and review the relevant literature.

Key words: Gastrointestinal stromal tumor, Upper GI Endoscopy, Endoscopic ultrasound, subepithelial tumor, Submucosal lesion, Endoscopic submucosal dissection

After the discovery of c-Kit mutations, it became possible to accurately diagnose gastrointestinal stromal tumors (GISTs) and differentiate them from other mesenchymal tumors. Moreover, use of imatinib mesylate provided a new therapeutic option. Consequently, interest in these tumors increased and their management and prognosis has been extensively investigated and standardized.

GISTs are the most common mesenchymal neoplasms of the gastrointestinal tract. However, esophageal GISTs are rare among mesenchymal esophageal tumors. Because of the rarity of esophageal GISTs, their natural clinical course, management, and prognosis are unclear. In particular, small (<2 cm) esophageal GISTs and microGISTs (<1 cm) pose unique management challenges. Here we present the case of a patient with an esophageal microGIST and review the relevant literature.

*Correspondence to: Chung-Cheng Liu, MD., Department of Gastroenterology, Tungs' Taichung Metro Harbor Hospital, No. 699, Sec. 8, Taiwan Blvd., Wuqi Dist., Taichung City 43503, Taiwan (R.O.C.)

Case presentation

A 55-year-old female had a past history of viral hepatitis B under stable drug control. She developed invasive ductal carcinoma of the right breast and underwent right simple mastectomy and right axillary sentinel lymph node biopsy. After implantation of left-side Port-A on April 7, 2015, she received neoadjuvant chemotherapy and exhibited pathological complete response.

Approximately 5 years ago, she suffered from epigastric pain and acid regurgitation for approximately 1 month. Esophagogastroduodenoscopy (EGD) performed on November 22, 2011 revealed gastroesophageal reflux disease (GERD) (grade A) and a subepithelial esophageal lesion approximately 0.8 cm in size, located 21 cm from the incisor tooth (IT). We suspected leiomyoma. The esophageal lesion was biopsied, and it proved to be an esophageal GIST. The pathological findings of immunohistochemical staining revealed the following: smooth muscle actin: 90%, +++ in tumor; S100: 20%, ++ in tumor; c-Kit (CD117): positive in tumor cells, 20%, ++; spindle cell type; mitotic rate: no mitosis; histologic grade: G1, low grade with a mitotic rate of ≤5/50 high-power

field. From these findings, she was diagnosed with GIST, determined to be at very low risk of malignancy.

Endoscopic ultrasound (EUS) was performed on December 8, 2012, using a 12-MHz miniprobe. EUS showed an esophageal GIST (confirmed via biopsy on November 22, 2011). The lesion arose from the second layer of the esophagus, measuring 0.8 cm in size with a homogenously hypoechoic pattern. No periesophageal lymph nodes were detected.

Repeat EGD and EUS on March 3, 2016 confirmed the above findings (Fig. 1 and 2). The subepithelial tumor of the esophagus, located 21 cm from IT and measuring 0.8 cm, remained the same size for 5 years. The pathological figures 3–6 show the c-Kit (CD117), spindle cell, S100 nerve, smooth muscle actin, and tumor cell positivity.

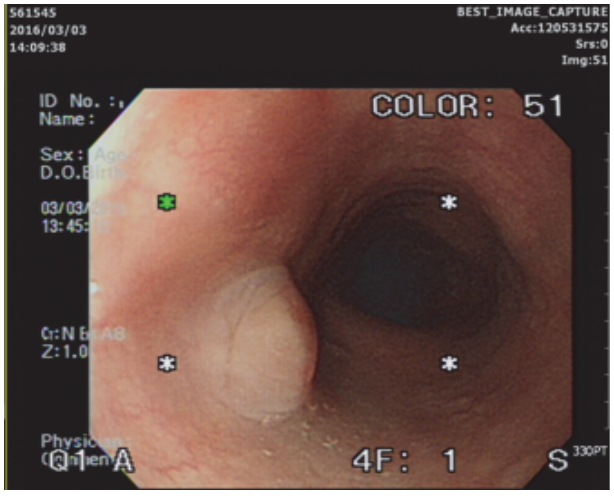

Fig. 1 EGD revealed: Esophageal lesion, a subepithelial lesion about 0.8 cm at 21 cm from incisor tooth.

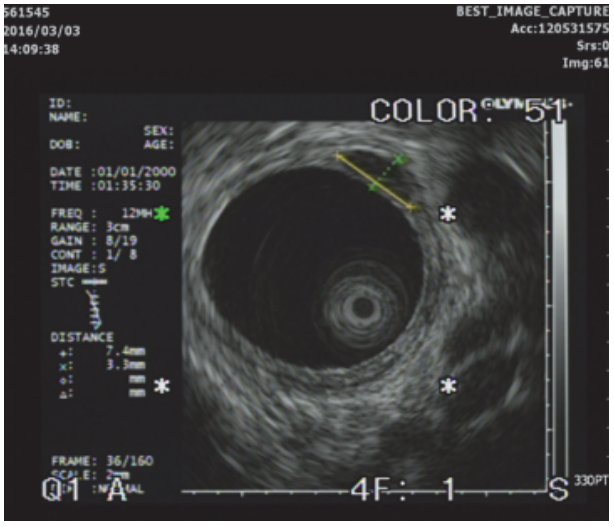

Fig. 2 EUS revealed: The lesion arised from 2nd layer of esophagus, measuring 0.8cm in size, homogenously hypoechoic pattern, no peri-esophageal LN.

Discussion

Incidence, sex, and age

GISTs are the most common mesenchymal tumors of the gastrointestinal tract[1], occurring predominantly in the stomach (60%–70%), followed by the small intestine (20%–30%)[2–5]. In contrast, esophageal GISTs are extremely uncommon, accounting for <2% of all GISTs. Other reports indicate that esophageal GISTs only account for 0.7% of all GISTs[6,7]. Esophageal leiomyomas, in contrast, are the most common mesenchymal tumors of the esophagus but are seldom found in other regions of the gastrointestinal tract[5].

Most patients with GIST are aged 40–80 years, with a median age at diagnosis of 60 years[8-9]. Regarding sex ratios, the male to female ratio was previously reported to be 3:2[6]. Our patient was a female diagnosed with esophageal GIST at the age of 55 years.

Clinical characteristics and symptoms

Fan Feng et al. reported that the most common symptom was dysphagia (38.76%), followed by chest pain (14.68%), bleeding (8.26%), and other symptoms including fatigue, cough, and dyspnea (9.17%)[6].

Our patient was incidentally diagnosed with esophageal GIST during an endoscopic examination for GERD; however, no symptoms were related to the upper esophageal GIST itself, possibly owing to its small size of 0.8 cm.

Esophageal location of GIST and interstitial cells of Cajal

The most common location of esophageal GISTs is the lower esophagus (86.84%), followed by the middle (11.40%) and upper esophagus (1.76%). GISTs arise from interstitial cells of Cajal (ICCs). Thus, the esophageal location of some GISTs may be attributed to the distribution of ICCs throughout the esophagus[10]. The authors investigated the distribution of ICCs in the human embryonal and fetal esophagus. They found that ICCs were abundant in the lower esophagus, less numerous in the middle esophagus,

and rare in the upper esophagus. This confirmed the fact that the distribution of ICCs was in accordance with the distribution of esophageal GISTs and appeared to mirror it. Our patient exhibited a rare case of esophageal GIST located in the upper third of the esophagus.

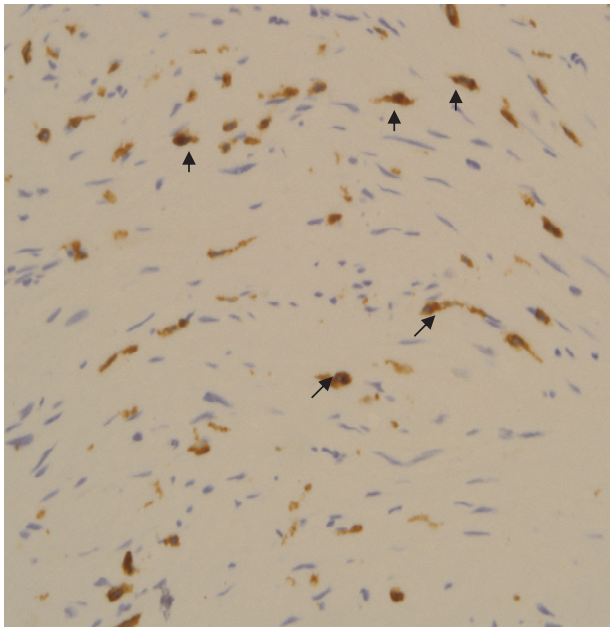

Fig. 3 C-Kit immunohistochemistry stains of spindle tumor cells.

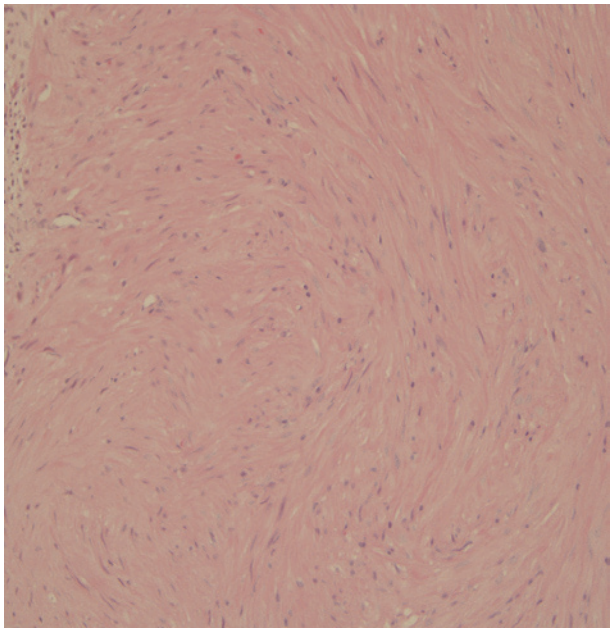

Fig. 4 H & E stains of spindle tumor cells.

Diagnosis

Preoperative diagnosis of esophageal GIST is difficult because of its rarity and submucosal location. The rate of accurate identification of the causes of submucosal lesions (SML) by endoscopy alone is only 40%[16]. EUS can provide information about the echoarchitecture and origin layer of SML. This information may be helpful for reaching a definite diagnosis or narrowing the diagnostic possibilities. On EUS,

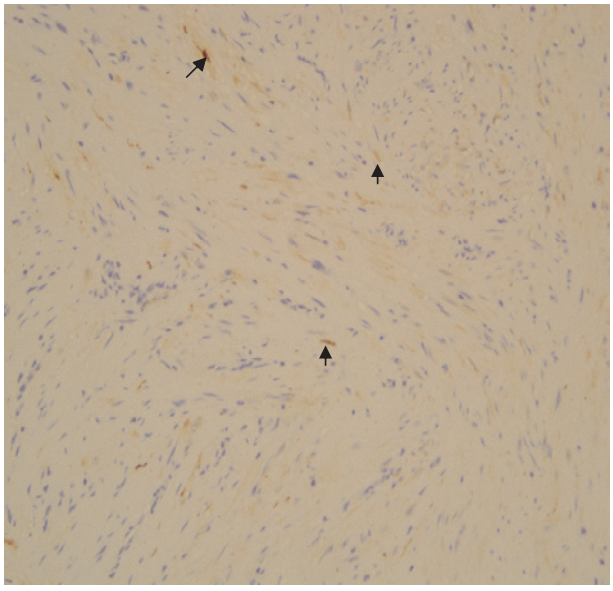

Fig. 5 S-100 immunohistochemistry stains of spindle tumor cells.

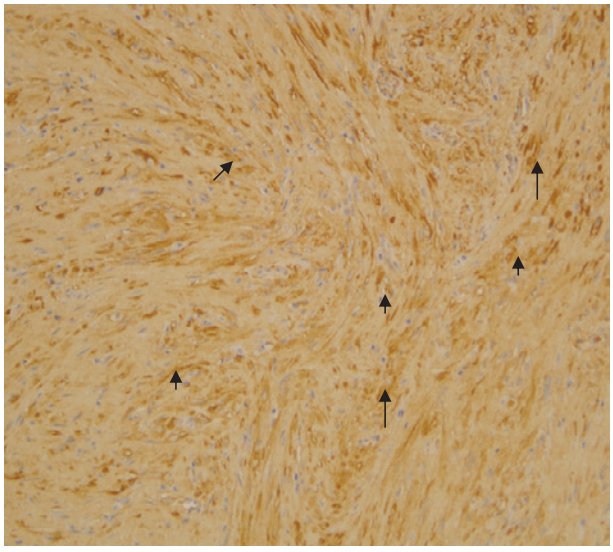

Fig. 6. Immunohistochemistry stain of smooth muscle actin in spindle tumor cells.

a GIST appears as a hypoechoic tumor arising from the fourth sonographic layer (muscularis propria) or arising from the second sonographic layer (muscularis mucosa). The appearance of GIST on EUS resembles other mesenchymal tumors, such as leiomyomas and schwannomas, rendering diagnosis based on EUS alone difficult[8].

Although EUS can provide more information than endoscopy, it is not an accurate means of carrying out differential diagnosis because of overlapping echo and endoscopic features. Thus, biopsy specimen analysis is often necessary. The immunohistochemical demonstration of c-Kit (CD117) expression is presently the most important diagnostic criteria for GIST[4].

Endoscopic biopsies of GIST are frequently nondiagnostic, except in the setting of an ulcerated mass. Hence, EUS-guided fine needle aspiration biopsy is most commonly used to make a tissue diagnosis of SML, when required[8]. In our patient, endoscopic biopsy of the small esophageal SML was fortunately proved to be GIST.

Management

From the guidelines of the National Comprehensive Cancer Network (NCCN)[12] and the European Society of Medical Oncology (ESMO)[13], all GISTs ≥2 cm in size require resection. Unfortunately, there is no consensus on the management of smaller GISTs. Furthermore, the natural history of smaller GISTs (1–2 cm), including their growth rate and metastatic potential, remains unknown. The optimal frequency of follow-up and specific risks associated with this strategy are also unclear. Successful endoscopic resection is reported, but remains controversial because of the risk of positive margins, tumor spillage, and perforation[12].

An algorithmic approach for the management of gastric GISTs based on size and EUS findings has been proposed[14]. This approach was adopted by NCCN[12] for gastric GISTs, but not for GISTs at other sites throughout the gastrointestinal tract.

Esophageal GISTs and small GISTs

Esophageal GISTs are more difficult to manage than GISTs arising from the serosa-lined intraabdominal organs because of the lack of tumor confinement by a serosal layer. In addition, there is a relative contraindication to segmental resection given the blood supply of the esophagus. Although local resection of small tumors confined to the wall of the distal esophagus is reasonable if negative resection margins can be achieved[1,15], an open en bloc esophagectomy may be required for tumors ≥2 cm in size and for those involving the gastroesophageal junction.

The optimal management of esophageal GISTs <2 cm in size is controversial. ESMO guidelines recommend EUS and follow-up, reserving excision only for those esophageal nodules that increase in size[13]. Canadian guidelines suggest that all GISTs, even those <1 cm, should be excised because of the risk of metastases[16].

A study by Kawanowa et al.[17] demonstrated that the incidence of subclinical GISTs is higher than expected. Their findings were consistent with those reported by Agaimy et al.[18], who found that gastric GISTs <1 cm were present in 22.5% of 98 consecutive adult autopsies, confirming their high frequency. GISTs <6 mm have also been reported in approximately 10% of gastroesophageal junction resections[19,20].

GISTs affect approximately 0.0014% of the population, and microGISTs are detected in approximately 20%–30% of elderly individuals. This suggests that microGISTs likely represent premalignant lesions that evolve into overt GISTs in only a very small fraction of cases. MicroGISTs display an overall lower frequency of mutations, particularly canonical KIT mutations, and also carry rare and novel mutations. These molecular features, together with the peculiar pathological characteristics, suggest that the proliferation of these lesions is likely sustained by weakly pathogenic molecular events, supporting the epidemiologic evidence that microGISTs seemed to be self-limiting lesions. However, the malignant potential of these lesions should be kept in mind at all times.

At present, all guidelines recognize that the management of small incidentally discovered GISTs remains controversial. Taken together, these guidelines suggest that surveillance is probably a safe approach for the management of an asymptomatic patient with an incidentally discovered small GIST (<2 cm) without suspicious EUS features such as irregular borders, cystic spaces, ulceration, echogenic foci, or heterogeneous appearance[14,21].

With the development of endoscopic resection therapies for subepithelial tumors, ESD has become a popular therapeutic choice[22-25]. The efficiency and

safety of ESD in the management of gastric SMTs is good[23,24], in addition to the management of SMTs of the gastroesophageal junction originating from the muscularis propria layer[25]. A study by Zhi-Gang Huang et al.[26] reported that 20 patients with esophageal and gastric SMTs emerging from the muscular layer underwent ESD and achieved very good results. The authors concluded that ESD for SMTs is a relatively safe and feasible technique to treat small SMTs <3 cm in the upper gastrointestinal tract. However, further clinical trials involving many more subjects and a longer follow-up period are needed.

Conclusion

Esophageal GIST is a rare disease, and the diagnosis and management of these lesions is challenging. Esophageal GISTs are difficult to diagnose without preoperative tissue biopsy. Complete resection of the tumor is sufficient for small, less-mitotic GISTs. Esophagectomy and imatinib mesylate therapy should be considered for patients with large or highly mitotic tumors.

At present, there are insufficient data to guide the management of GISTs <1 cm that are incidentally discovered on endoscopy. These lesions rarely exhibit clinical progression, thereby supporting the epidemiologic evidence that microGISTs are self-limiting lesions. As illustrated in this case, the patient's esophageal microGIST did not change in size for over 5 years. However, because it was a GIST, the malignant potential was still present. Therefore, endoscopic resection, such as ESD, seemed a safe and reasonable therapeutic choice.

References

1. H. J.Lee, S. I.Park, D. K. Kim, and Y.H. Kim, "Surgical resection of esophageal gastrointestinal stromal tumors," The Annals of Thoracic Surgery, vol. 87, no. 5, pp. 1569-1571, 2009.
2. Abraham SC, Krasinskas AM, Hofstetter WL, Swisher SG, Wu TT. "Seedling" mesenchymal tumors (gastrointestinal stromal tumors and leiomyomas) are common incidental tumors of the esophagogastric junction. Am J Surg Pathol 2007; 31: 1629-35.
3. Ji F, Wang ZW, Wang LJ, Ning JW, Xu GQ. Clinicopathological characteristics of gastrointestinal mesenchymal tumors and diagnostic value of endoscopic ultrasonography. J Gastroenterol Hepatol 2008; 23(pt 2): e318-24.
4. Miettinen M, Lasota J. Gastrointestinal stromal tumors: review on morphology, molecular pathology, prognosis, and differential diagnosis. Arch Pathol Lab Med 2006; 130: 1466-78.
5. Miettinen M, Sarlomo-Rikala M, Sobin LH, Lasota J. Esophageal stromal tumors: a clinicopathologic, immunohistochemical, and molecular genetic study of 17 cases and comparison with esophageal leiomyomas and leiomyosarcomas. Am J Surg Pathol 2000; 24: 211-22. (original ref. 4)
6. Fan Feng, PhD, Yangzi Tian, MD, Zhen Liu, MM, Guanghui Xu, MM, Shushang Liu, MM, Man Guo, BM, Xiao Lian, MStat, Daiming Fan, PhD, and Hongwei Zhang, PhD, Clinicopathologic features and clinical outcomes of esophageal gastrointestinal stromal tumor: evaluation of a pooled case series. Medicine Volume 95, Number 2, January 2016, e2446.
7. C. D. M. Fletcher, J. J. Berman, C. Corless et al., "Diagnosis of gastrointestinal stromal tumors: a consensus approach," Human Pathology, vol. 33, no. 5, pp. 459-465, 2002.
8. V. Bhatia, M. Tajika, and A. Rastogi, "Upper gastrointestinal submucosal lesions—clinical and endosonographic evaluation and management," Tropical gastroenterology, vol. 31, no. 1, pp. 5-29, 2010.
9. DeMatteo RP, Lewis JJ, Leung D, Mudan SS, Woodruff JM, Brennan MF. Two hundred gastrointestinal stromal tumors: recurrence patterns and prognostic factors for survival. Ann Surg. 2000; 231: 51-8.
10. Radenkovic G, Ilic I, Zivanovic D, et al. C-kit-immunopositive interstitial cells of Cajal in human embryonal and fetal esophagus. Cell Tissue Res. 2010; 340: 427-436.
11. Rosch T, Kapfer B, Will U, et al. Accuracy of endoscopic ultrasonography in upper gastrointestinal submucosal lesions: a prospective multicenter study. Scand J Gastroenterol 2002; 37: 856-62.
12. Demetri, GD, Benjamin, RS, Blanke, CD, et al. NCCN task force report: optimal management of patients with gastrointestinal stromal tumor (GIST)- Update of NCCN Clinical Practice Guidelines J Natl Comprehensive Cancer Network. 2007; 5(2 suppl): S-1.
13. Casali PG, Jost L, Reichardt P, Schlemmer M, Blay JY, ESMO Guidelines Working Group. Gastrointestinal stromal tumours: ESMO clinical recommendations for diagnosis, treatment and follow-up. Ann Oncol. 2009; 20 Suppl 4: 64.
14. Sepe PS, Brugge WR. A guide for the diagnosis and management of gastrointestinal stromal cell tumors. Nat Rev Gastroenterol Hepatol. 2009; 6(6): 363.
15. Blum MG, Bilimoria KY, Wayne JD, et,al. Surgical considerations for the management and resection of esophageal gastrointestinal stromal tumors. Ann Thorac Surg. 2007; 84(5): 1717-1723.
16. Blackstein ME, Blay JY, Corless C, Driman DK, Riddell R, Soulières D, Swallow CJ, Verma S, Canadian Advisory Committee on GIST. Gastrointestinal stromal tumours: consensus statement on diagnosis and treatment. Can J Gastroenterol. 2006; 20(3): 157.
17. Kawanowa K, Sakuma Y, Sakurai S, et al. High incidence of microscopic gastrointestinal stromal tumors in the stomach. Hum Pathol. 2006; 37: 1527-1535.
18. Agaimy A, Dirnhofer S, Wunsch PH, et al. Multiple sporadic gastrointestinal stromal tumors (GISTs) of the proximal stomach are caused by different somatic KIT mutations suggesting a field effect. Am J Surg Pathol. 2008; 32: 1553-1559.
19. Abraham SC, Krasinskas AM, Hofstetter WL, et al. "Seedling" mesenchymal tumors (gastrointestinal stromal tumors and leiomyomas) are common incidental tumors of the esophagogastric junction. Am J Surg Pathol. 2007;

31: 1629-1635.
20. Agaimy A, Wunsch PH. Sporadic Cajal cell hyperplasia is common in resection specimens for distal oesophageal carcinoma. A retrospective review of 77 consecutive surgical resection specimens. Virchows Arch. 2006; 448: 288-294.
21. Hwang, J. H., rulyak, s. D. & Kimmey, M. B. American Gastroenterological Association institute technical review on the management of gastric subepithelial masses. Gastroenterology 130, 2217-2228 (2006).
22. Pedro Pimentel-Nunes, Mário Dinis-Ribeiro, Thierry Ponchon, Endoscopic Submucosal dissection: European Society of Gastrointestinal Endoscopy(ESGE) Guideline. Endoscopy 2015; 47(09): 829-854.
23. Huang LY, Cui J, Lin SJ, et al. Endoscopic full-thickness resection for gastric submucosal tumors arising from the muscularis propria layer. World J Gastroenterol 2014; 20: 13981-13986.
24. He Z, Sun C, Wang J, et al. Efficacy and safety of endoscopic submucosal dissection in treating gastric subepithelial tumors originating in the muscularis propria layer: A single-center study of 144 cases. Scand J Gastroenterol 2013; 48: 1466-1473.
25. Li QL, Yao LQ, Zhou PH, et al. Submucosal tumors of the esophagogastric junction originating from the muscularis propria layer: A large study of endoscopic submucosal dissection (with video). Gastrointest Endosc 2012; 75: 1153-1158.
26. Zhi-Gang Huang, Xue-Song Zhang, Shi-Liang Huang, Xiao-Gang Yuan. Endoscopy dissection of small stromal tumors emerged from the muscularis propria in the upper gastrointestinal tract : Preliminary study. World J Gastrointest Endosc 2012 December 16; 4(12): 565-570.

食道基質瘤：一病例報告及文獻探討

徐承毓[1] 劉忠政[1,*] 林連福[1] 金忠孝[2] 于家珩[3]

童綜合醫療社團法人童綜合醫院 [1]內科部胃腸肝膽科 [2]病理科 [3]一般外科

受文日期：民國 105 年 11 月 03 日；接受刊載：民國 105 年 12 月 23 日

摘要

食道基質瘤是種罕見疾病，儘管完全的外科切除是標準的治療方法，但是由於食道基質瘤罕見，它們的自然臨床過程，處置方式及預後，都不清楚。尤其是小於 2 公分，甚至小於 1 公分的微基質瘤，它們處置的策略更具挑戰性。因此我們提出一個食道微基質瘤的病例報告並做文獻上的探討。我們提出的病例是 55 歲女性，她的食道基質瘤位於食道上段，且持續保持同一大小 0.8 公分，有五年之久，它病理的癌風險評估是“非常低癌症風險”。

關鍵詞：胃腸道基質瘤、上消化道內視鏡、內視鏡超音波、上皮下腫瘤、黏膜下病灶、內視鏡黏膜下剝離術

* 通訊作者：劉忠政醫師 童綜合醫療社團法人童綜合醫院內科部胃腸肝膽科 43503 臺中市梧棲區臺灣大道八段 699 號

Case Report

Tracheal Tuberculosis Diagnosed by Bronchoscopy: A Case Report

Chia-Te Huang*

Thoracic Department, Show Chwan Memorial Hospital, Changhua

Received: May. 20, 2016; Accepted: Oct. 06, 2016

Abstract

A 35-year-old male presented to our hospital with persistent cough. Previous visits and examinations elsewhere included chest computed tomography scans and chest X-ray with no specific diagnosis found. Because a tracheal or bronchial lesion was suspected, bronchoscopy was performed, and caseous lesions were found isolated throughout a large area. Tracheal tuberculosis was suspected. Sputum was sampled after bronchoscopy and stained for acid-fast bacilli with a positive result. Biopsy was obtained via bronchoscopy and cultured for *Mycobacterium tuberculosis* with a positive result. Antituberculosis therapy resulted in a smooth progress. Steroids were administered to prevent stenosis caused by scar formation. An acid-fast bacilli test and *M. tuberculosis* culture revealed negative results after 4 months of continuous treatment and follow-up.

Key words: Bronchoscopy, Acid-fast bacilli, Mycobacterium tuberculosis, Tracheal tuberculosis

Introduction

Tracheal tuberculosis (TB) is uncommon [1]. General symptoms are persistent cough, dyspnea, hoarseness, and stridor. Chest X-ray (CXR) generally shows normal results with a clear image in the lung area [2]. In general, for patients with tracheal TB, histological examination by sputum smears stained for acid-fast bacilli (AFB) and biopsy culture for *Mycobacteria tuberculosis* do not always reveal positive results [3]. In the early stage, patients with tracheal TB are usually treated for asthma or bronchiolitis, and even in serious situations, patients can be misdiagnosed with lung cancer [4]. Thus, bronchoscopy is a requirement for the diagnosis of tracheal TB. Computed tomography (CT) scans have also been suggested [2, 5]. Herein, we report a 35-year-old male with chronic cough but a clear CXR. Tracheal TB was suspected via bronchoscopy. Antituberculosis therapy in combination with steroids revealed a smooth progress.

*Correspondence to: Chia-Te Huang, MD. Thoracic Department, Show Chwan Memorial Hospital, Changhua, No. 542, Sec. 1, Chung-Shan Rd., Changhua, 500, Taiwan (R.O.C.)

Case Report

A 35-year-old male patient presented to our hospital complaining of chronic cough with yellow sputum retention, hiccup, some chest tightness, and postnasal drip. Auscultation revealed lung rales or wheeze. Blood pressure was 121/81 mmHg, with a heart rate of 97 beats per minute and body weight of 68 kg. Laboratory workup showed a hemoglobin of 15.7 g/dL, hematocrit of 45.6%, white blood count (WBC) of 4900/uL, and platelet count of 185,000/uL. Blood chemistry showed blood urea nitrogen (BUN) of 11 mg/dL, creatinine of 0.72 mg/dL, glutamic oxaloacetic transaminase (GOT) of 18 U/L, glutamic pyruvic transaminase (GPT) of 19 U/L, alkaline phosphatase of 249 U/L, and uric acid of 4.6 mg/dL. Chest CT scans and CXR performed elsewhere revealed no specific diagnosis. He was referred for bronchoscopy because the CXR results showed only increased infiltration of the left lower lobe (LLL) of the lung.

Bronchoscopy revealed that the vocal cord was normal, the carina was sharp and not fixed, and the bronchial tree was patent bilaterally. However, the middle and lower trachea showed irregular swelling

of the mucosa with a necrotic surface (Fig. 1). The lesion extended to the orifice of the right main bronchus. Isolated tracheal or bronchial TB or malignancy was suspected and treated with antibiotics. Bronchial biopsy of the tracheal lesion was smoothly performed, and the specimens were sent for pathological examination.

The specimen section under microscopy revealed necrotic tissue with acute and chronic inflammatory cell infiltration. AFB were positive with special stain. No visible tissue was observed. Immunohistochemical stains for AE1/AE3, TTF-1, and CD56 were also negative. Pathological diagnosis was a mycobacterial infection, consistent with TB, and tissue culture was suggested. Antituberculosis therapy was continued while steroids were administered to prevent scar formation and tracheal stenosis. AFB were isolated upon further ABF culture using the Mycobacteria Growth Indicator Tube (MGIT) method on December 9, 2014. Immunochromatographic assay (ICA) revealed growth of *M. abscessus* on December 11, 2014 and *M. tuberculosis* on December 18, 2014. Follow-up AFB culture and ICA of a sputum specimen in February 2015 remained positive for AFB and *M. abscessus* but not for *M. tuberculosis*.

The patient was followed up for tracheal TB by bronchoscopy at our outpatient department. The vocal cord was normal, carina was sharp, and right main bronchus showed minimal narrowing of the orifice. The lower trachea showed resolution of the previous lesion. The lower third mucosa showed some erythema and mild focal scar formation with

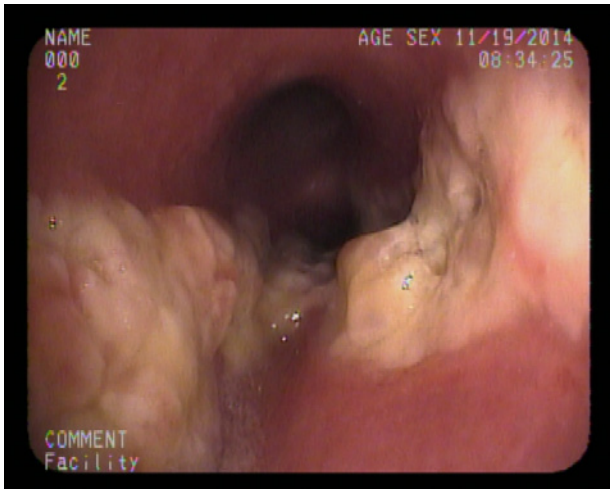

Fig. 1 Caseous lesions are found isolated throughout a large area on bronchoscopy.

significant narrowing of the lumen. Follow-up in May 2015 showed a normal CXR, negative AFB stain test, and no growth of AFB.

Discussion

According to statistics, the incidence of tracheobronchial TB is 10%–36.8% of patients with pulmonary TB [3, 5]. In particular, tracheal TB is an uncommon form of pulmonary TB with fewer than 150 reported cases [1]. Research reported that there are more female patients with tracheal TB than male patients. Most of these cases were primarily involved with the main trachea. The tracheobronchial lumen was reportedly thinner in females than in males, making it weaker against direct invasion of *M. tuberculosis* [2].

The etiological sources of tracheal TB were sputum infection by other patients, lymphatic fluid infection, lymph node erosion, expansion of infection from a nearby location, and extension of hematological infections. If the tracheal TB was due to spread from the lymphatic submucosa, negative results have been reported for the sputum smear stain of AFB [1, 5, 6]. The foci in our case were found in the distal trachea on bronchoscopy. No lesions were found in the bronchi and lung areas. This indicated that tracheal TB in our case was not due to infection from nearby locations. It was more likely due to a higher chance of implantation of AFB or spread from the lymphatic submucosa [5].

The most common symptoms of tracheal TB are chronic cough, with an occasionally bloody sputum, dyspnea, and chest pain, accompanied with fever, weight loss, and night sweats [2, 6]. Infection with *M. tuberculosis* would present in some patients with caseous material deposited in the lumen of the trachea, resulting in obstruction of airflow. At the expiratory stage, airflow went through the narrowing airway, causing hoarseness, stridor, and wheezing detected during auscultation. Occasionally, CXRs were normal with clear images at the lung areas. Serious cases of obstruction may cause atelectasis of the lungs [2]. Histopathological examinations of tracheal TB include microscopic examination of the AFB with special stain and culture for *M. tuberculosis*. However, sputum smears stained for AFB and biopsy culture for *M. tuberculosis* do not always reveal positive results for tracheal TB [3]. In addition, if the

infections were spread from lymphatic submucosal areas, tests for AFB may be negative [5]. Our case revealed intermittent negative results for sputum smears stained for AFB and biopsy culture for *M. tuberculosis*. This is similar to findings reported in the literature. A prolonged observation is required for patients with tracheal TB showing this phenomenon. The duration from observation of cough to diagnosis of tracheal TB took an average of 6 months. In other words, the difficulty in the diagnosis of tracheal TB is that it usually takes a long time before correct treatments can be given. In some patients with mild symptoms, tracheal TB was usually treated for asthma or bronchiolitis, whereas some patients with serious symptoms were misdiagnosed with lung cancer [4]. For this reason, bronchoscopy is required to rule out the diagnosis of tracheal TB with unexplained persistent cough. CT scans have also been suggested as a supportive diagnostic tool [2, 5].

Patients with tracheal TB should be treated with antituberculosis therapy, which requires a long compliance with medication. For drug resistance in many mycobacteria species, drug susceptibility testing is required to select appropriate medications [4, 7]. Steroids are prescribed to control tracheal stenosis and bronchi; however, further empirical evidence is required to elucidate which subtypes are suitable for the use of steroids [3].

Bronchoscopy is useful to distinguish the subtypes of tracheal TB, including the stenotic type with and without fibrosis, and actively caseating, tumorous, ulcerative, granular, and nonspecific bronchitic types. The most common bronchoscopic manifestations are mucosal granularity with or without caseous material and mucosal ulceration in actively caseous diseases. Extensive granulation tissue associated with these ulcerations narrows the lumen. Two of three patients with the caseating subtype of tracheal TB have shown sequelae of tracheal stenosis caused by fibrosis [1]. Tracheobronchial TB can lead to tubercle formation in the lumen of the trachea or bronchi. Mucosa and submucosa can be destroyed, and tracheobronchial narrowing can occur due to fibrosis. Bronchoscopy has an important role in detecting tracheobronchial stenosis. Caseous tracheal TB requires early detection and prevention of stenosis as well as wall thickening of the trachea or bronchi to avoid permanent narrowing of the airways [5].

Standard antituberculosis regimens can be provided for effective treatment of tracheal TB, but the formation of tracheal stenosis for some subtypes of the disease is unavoidable. Early treatment with antituberculosis therapy in combination with steroid medications can effectively control tracheal stenosis. Sequelae can be effectively diminished if an early diagnosis is made before fibrosis formation. Our case was treated with antituberculosis therapy, and steroids were prescribed because tracheal TB was suspected. There was a smooth progress of recovery, and stenosis was effectively prevented.

Conclusion

Tracheal TB should be highly suspected by clinicians in patients with unexplained chronic and persistent cough. CXR, AFB test, and mycobacteria culture can present negative results. The use of bronchoscopy can be helpful in detecting tracheal TB. Antituberculosis therapy in combination with steroids can effectively treat the patient and prevent tracheal stenosis.

References

1. Smati, B., et al., Tuberculosis of the Trachea. The Annals of Thoracic Surgery, 2006; 82(5): 1900-1901.
2. Cary, C., et al., A rare case of fibrostenotic endobronchial tuberculosis of trachea. Annals of Medicine and Surgery, 2015; 4(4): 479-482.
3. Rikimaru, T., et al., Diagnostic features and therapeutic outcome of erosive and ulcerous endobronchial tuberculosis. The International Journal of Tuberculosis and Lung Disease, 1998; 2(7): 558-562.
4. Hochhegger, B., G. Zanetti, and E. Marchiori, Mass invading the trachea: a rare presentation of tuberculosis simulating lung cancer. Infection, 2013; 41(2): 599-600.
5. Kim, Y., et al., Tuberculosis of the trachea and main bronchi: CT findings in 17 patients. American Journal of Roentgenology, 1997; 168(4): 1051-1056.
6. Knappe, M.V., J.W. Schneider, and R. Gregor, Pathologic quiz case 2. Archives of Otolaryngology–Head & Neck Surgery, 1998; 124(4): 469-471.
7. Mok, J.H., et al., Extensively drug-resistant tuberculosis presenting as primary lymphadenitis eroding into the trachea in an immunocompetent patient. Journal of the Formosan Medical Association, 2014; 113(10): 764-765.

以支氣管鏡診斷之氣管結核病例報告

黃嘉德*

彰化秀傳紀念醫院　胸腔內科

受文日期：民國 105 年 05 月 20 日；接受刊載：民國 105 年 10 月 06 日

摘要

一名 35 歲男性病患因久咳不癒至本院求診，先前於友院電腦斷層及胸部 X 光均無法確認診斷。本院診斷疑似氣管或支氣管損傷，因此進行支氣管鏡檢查，發現大面積分散之乳酪狀損傷。因此診斷為氣管結核。後來的痰液採檢嗜酸性菌染色結果陽性，支氣管鏡採檢體培養結核桿菌結果陽性。抗結核菌治療結果反應良好，為避免疤痕形成導致氣管狹窄，給予類固醇治療。經 4 個月後的持續治療與追蹤，嗜酸性菌檢查及結核桿菌培養均呈陰性。

關鍵詞：支氣管鏡檢查、嗜酸性菌、結核桿菌、氣管結核

* 通訊作者：黃嘉德醫師　彰化秀傳紀念醫院胸腔內科主治醫師　500 彰化縣彰化市中山路一段 542 號

Case Report

Pelvic Presentations of Dengue fever in female, Mimicking a Pelvic Inflammatory Disease

Chui-Na Wong*

Department of Obstetrics and Gynecology, Show Chwan Memorial Hospital, Changhua, Taiwan

Received: May. 20, 2016; Accepted: Oct. 06, 2016

Abstract

Dengue is caused by infected mosquito bites. There are four viral serotypes that cause dengue: dengue virus 1 (DENV-1), DENV-2, DENV-3, and DENV-4. The vector mosquito harbors the virus and transmits it when it bites a person. The population of Tainan or of that of the south of Taiwan experienced the largest outbreak of dengue fever in an endemic area in 2014 with at least 15,000 reported cases. In this case study, we report a delayed and unusual case of dengue fever that was misinterpreted as female pelvic inflammatory disease. A 40-year-old, multiparous woman presented with a 4-day history of lower abdominal pain radiating to the back and associated with increased and unpleasant vaginal discharge. Intermittent fever was also noted during this period. The patient also presented with other constitutional symptoms, such as headache, anorexia, nausea, and vomiting; but denied eye socket or joint pain, myalgia, and arthralgia. On clinical examination, she was alert, lethargic, restless, and febrile (38°C). The patient's travel history was ignored during admission, but on the 2nd day after admission, the patient revealed a recent trip to her hometown, Kaoshiung City. She and her two sons had been admitted to a pediatric department the day before her admission because of fever of unknown origin. Laboratory testing for dengue fever was ordered and was positive for DENV NS 1 Ag and DENV IgM, but negative for IgG. Serological assays should be used in the early stage when a patient is suspected of viral outbreak of dengue fever as he/she presents with abdominal pain and cytopenia. Physicians in tropical and endemic geographical regions, such as Southern Taiwan-Kaoshiung or Tainan City, should be aware of this type of presentation of DENV infection. Warm temperatures and rainfall in Southern Taiwan are factors leading to outbreaks of dengue fever because they promote mosquito breeding and facilitate DENV transmission.

Key words: Dengue fever, Inflammation of the uterus, Women's medicine, Mother and son case report, Abdominal pain

Introduction

Dengue infection is caused by infected mosquito bites; its name was coined in 1828 A.D. in Cuba [1]. There are four viral serotypes that are antigenically distinct: dengue virus 1 (DENV-1), DENV-2, DENV-3, and DENV-4 [2]. The mosquito harboring the virus is called *Aedes aegypti*, and it acts as a host and a vector that transmits this disease to humans. In Kaohsiung, Southern Taiwan, dengue fever outbreaks because of DENV-1 have been reported since 1981. However, DENV-2 and DENV-3 have replaced the predominant serotype (DENV-1) in more recent outbreaks. Tainan (in Southern Taiwan) experienced the largest outbreak of dengue fever in any endemic area in 2014 with at least 15,000 reported cases. In this case study, we report a delayed and unusual presentation of dengue fever, which was first misinterpreted as a pelvic inflammatory disease (PID) in a woman.

Age and gender were found to be associated with *Aedes aegypti* exposure in a study on six Asian countries that spanned a period of 6–10 years and where the number of male and female dengue cases was available for four age groups (<1, 1–4, 5–14 and ≥15 years) [3]. The authors found that both sex and age since collapsing data over all ages would have masked some of the male–female differences. The

*Correspondence to: Chui-Na Wong, MD., Department of Obstetrics and Gynecology, Show Chwan Memorial Hospital, No. 542, Sec. 1, Chung-Shan Rd., Changhua, 500, Taiwan (R.O.C.)

biological or gender-related factors would be relative to dengue. Helinski and Harrington [4] studied *Aedes aegypti* and observed that small and large males mated in rapid succession with up to five females. Large males had greater mating capacity than small males. Because of the physiological characteristics of mosquito, the human infected with dengue fever would be different in gender situation.

A Case Report

A 40-year-old, multiparous woman presented with a 4-day history of lower abdominal pain radiating to the back and associated with increased and unpleasant vaginal discharge. Intermittent fever was also noted during the symptomatic periods. Because of a history of PID with tubo-ovarian abscess formation, the patient interpreted the clinical presentation to be related to that same event. However, she also had reported other constitutional symptoms, such as headache, anorexia, nausea, and vomiting, but denied eye socket or joint pain, myalgia, and arthralgia. Upon clinical examination, she was alert, lethargic, restless, and febrile (38°C). Abdominal examination revealed tenderness in the suprapubic region but no rebound pain. On pelvic examination, typical PID signs were present, with cervical motion tenderness and massive whitish discharge. A vaginal wet mount preparation was positive for clue cells with bacterial vaginosis. Skin examination failed to reveal signs of bleeding tendency, including petechiae or ecchymosis. Clinical presentation and pelvic examination were consistent with the preliminary impression of PID. Routine blood tests before admission revealed a hemoglobin level of 12.2 g/dl with leucopenia (1250 cells/uL) and thrombocytopenia (>10^4 cells/uL). All other biochemical investigations were normal. The patient's travel history was ignored first, but on the 2nd day after admission, the patient mentioned a recent trip to her hometown, Kaoshiung City. She and her two sons had been admitted to the pediatric department the day before her admission for fever of unknown origin. We ordered dengue fever laboratory testing and results were positive for DENV NS 1 antigen and DENV IgM, but negative for IgG. With these serum results, we modified our strategy to focus on treating the patient for dengue fever. We provided mosquito bed nets, used acetaminophen to control the fever, and provided parenteral hydration. The fever lasted for 3 days after admission. Routine blood reinvestigation performed 2 days after the afebrile period showed recovered platelet and leukocyte counts. The patient recovered with a favorable outcome and was discharged uneventfully.

Discussion

Dengue fever usually presents as a febrile viral illness, but rarely presents as an acute abdominal emergency mimicking PID. This presentation should be considered to rule out the infection with serological assays during early stages in patients presenting with abdominal pain and cytopenia in endemic regions or after travel to such regions (Southern Taiwan-Kaoshiung or Tainan City in our case). Dengue fever outbreaks in Southern Taiwan are due to its warm temperature and frequent rainfall, which enhance mosquito breeding and facilitate DENV transmission. Dengue fever is usually a self-limited illness, and no specific antiviral treatment is currently available for its treatment. Supportive care with analgesics, fluid replacement, and bed rest are usually sufficient. Acetaminophen is used for treating fever and relieving pain. Aspirin, nonsteroidal anti-inflammatory drugs (NSAIDs), and corticosteroids should be avoided.

Acknowledgment

I would like to acknowledge the medical doctor Chun-Yi Lin, Dr.PH. Expert of long term study of Dengue Fever, Rong-Fu Chen, Ph.D. gave me ideas. Thanks for Infection Dept, Wang, Yi-Ren, MD. Special thanks for Zih-Ping Ho, Ph.D.'s helps, and his assistance Wei-Zen Chang. Thanks for proofreading and content support, provided by Research Assistant Center, Show Chwan Health Care System.

Reference

1. Pan CZ, Lee BY. Introduction to Dengue hemorrhagic fever and case report. The J Phar on Taiwan 2003;19:134-9.
2. Wang SF, Wang WH, Chang K, Chen YH, Tseng SP, Yen CH, et al. Severe Dengue Fever outbreak in Taiwan. Am J Trop Med Hyg 2016;94:193-7.
3. Anker M, Arima Y. Male-female differences in the number of reported incident dengue fever cases in six Asian countries. Western Pac Surveill Response J 2011;2:17-23.
4. Helinski ME, Harrington LC. Male mating history and body size influence female fecundity and longevity of the dengue vector Aedes aegypti. J Med Entomol 2011;2:202-11.

女性盆腔炎的登革熱個案研究 - 仿如類似盆腔炎疾病

黃翠娜*

彰化市秀傳紀念醫院　婦產科

受文日期：民國 105 年 05 月 20 日；接受刊載：民國 105 年 10 月 06 日

摘要

登革熱的感染主要起因於感染過登革熱的蚊蟲所叮咬的結果。它有四種病毒血清：登革熱病毒 1（DENV-1），登革病毒 2（DENV-2），登革熱病毒 3（DENV-3），和登革病毒 4（DENV-4）。蚊子是登革熱病毒的載體。在 2014 年臺灣臺南經歷了登革熱大爆發，該年至少被報導 15000 個通報個案。在本病例報告，我們找到一例女性子宮發炎之登革熱感染及不尋常的個案。一位四十歲中年婦女，有四天的下腹部持續疼痛及白帶增多，在此期間伴隨著發燒。她曾發生以下全身症狀，如頭痛、厭食、噁心、嘔吐，但卻沒有眼痛、肌痛和關節痛。臨床檢查中發現，警覺、嗜睡、躁動和發熱（38 攝氏度）。在入院前沒有旅遊史記錄，但在第二天的巡房時，病人告訴我們她最近曾回過她的高雄老家。她送她二個兒子去小兒科檢查，因為他們發生了不明的高燒。經登革熱生化檢查試驗，陽性登革病毒 NS1 Ag 和登革病毒 IgM 抗體，但陰性 IgG 抗體。此報告應在早期的時候，患者因登革熱而腹痛，使用血清學檢測而不讓病毒爆發。這種意識應該在熱帶和亞熱帶區域，如南臺灣 - 高雄市或台南市地理位置而加高。主要的因素是由於溫暖的氣溫和降雨，也增強了蚊子的繁殖和促進登革熱病毒傳播。

關鍵詞：登革熱、子宮發炎、婦女醫學、母子病例、腹痛

* 通訊作者：黃翠娜醫師　彰化市秀傳紀念醫院婦產科　500 彰化縣彰化市中山路一段 542 號

Tungs' Medical Journal 12 (2018) 62-65

Case Report

Brain Abscess Masquardered As Bacterial Meningitis

Hueng-Chuen Fan[1], Chii-Wen Chou[2], Bei-Rong Su[3], Pin-Ho, Pan[2], Hao-Chun Hung[3,*]

[1]Department of Pediatrics, [2]Department of Neurosurgery, [3]Department of Radiology, Tungs' Taichung MetroHarbor Hospital, 43503, Taichung, Taiwan

Received: May. 23, 2016; Accepted: Jan. 05, 2017

Abstract

We report the case of a 10-year-old girl who initially presented with bacterial meningitis, andempiric antibiotics only partially alleviated her symptoms. However, electroencephalography (EEG) findings showed prominent slow waves over her right hemisphere. Brain magnetic resonance imaging (MRI) further revealed an encapsulated cystic lesion, which suggested an abscess, which ruptured into a lateral ventricle andlead to a meningitis-like presentation. Craniotomy with ultrasound-guided aspiration displayedcloudy fluid that grew ampicillin-sensitive *Streptococcus viridans*. After six weeks of antibiotics administration, she completely recovered without the presence of any neurological sequelae.

Key words: Brain abscess, Meningitis

Introduction

Brain abscess (BA)initiates as a localized area of cerebritis and develops into a collection of pus surrounded by a well-vascularized capsule[1]. BA is potentially lethalwhen left untreated. Patientmortality rate increases if BA ruptures into the ventricle[2]. Wereported a girl whoinitiallypresentedwithbacterial meningitis, andempiric antibioticscould only partially alleviate her symptoms. Results of electroencephalography (EEG) indicatedthe presence of organic lesions within her right brain. Brain magnetic resonance imaging (MRI) displayeda large ring-enhancing lesion that invaded into her right lateral ventricle. She completely recovered without the presence of any neurological sequelae after aspiration and six weeks of antibiotics administration.

Case Report

A 10-year-old girl without a history ofremarkable illness presented with intermittent fever, neck pain and stiffness, headache, and vomiting for two days. She was alert and interactiveon physical examination. Her blood pressure, body temperature, heart rate, and respiratory rate were noted to be 115/79 mmHg, 37.8°C, 96/min, and 20/min, respectively. Neurological examination revealed typicalmeningismwithout focal neurological deficits. Blood analysisfindings revealed a total white cell count of 18,400/mm^3, hemoglobin concentration of 11.3 g/dL, platelet count of 467,000/mm^3, and C-reactive protein concentration of 10.8 mg/dL. Blood glucose and serum electrolytes were within the normal range. Intracranial pressure was 40 cmH_2O. Cerebrospinal fluid (CSF) analysis showed turbid fluid with a total protein of 243 mg/dL, glucose of 18 mg/dL, leukocyte count of 6410/mm^3 with 77% polymorphonuclear leukocytes, and erythrocyte count of 220 /mm^3. Bacterial meningitis was suspectedon the basis of these findings. Her stiff neck alleviated afterempiric antibiotic therapy (cefotaxime 200mg/kg/day and vancomycin 30mg/kg/day) and mannitol 0.25 g/kg/day, but fever and headache still fluctuated. EEGfindings showed intermittent arrhythmic delta waves over her right hemisphere (Fig. 1a). Brain MRIshoweda large ring-enhancing

*Correspondence to: Hao-Chun Hung, MD., Department of Radiology, Tungs' Taichung MetroHarbor Hospital, No. 699, Sec. 8, Taiwan Blvd., Wuqi Dist., Taichung City 43503, Taiwan (R.O.C.)

lesion with a thick wall in the right occipital lobe that invaded into the right lateral ventricle and suggesteda BA with ventriculitis (Fig. 1b). Craniotomy with ultrasound-guided aspiration showed cloudy fluid, which grew ampicillin-sensitive *Streptococcus viridans*. Detailed ear, nose, and throat; cardiovascular; immune; and dental examinationsdidnot reveal any pathology. After six weeks of antibiotics administration, she did not have any neurological sequelae. A follow-up EEGshowednormalfindings (Fig. 1c), and a follow-up brain MRI demonstrateda shrinkingBA with residual enhancement (Fig. 1d).

Discussion

BA is notorious for a high mortality rate whenmisdiagnosed or left without any aggressive treatment[3]. Pathogens can insidiously invade the brain and cause single or multiple abscesses through direct extension and/or a hematogenous route[3]. Direction extension, whichinvolves any of the paranasal sinuses, ears, face, and oral cavity infections, frequently occurs in the pathogenesis of BA[4]. However, none of these infections was identified in the present case. The patient's blood cultures did not grow any bacteria. We were unable to detect how *S. viridans* infected her brain, and the percentage of obscure causes for BA was reportedlyhigh at 37%[5].

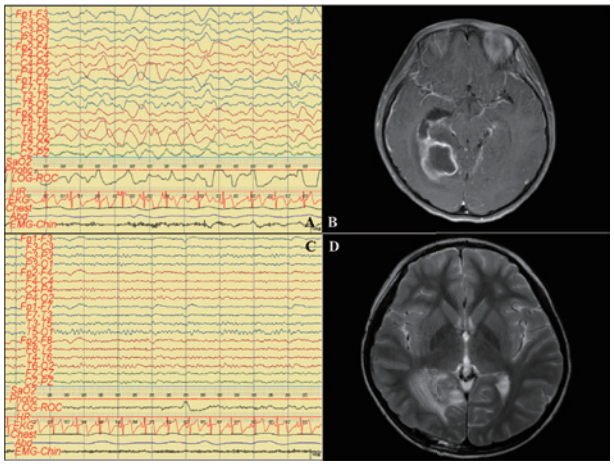

Fig. 1 (A) EEG demonstrates arrhythmic delta waves over the right parietal (P4) and temporal (T6) regions. The recording parameters include a longitudinal bipolar montage with asensitivity 7 μv and filter settings of 1–70 Hz. (B) Axial T1-weighted brain MRI shows a largering-enhancing lesion with a thick wall in the right occipital lobe invading intothe right lateral ventricle. (C) EEG demonstrates a normal background. (D) Axial contrast-enhanced T2-weighted MRI showsa shrinking abscess with residual enhancement.

The patientdid not manifest the classic triad of BA, which includesheadache, fever, and focal neurologic deficit[6]. Furthermore,the lesion in her brain had ruptured into the right lateral ventricleand lead to a meningitis-like picture, such asfever, neck pain, headache, vomiting, typical meningeal signs, and clouded CSF. If BA had not been promptly identified in this patient, she would have expiredconsidering thatthe mortality rate was >80%[2]; thus,any efforts at diagnosingareimperativein planning appropriate therapy. However, a lumbar puncturepotentially causescatastrophic herniation and subsequent death. A cranial image, CT or MRI, with contrast administration showing a ring-enhancing lesion suggests the presence of BA[6]. EEG also is useful in the detection of BA by the appearance of focalarrhythmic delta waves[7], which were found in our case and which correlated with the location of the abscess lesion. A combination of EEG and cranial imaging may offer a sensitive aid in thedetection of BA.

BA requires urgent neurosurgical intervention, and treatment is prone to failure if therapy consists of antimicrobial agents alone[6]. The initial approach consists of draining the abscess through a twist drill craniotomy. If the capsule is thick, the next procedure entails therapeutic burr-hole drainage. A deep-seated abscess, like in the present case, requires tobe drainedusingbrain image-guided aspiration. The recommended duration of parenteral antibiotic therapy is six to eight weeks following aspiration. Craniotomy and excisionare often performed for multiloculated abscesses and larger lesions with significant mass effect that are superficial and located in the non-eloquent regions of the brain and for abscesses that enlarge after two weeks of antibiotic therapy or that fail to shrink after three to four weeks of antibiotic administration.

In conclusion, the diagnosis of BArequires a careful consideration of the patient's history, astute physical examination, a combination oflaboratory studies, EEG and cranial imaging, anda high index of suspicion. Therapy should include neurosurgical intervention and aggressive antibiotics.

References

1. Alvis MH, Castellar-Leones SM, Elzain MA, Moscote-Salazar LR. Brain abscess: Current management. J Neurosci Rural Pract. 2013; 4: S67-S81.

2. Ferre C, Ariza J, Viladrich PF et al. Brain abscess rupturing into the ventricles or subarachnoid space. Am J Med. 1999; 106: 254-257.
3. Mathisen GE, Johnson JP. Brain abscess. Clin Infect Dis. 1997; 25: 763-779.
4. Helweg-Larsen J, Astradsson A, Richhall H et al. Pyogenic brain abscess, a 15 year survey. BMC Infect Dis. 2012; 12: 332.
5. Tseng HM, Lin SM, Kao MC, Hung CC. Reappraisal of management of brain abscess: analysis of 26 cases treated with various methods. Taiwan Yi Xue Hui Za Zhi. 1987; 86: 137-143.
6. Brouwer MC, Tunkel AR, McKhann GM, van de Beek D. Brain abscess. N Engl J Med. 2014; 371: 447-456.
7. Vignadndra V, Ghee LT, Chawla J. EEG in brain abscess: its value in localization compared to other diagnostic tests. Electroencephalogr. Clin Neurophysiol. 1975; 38: 611-622.

偽裝成腦膜炎的腦膿瘍

范洪春[1] 周啟文[2] 蘇碧榕[3] 潘品合[1] 洪豪駿[3,*]

童綜合醫療社團法人童綜合醫院 [1]小兒部 [2]神經外科部 [3]放射線部

受文日期：民國 105 年 05 月 23 日；接受刊載：民國 106 年 01 月 05 日

摘要

我們報告一個 10 歲女童有頭痛、發燒與頸部僵直，腦脊髓液分析顯示高腦壓、高蛋白、低葡萄糖以及白血球上升，臨床醫師一開始以腦膜炎處理。使用第三線抗生素後，女童仍有輕微頭痛，但無任何局部的神經症狀。進一步檢查，腦電圖發現有右大腦不規律的慢波，腦部核磁共振掃瞄在右側枕葉呈現環狀病灶，內容物破入右側腦室，腦膜在 T2 有訊號增強，可能是腦膿瘍合併腦室炎與腦膜有受波及。經開顱手術與術中超音波定位的膿瘍抽出後，細菌培養証實是草綠色鏈球菌。以抗生素治療 6 週後，女童病情完全改善無任何後遺症。

關鍵詞：腦膿瘍、腦膜炎

* 通訊作者：洪豪駿醫師 童綜合醫療社團法人童綜合醫院放射線部 43503 臺中市梧棲區臺灣大道八段 699 號

Tungs' Medical Journal 12 (2018) 66-68

Pathology Page

Pathology Page in Clinical Medicine: Leprosy, Borderline – Tuberculoid Type

Chien-Chang Wu[1], Kuo-Hsi Lin[2], Chih-Chuan Kao[2,*]

[1]Departments of Family Medicine, [2]Infectious Disease, Tungs' Taichung MetroHarbor Hospital

Received: Aug. 10, 2015; Accepted: Dec. 03, 2015

Abstract

Leprosy, or Hansen's disease, is caused by *Mycobacterium leprae*, causing skin lesions and nerve damage. Less than 5% of people exposed to *M. leprae* develop clinical disease. Host cell-mediated resistance determines whether an individual will develop paucibacillary or multibacillary disease. We report here the case of a 32-year-old Indonesian male worker with a 3-year history of hypoesthetic erythematous plaque lesions over his right forearm and 10-day history of multiple nontender papules and nodules located in both forearms, back, and face. Neurologic examination showed decreasing tactile sensation over dermatome of the 1st branch of the 5th cranial nerve (also called as ophthalmic nerve). Skin biopsy revealed histiocytic granulomas. Borderline-tuberculoid type of leprosy was diagnosed based on the classical clinical and pathologic manifestations. Although no indigenous case has been reported in Taiwan hitherto, imported case, as shown in this report, can occur.

Key words: Borderline-tuberculoid, Leprosy, Hansen's disease

A 32-year-old male laborer from Indonesia presented with a 3-year history of hypoesthetic with well-demarcated erythematous plaque, about 3 × 10 cm in diameter, on the right forearm (Fig. 1). Ten days before presentation, generalized discrete erythematous papules and nodules appeared on both forearms, back, and face (Fig. 2). Even in a low temperature environment, he felt tingling sensation over his right forearm and face. Physical examination revealed mild sensory loss of tactile sensation over the dermatome of the 1st branch of the 5th cranial nerve. Histopathological examination of skin biopsy of the right forearm revealed multiple non-caseous granulomas, which contained spindle-shaped histiocytes with pyknotic nuclei (Fig. 3) in the upper dermis (arrows, Fig. 4). Based on the classical clinical manifestations of erythematous skin patches with definite loss of sensation and well-formed granulomas with differentiated macrophages and giant cells, leprosy

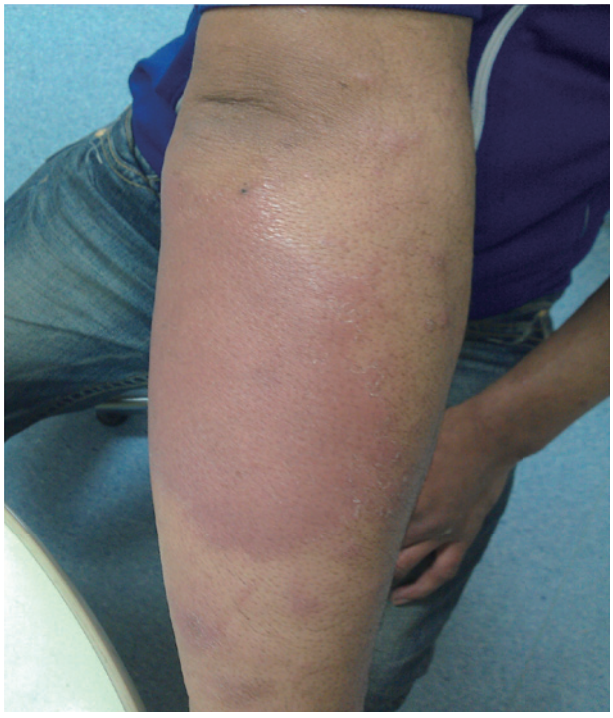

Fig. 1 well-defined margin and erythematous plaque on the posterior forearm with elevated external borders, presenting significant change in sensitivity.

*Correspondence to: Chih-Chuan, Kao, MD. Department of Infectious Disease, Tungs' Taichung MetroHarbor Hospital, No. 699, Sec. 8, Taiwan Blvd., Wuqi Dist., Taichung City 43503, Taiwan (R.O.C.)

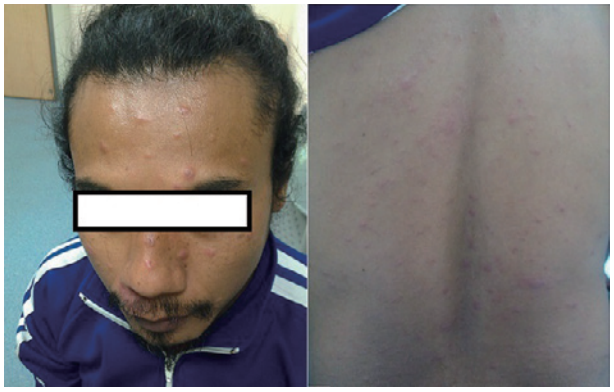

Fig. 2 numerous dry surface erythematous nodules and papules over his face and variable size, ill-defined macules and plaque on his back.

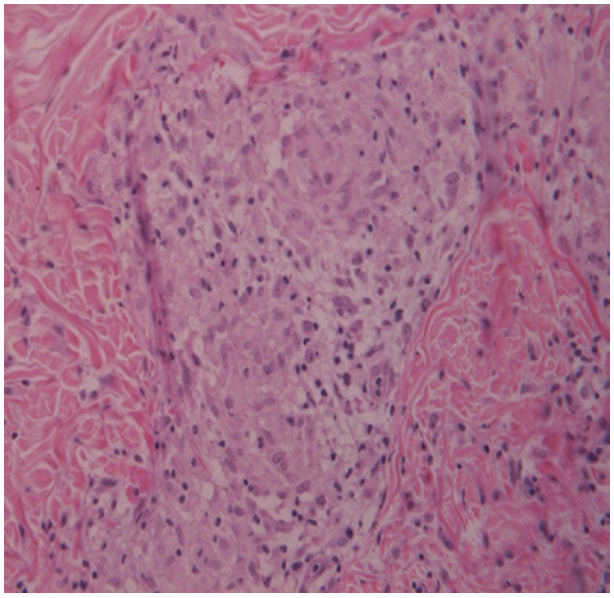

Fig. 3 noncaseating granuloma with pseudocapsule formation and lymphocytes infiltration (Hematoxylin & eosin, X400).

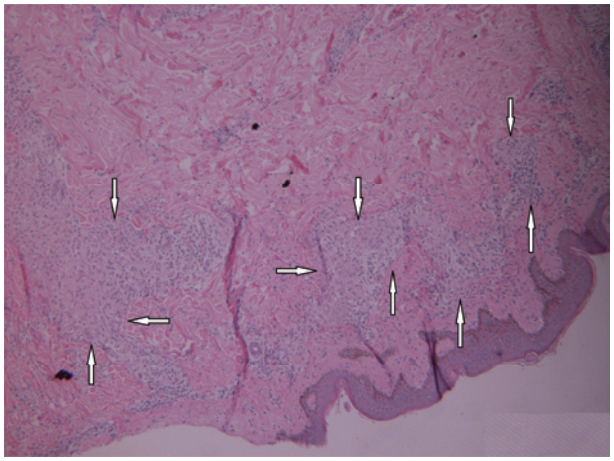

Fig. 4 numerous infiltrative noncaseating granuloma composed of lymphocytes and histiocytes located in the dermis (Hematoxylin & eosin, X100).

was diagnosed. A skin smear for acid-fast bacilli was negative. Without cardinal signs of leprosy, the differential diagnoses would include deep fungal infection, atypical mycobacterial infection, and even tuberculosis verrucosa cutis. He received 1-week of anti-leprosy treatment with dapsone 100 mg and rifampin 600 mg per day and then was repatriated.

According to the World Health Organization (WHO) in 2014[1], leprosy, or Hansen's disease, caused by *Mycobacterium leprae*, annually affected approximately 220,000 persons worldwide, mainly in India, Brazil, Indonesia, Ethiopia, and the Democratic Republic of the Congo. The diagnosis of leprosy, according to the guidelines concluded by WHO[2], is based on the findings consistent skin lesions with associated sensory loss, with or without associated thickened nerves, or the presence of acid-fast bacilli on slit-skin smears or tissue biopsy. Slit-skin smear is currently the most important adjunctive examination in leprosy patients because, by demonstrating acid-fast bacilli, it can confirm the diagnosis of leprosy and help in determining its clinical stage and prognosis. Histologic features include well-organized epithelioid granulomas surrounded by lymphocytes. However, compared to other types of leprosy, the number of bacilli in the borderline-tuberculoid type of leprosy is not abundant, which might explain why the patient's skin biopsy revealed non-caseous necrosis. Therefore, the combination and correlation of clinicopathological criteria might be helpful in an operational classification of leprosy.

References

1. World Health Organization. WHO Leprosy: Regional elimination on the horizon. http://www.searo.who.int/entity/leprosy/regional-elimination-on-the-horizon/en/. Accessed July 21, 2015.
2. World Health Organization Expert Committee on Leprosy. Seventh Report. Technical Report Series 1998, 874.

病理醫學判讀：痲瘋病 - 偏結核樣型

吳建璋[1] 林國璽[2] 高智泉[2,*]

童綜合醫療社團法人童綜合醫院 [1]家庭醫學部 [2]感染醫學科

受文日期：民國 104 年 08 月 10 日；接受刊載：民國 104 年 12 月 03 日

摘要

痲瘋病，亦稱為漢生病，是由痲瘋分支桿菌感染所造成的皮膚病灶和神經損傷。而曾接觸過痲瘋桿菌的人，其中不到 5% 會造成臨床疾病，此取決於個案本身的免疫能力。免疫能力會影響痲瘋病是否會發展為寡菌量（paucibacillary）或是多菌量（multibacillary）。在這篇病例報告中，一名 32 歲印尼男性勞工，右手前臂有一個持續三年、局部感覺遲鈍的紅色斑塊以及在十天前，在他的背部、臉部以及雙手前臂出現結節丘疹。神經學檢查出現三叉神經的第一分支皮區觸覺反應減低。針對右手前臂斑塊的皮膚切片，蘇木素伊紅染色出現組織細胞肉芽腫。最終依據典型臨床表現診斷為偏結核樣型痲瘋病。儘管目前台灣並無本土痲瘋病個案，但境外移入案例，如這篇個案報導，卻是有可能發生的。

關鍵詞：偏結核樣；痲瘋病；漢生病

* 通訊作者：高智泉醫師 童綜合醫療財團法人童綜合醫院 感染醫學科 43503 臺中市梧棲區臺灣大道八段 699 號

Image

Infected Aneurysm of the Thoracic Aorta

Ming-Chang Yin*

Chest Department of Tungs' Taichung MetroHarbor Hospital, Taichung, Taiwan

Received: Jan. 09, 2017; Accepted: Apr. 10, 2017

Abstract

An infected aneurysm involves localized dilation of an artery due to destruction of the vessel wall by infection. An infected aneurysm of the thoracic aorta is rare. Here, we report a case of an infected thoracic aneurysm presenting as an anterior mediastinum tumor initially. The patient was an 82-year-old man. He was diagnosed with an infected thoracic aneurysm and was successfully treated with antibiotics and endovascular aortic arch repair with Gore thoracic stenting. Endovascular stenting combined with antibiotic therapy may be a good alternative to conventional thoracotomy for managing an infected aneurysm in the thoracic aorta.

Key words: Infected aneurysm, Thoracic aorta

Introduction

An infected aneurysm involves localized dilation of an artery due to destruction of the vessel wall by infection. It can occur in any artery, but is most commonly seen at the bifurcation points of extremity, splanchnic, and cerebral circulations. It is a serious clinical condition associated with significant morbidity and mortality, unless a diagnosis is made early. The clinical symptoms include fever, chest pain, hemoptysis, respiratory failure, hoarseness, loss of consciousness, and stroke[1]. Here, we report a case of an infected thoracic aneurysm presenting as an anterior mediastinum tumor.

An 82-year-old man was admitted to the hospital because of cough and fever with yellowish sputum. His medical history included interstitial pneumonitis, atrial fibrillation, hypertensive cardiovascular disease, and diabetes mellitus. Chest radiography revealed an alveolar patch over the left lower lobe and a mass over the left upper lobe. Pneumonia was considered, and antibiotics were prescribed. However, progressive hemoptysis and dyspnea occurred four days after admission. Chest computed tomography (CT) with intravenous contrast showed a large left anterior superior mediastina mass (size 8 × 6 × 7 cm) with a surrounding hematoma, which compressed the trachea. Under the suspicion of an anterior mediastinum tumor, CT-guided biopsy was performed.

On pathological assessment of the tumor, acute necrotizing inflammation with bacterial infection was identified. Gram staining of the biopsy specimen showed many bacteria, including cocci and filament bacilli. Based on these results, the CT report was revised from an anterior mediastinum mass to an aortic arch aneurysm with complicated thrombosis. Unfortunately, sputum impaction with asphyxia was noted during admission, and he was resuscitated for five minutes. He had a poor performance status, and thus, he was admitted to the intensive care unit. As his condition was unstable, he was treated with antibiotics initially. Cardiovascular surgery involving endovascular aortic arch repair with Gore thoracic stenting was performed after 20 days of intensive care. His condition improved within six months after surgery and medical treatment. Because of poor pulmonary function and a request from his family to provide nearly home care, he was transferred to a local hospital with ventilatory support.

A diagnosis of an infected aneurysm is made

*Correspondence to: Dr. Ming-Chang Yin. Division of Pulmonary and Critical Care Medicine, Tungs' Taichung MetroHarbor Hospital, No 699, Sec. 8, Taiwan Bivd., Wuchi Dist., Taichung City, 43503, Taiwan (R.O.C).

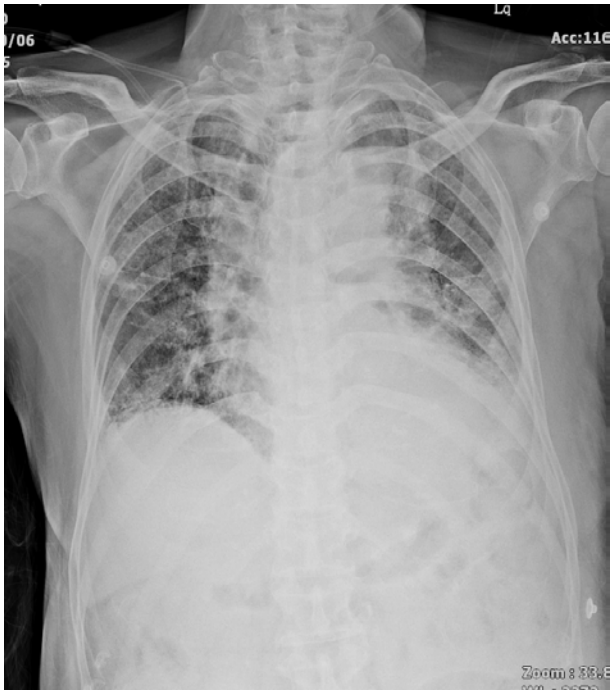

Fig. 1 CXR showed left upper lung mass lesion with trachea deviation to right side, bilateral lung infiltration .especially left lower lung field.

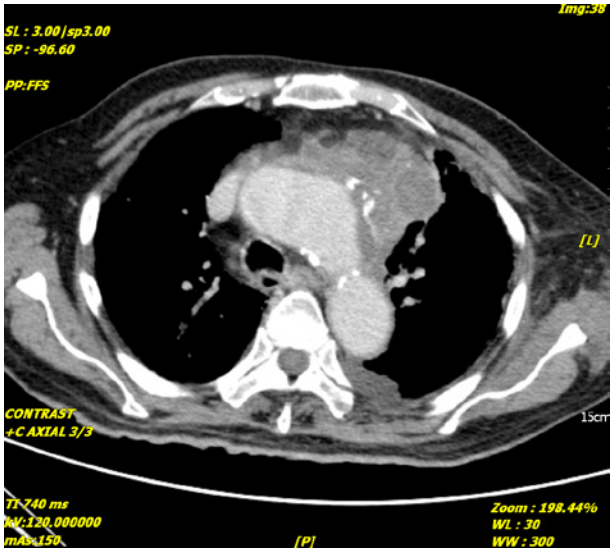

Fig. 2 Computed tomography of the chest showed a large left anterior superior mediastinal tumor (8 × 6 × 7 cm) with Surrounding hematoma compressing the trachea (arrow).

according to the imaging findings of the aneurysm and confirmation of infection on culture. CT angiography can be used to definitively diagnose the aneurysm. There have been no randomized trials to guide the management of infected aneurysms. Management strategies are primarily based on clinical experience guided by case series. The gold standard for treatment is surgery involving open surgical resection of the infected aorta, wide debridement of tissues, and reconstruction to re-establish blood flow. However, this approach has been reported to be associated with a high mortality rate (up to 40%)[2]. The mortality rate among patients managed without surgery (antibiotics only) has been reported to be 85%, and two-thirds of these patients died from in-hospital rupture[3]. Endovascular therapy may be the most suitable approach for the management of infected aneurysms in patients at high risk for issues with open surgery. Our patient's age and clinical condition made him a poor candidate for surgery, and he successfully underwent endovascular aortic arch repair. Endovascular stenting combined with antibiotic therapy may be a good alternative to conventional thoracotomy for managing an infected aneurysm in the thoracic aorta.

References

1. Lopes RJ, Almeida J, Dias PJ, et al. Infectious thoracic aortitis: a literature review. Clin Cardiol 2009; 32: 488.
2. Vallejo N, Picardo NE, Bourke P. The changing management of primary mycotic aortic aneurysms. J Vasc Surg 2011; 54: 334-40.
3. Weis-Müller BT, Rascanu C, Sagban A, et al. Single-center experience with open surgical treatment of 36 infected aneurysms of the thoracic, thoracoabdominal, and abdominal aorta. Ann Vasc Surg 2011; 25: 1020.

感染性的胸主動脈瘤──罕見的前縱膈腫塊

殷明昌*

童綜合醫療社團法人童綜合醫院　胸腔內科

受文日期：民國 106 年 01 月 09 日；接受刊載：民國 106 年 04 月 10 日

摘要

感染性的主動脈瘤在臨床上並不常見，發生在胸主動脈更是罕見。提早發現，外科和抗生素的治療可降低死亡風險。在此我們提出一複雜案例，同時合併肺炎和感染性的胸主動脈瘤，影像學初步判斷為前縱膈腫塊，並討論此疾病的臨床表現與治療。

關鍵詞：感染性的主動脈瘤、胸主動脈

* 通訊作者：殷明昌醫師　童綜合醫療社團法人童綜合醫院胸腔內科　43503 台中市梧棲區台灣大道八段 699 號

Instruction to contributors

The Tungs' Medical Journal provides a forum for all fields of medicine, including Editorials, Review Articles, Original Articles, Case Reports, Brief Communications, Images, and Pathology Page. Authors are welcome to submit manuscripts to Tungs' Medical Journal.

Preparing Your Manuscript:

1. Three copies of the manuscript must be submitted as a Word document to the Editor, Tungs' Medical Journal, Tungs' Taichung MetroHarbor Hospital, No.699, Sec.8, Taiwan Blvd., Wuqi Dist., Taichung 43503, Taiwan (R.O.C.) and an electronic copy of the manuscript to E-mail address: Tungs_Journal@ms.sltung.com.tw.
2. The author is responsible for the content of the manuscript. If the content is related to copyright, author needs to obtain the right to use and is legally responsible for it.
3. Please attached the copyright and consent form on submission. All author(s) listed must actually participate in and agree with the conclusion. Upon receiving and completion of printing, the author(s) will receive 20 free copies and compensation. If extra copy is needed, please notify during editing, and this is subjected to charges.
4. The manuscript may be rejected if incompatible with the journal's mission. After acquiring consent from the author(s), the editor may edit the manuscript.
5. For any the manuscript related to "the human specimen for research" or "clinical trial", must follow the guidelines to obtain an IRB approval for the right of participants.
6. For any the manuscript related to the use of animals, it needs to be approval of The Institutional Animal Care and Use Committee to ensure the humane management.

Manuscript format:

1. Editorials are limited to 2000 words, with 150 words of abstract and 7 references.
2. Review articles should provide the reader with a balanced overview of an important and topical subject in the field. This should be limited to 3500 words, with 300 words of abstract and 40 references.
3. Original articles should be presented in the following order: Abstract, Introduction, Materials and Methods, Results, Discussion and Conclusion, Acknowledgements, References, Attachments, Tables, Legends for illustration, and Figures (photographs). This should be limited to 3000 words, with 300 words of abstract and 40 references.
4. Case reports should be arranged by the following sequence: Abstract, Introduction, the Clinical case, Discussion, References, Attachments, Table, Legends for illustration, and Figures. Patients' eyes should be covered for privacy. Diagnosis information or the chart of clinical process should be within 6 months. This should be limited to 1500 words, with 150 words of abstract and 10 references.
5. Brief communications should be concise presentations of preliminary clinical results and technological improvements. This should be exceeded 750 words, 150 words of abstract and 7

references.

6. Images and Pathology page should be limited to 500 words, with 150 words of abstract and 3 references.
7. For other details, please refer to International Steering Committee, for Uniform Requirements for Manuscripts Submitted to Biomedical Journals, please refer to The New England Journal of Medicine 336:309-315,1997.

Specifications for the different article categories

Article Category	Word count limit		No. of references allowed	No. of tables/ figures allowed
	Abstract	Min text*		
Original Articles	≦300	≦3000	≦40	≦5
Case Reports	≦150	≦1500	≦10	≦3
Review Articles	≦300	≦3500	≦60	≦6
Brief Communications	≦150	≦750	≦7	≦1
Images, Pathology Page	≦150	≦500	≦3	≦2
Editorials	≦150	≦2000	≦7	≦1

*Refers to the main body of text only, i.e., does not include article title, abstract, table headings/tables, figure legends and references.

Manuscript preparation:

Manuscript should be double-spaced and numbered pages, and comply with the "uniform requirements for manuscripts submitted to biomedical journals". The first page is the title page, which include title, name of author(s), organization and unit, contact name, phone number, e-mail address and mail address (in both Chinese and English). The second and the third page is for abstract (Chinese content needs to consist with English content) and key words (please include 3 to 5 keywords or phrases in Chinese and English), and should be written in paragraphs following by background and purpose, methods, results and discussion.

Co-corresponding author should mention the contributions on manuscript, such as initiation of research topics, the study design, statistical analysis, interpretation of findings, chapters writing involved, et al.

Please attach two original copies including attachments, charts and legends. Chart should be professional, with only one figure or one table per page, and is arranged in consecutive orders and numbered in Arabic characters. Table should have a title and appropriate interpretation. Picture should be 5" x 7" in size, black and white, glossy and numbered in consecutive orders of appearance.

Reference:

Unpublished articles or abstracts cannot be listed as references, but could be noted as "unpublished observations". Doctoral dissertation or master thesis can be used. Any articles being accepted by magazines but not published yet, please note the name of magazine, year and note "in press".

Original researches, case reports, review articles, communications (includes brief communications), images in clinical medicine, editorial follows the following format:

1. Abbreviations used should follow the format of Index Medicus for all journal titles. When authors are less than 6 people, list all author(s), when more than 6, only list the first 6 followed by "et al." for the rest.
2. References in the text should be placed where relevant. When a reference article is cited, only the primary author is cited; however, if only two authors are present, both should be listed.
3. Example of references:

Examples of Reference:

1. Periodicals:

   Yang KTA, Chen HD: A semi-automated method for edge detection in the evaluation of left ventricular function using ECG-gated single-photon emission tomography. Eur J Nucl Med 1994;21:1206-11.

2. Monographs:

   Plum F, Posner JB: Diagnosis of Stupor and Coma. 3rd ed. Philadelphia: Davis, 1980:132-3.

3. Monographs with multiple authors:

   Levinsky NG: Fluid and electrolytes. In: Thorn GW, Adams RD, Braunwald E, Isselbacher K, Petersdprf RG eds. Harrison's Principles of Internal Medicine, 8th ed. New York: Mcgraw-Hill, 1977:364-75.

4. References from website

   please indicate the title, source, and the retrieving date

   (Accessed Month day, 2016, at http://www.house.gov/xxxx/min/inves_xxx/index_accord.htm.)

Copyright:

童綜合醫學雜誌投稿相關規則

95.9.01 製訂
99.08.17 修訂
100.07.11 修訂
102.07.08 修訂
102.12.27 修訂
103.07.14 修訂
103.12.12 修訂
104.03.13 修訂
104.11.19 修訂
107.01.10 修訂

本雜誌刊載與醫學有關之論述，包括原著論文（Original Articles）、病例報告（Case Reports）、綜論（Review Articles）、短論（Communications 、包括 Brief Communications）、影像判讀（Images）、臨床病理討論（Pathology Page）、編著的話（Editorials）等。惠稿請送 43503 臺中市梧棲區臺灣大道八段 699 號童綜合醫學雜誌編審委員會。（E-mail:Tungs_Journal@ms.sltung.com.tw）

壹、投稿前注意事項

1. 惠稿請以英文撰寫，本雜誌接受電子檔投稿或紙本投稿，電子檔投稿請直接將稿件 WORD 檔寄至編審委員會信箱 Tungs_Journal@ms.sltung.com.tw)，紙本投稿需檢附紙本稿件三份及電子檔一份寄至編審委員會（43503 臺中市梧棲區臺灣大道八段 699 號童綜合醫學雜誌編審委員會）。
2. 文件內容需清晰，內容與原稿一致，若複印稿與原稿有差異或遺漏，由作者自行負責。著作中若牽扯到版權所有之內容，作者需取得其使用權，法律責任由作者負責。
3. 投稿同時請附上著作權讓與同意書。所有作者必須實際參與並同意該論述。本院於接受稿件且印刷完成後，將致贈稿酬並贈送 20 份抽印本給通訊作者，如需額外抽印本請於校稿時言明，並酌收成本費用。第一作者若需抽印本可提出申請，依份數酌收成本費用。
4. 本刊對於原稿經徵得著者之同意得伸縮或修改之。如不合本刊宗旨者，得退還之。
5. 凡刊載於本雜誌之著作，若涉及「研究用人體檢體採集」及「人體試驗」等情事，應遵守該注意事項，以落實保障受檢人權益。詳文請參考須附上相關審議認可之文件。
6. 論文中如涉及使用脊椎動物進行科學應用計畫者，應檢附該計畫業經所屬機構動物實驗管理小組審議認可之文件，以落實實驗動物之人道管理。

貳、寫作原則

1. 原著論文（Original Articles）按下列順序撰寫：摘要、前言、材料與方法、結果、討論與結論、誌謝、參考文獻、附表、圖片說明、圖片（含照片）。每篇字數 3000 字以內，摘要 300 字以內，參考文獻 40 篇以內。
2. 病例報告（Case Reports）按下列順序撰寫：摘要、前言、病例、討論、參考文獻、附表、圖片說明、附圖、照片。凡病患顏面部位之相片必須遮去眼睛部位，表示尊重隱私。診療資料或臨床經過之圖表，原則上均限六個月以內。每篇字數 1500 字以內，摘要 150 字以內，參考文獻 10 篇以內。
3. 綜論（Review Articles）不必按原著論文格式撰寫，但每篇字數 3500 字以內，摘要 300 字以內，參考文獻 60 篇以內。
4. 短論（Brief Communications），臨床上、技術上的精簡論著，每篇字數 750 字以內，摘要 150 字以內，參考文獻 7 篇以內。

5. 影像判讀（Images）、臨床病理討論（Pathology Page）圖例說明每篇字數 500 字以內，摘要 150 字以內，參考文獻 3 篇以內。
6. 編者的話（Editorials），每篇字數 2000 字以內，摘要 150 字以內，參考文獻 7 篇以內。
7. 其他細節，請參閱國際指導委員會（International Steering Committee）發表之生物醫學雜誌稿件統一規格（Uniform Requirements for Manuscripts Submitted to Biomedical Journals，見 The New England Journal of Medicine 336:309-315,1997）。
8. 將可接受投稿之稿件種類之摘要字數、字數、參考文獻及圖表相關上限規定，整理於下表：

稿件種類	字數限制		參考文獻	圖 / 表
	摘　　要	內文字數		
原著論文 (Original Article)	≦ 300	≦ 3000	≦ 40	≦ 5
病例報告 (Case Report)	≦ 150	≦ 1500	≦ 10	≦ 3
綜論 (Review Article)	≦ 300	≦ 3500	≦ 60	≦ 6
短論 (Brief Communication)	≦ 150	≦ 750	≦ 7	≦ 1
影像判讀 (Images)、 臨床病理討論 (Pathology Page)	≦ 150	≦ 500	≦ 3	≦ 2
編者的話 (Editorial)	≦ 150	≦ 2000	≦ 7	≦ 1

參、投稿須知

1. 稿件須符合「生物醫學雜誌投稿之統一規定」[1]，請以電腦隔行 double space 書寫，並編頁碼，中文字型以標楷體，英文字型以 Time New Roman 12 號字大小，稿紙之左右緣爲 2.54 公分，上下緣爲 3.17 公分。
2. 第一頁爲標題頁，須列出中文及英文之論文題目、中英文作者姓名、所屬機構及單位之中英文稱號（分屬不同單位，請以阿拉伯數字標出作者與單位）、聯絡人姓名、電話及中英文通訊錄。
3. 第二、三頁爲中文及英文之摘要及關鍵詞（請提供 3 至 5 個關鍵詞或簡短片語），中英文摘要須完全相同，摘要分段撰寫，依序爲背景及目的（Background and purpose）、方法（Methods）、結果（Results）及討論（Discussion）。
4. 相同貢獻作者請加註說明，如研究主題的設定、參與決定研究設計、進行統計分析、詮釋研究結果、以及各章節撰稿等貢獻。
5. 圖表應專業製作，一張紙僅一個附圖或附表，依引用順序以阿拉伯數字標出排列。附表須有標題及說明且不可以照片形式。圖片或照片電子檔（.jpg）必須清晰、分明。附圖須有簡單說明（Legend），並另頁撰寫。光學或電子顯微鏡照片，請註明擴大倍率或比例。

註：[1] 根據「生物醫學雜誌投稿之統一規定」第五版，刊載於 Annals of Internal Medicine 1997;126(1): 36-47.

肆、參考文獻

未經發表之論文或摘要不得列爲參考文獻，但可於本文中說明並註明「未發表」（unpublished observations）。博碩士論文可引用。已被任何雜誌接受刊發但仍未發表之著作，請列出雜誌名稱及年份，並註明「in press」。

原著論文、病例報告、綜論、短論、影像判讀、臨床病理討論、編著的話按下列格式撰寫：

A.雜誌及期刊

中文例〔作者姓名：題目 。雜誌簡稱 年號；卷數：起訖頁數〕

薛玉梅、陳建仁：皮膚砷癌之流行性病學特徵與危險因子。中華衛誌 1996; 15: 1-26。

英文例〔英文原稿中引用的參考文獻，其雜誌或期刊之簡稱應參照 Index Medicus 型式〕

1. Feely J, Wilkinson GR, Wood AJ. Reduction of liver blood flow and propranonol metabolism by cimetidine. N Engl J Med 1981;304:691-6.
2. Kaplan NM. Coronary heart disease risk factors and antihypertensive drug selection. J cardiovasc Pharmacol 1982; 4(suppl 2): 186-365.（引用雜誌附冊時）
3. Tada A, Hisada K, Suzuki T, Kadoya S. Volume measurement of intracranial hematoma by computedtomography. Neurol surg (Tokyo) 1981; 9: 251-6.〔In Japanese: English abstract〕（引用文獻之作者之本文爲非英文，但有英文摘要）。
4. Bhasin S, Storer TW, Berman N, Callegari C, Clecenger B, Phillips J, et al. The effects of supraphysiologic doses of testosterone on muscle size and strength in normal men. N Engl J Med 1996; 335: 1-7.（作者超過 6 位時，只須列出前 6 位，其它以「等」(et al) 代替）

＊期刊若有「數位物件識別碼 (digital object identifier, DOI)」，則於文獻末。

B.單行本：

中文例 [作者姓名：書名，版數（卷數）。發行地；出版公司，年代：引用部份頁數]。

楊志良：生物統計學新論，一版。台北；巨流圖書公司，1984：33-8.

英文例 [英文單行本的書名，除介系詞及連接詞外，第一字母需大寫]

(1) Plum F, Posner JB. Diagnosis of Stupor and Coma. 3rd ed., Philadelphia: Davis, 1980:132-3.

C.多重作者之單行本：

中文例 [有關文章作者姓名：題目 。編輯者姓名 : 書名 。版數（卷數）。發行地 : 出版公司，年代 ; 引用部份頁數]。

蔣欣欣：護理與健康。顧乃平：護理專業導論。一版。台北 : 匯華出版公司，1991：83-121。

英文例 Levinsky NG: Fluid and electrolytes. In: Thorn GW, Adams RD, Braunwald E, lsselbacher K, Petersdprf RG eds. Harrison’s Principles of Internal Medicine. 8th ed. New York: Mcgraw-Hill, 1977;364-75.

D.參考文獻引用時，若兩名以下作者請列出姓氏。兩名以上則列出第一名之姓氏，其他以「等」(et al) 代替，並以阿拉伯數字方括弧表示於引用之後。

例：One of the first well documented reports of ECH poisoning with fatality in young children was reported by Miller et al. in 1970[2].

E.參考文獻引用網路資料請列出文獻名稱及出處以及引用時間

(Accessed Month day, 2016, at http://www.house.gov/xxxx/min/inves_xxx/index_accord.htm.)

伍、著作權

若著作人投稿於本刊經收錄後，同意授權本刊得再授權國家圖書館或其他資料庫業者，進行重製、透過網路提供服務、授權用户下載、列印、瀏覽等行爲。並得爲符合各資料庫之需求，酌作格式之修改。若爲摘譯、譯稿或改寫稿，需附原作者之正本同意書，並附原文影本一份；來稿如涉及版權，概由作者自負文責。

童綜合醫學雜誌

編著的話

綜　論

原　著

病例報告

臨床病理討論

影像判讀

ISSN 2071-3592

童綜合醫學雜誌

中華民國九十六年十二月創刊
預定出版日期：每年六、十二月三十日出刊

出版編輯部：
童綜合醫學雜誌編審委員會
地址：43503 臺中市梧棲區臺灣大道八段 699 號
E-Mail：Tungs_Journal@ms.sltung.com.tw
Tel：〈04〉26581919 ext 59045　Fax：〈04〉26582193

印 刷 者：
大光華印務部　Tel：〈02〉2302-3939（代表號）
地址：10851 台北市萬華區廣州街 32 號 6 樓　Fax：〈02〉2302-2036